

Improved monitoring and decision-making to manage atypical *Aeromonas hydrophila* in catfish
aquaculture ponds

By

Bradley Michael Richardson

Approved by:

Michael E. Colvin (Co-Major Professor)

David Wise (Co-Major Professor)

Ryan M. Walker (Minor Professor)

Terrence E. Greenway

Matthew J. Griffin

Charles C. Mischke

Kevin M. Hunt (Graduate Coordinator)

George M. Hopper (Dean, College of Forest Resources)

A Dissertation
Submitted to the Faculty of
Mississippi State University
in Partial Fulfillment of the Requirements
for the Degree of Doctor of Philosophy
in Forest Resources (Wildlife, Fisheries, and Aquaculture)
in the College of Forest Resources

Mississippi State, Mississippi

August 2020

ProQuest Number: 28028553

All rights reserved

INFORMATION TO ALL USERS

The quality of this reproduction is dependent on the quality of the copy submitted.

In the unlikely event that the author did not send a complete manuscript and there are missing pages, these will be noted. Also, if material had to be removed, a note will indicate the deletion.



ProQuest 28028553

Published by ProQuest LLC (2020). Copyright of the Dissertation is held by the Author.

All Rights Reserved.

This work is protected against unauthorized copying under Title 17, United States Code
Microform Edition © ProQuest LLC.

ProQuest LLC
789 East Eisenhower Parkway
P.O. Box 1346
Ann Arbor, MI 48106 - 1346

Copyright by
Bradley Michael Richardson
2020

Name: Bradley Michael Richardson

Date of Degree: August 7, 2020

Institution: Mississippi State University

Major Field: Forest Resources (Wildlife, Fisheries, and Aquaculture)

Select Appropriate Title: Michael E. Colvin, David Wise

Title of Study: Improved monitoring and decision-making to manage atypical *Aeromonas hydrophila* in catfish aquaculture ponds

Pages in Study: 154

Candidate for Degree of Doctor of Philosophy

Commercial catfish production is an inveterate industry within the southeastern United States. Bacterial disease is a significant detriment to global aquaculture, including the United States catfish industry. Among them, an atypical strain of the bacterium *Aeromonas hydrophila* has plagued the industry since the late 2000s. Atypical *A. hydrophila* (aAh) outbreaks are largely acute, resulting in catastrophic losses. The disease ecology, prevalence, and genetic distribution are poorly understood. Atypical *Aeromonas hydrophila* displays a rapid onset with few warning signs of the impending disease, making it difficult for early detection.

At present there are two recognized haplotypes of aAh. This project aimed to investigate changes in the spatial and temporal distributions of these haplotypes. The analysis of clinical isolates from different geographic regions across multiple years revealed complete supplanting by the younger haplotype in the Mississippi Delta within 5 years of first isolation. Comparative genomics demonstrated distinct divergences in specific virulence components between the two strains, specifically the Type VI Secretion System, which may explain putative differences in outbreak dynamics and recent displacement of one strain by the other.

Also, a rapid, non-lethal screening method was validated that can detect aAh within the catfish host. This method affords data collection regarding infection severity prior to onset of disease and, can predict aAh prevalence at the fish- and pond-levels. The occupancy model indicates more than half the population within a pond may be infected with aAh despite no overt signs of disease. Additionally, aAh is commonly present in approximately 10% of the population, providing the first evidence of a carrier state in this disease.

Lastly, a compartmental SLIR model was used to investigate disease dynamics of aAh in catfish aquaculture ponds. Simulations suggest the introduction hypothesis does affect estimated pond profit and antibiotic intervention is an economical treatment for aAh. Routine monitoring was less economical and could dramatically reduce profit in some scenarios. Overall, this work expands our current knowledge of aAh in catfish aquaculture and lays the foundation for future studies investigating aAh management and mitigation of bacterial disease in catfish aquaculture.

DEDICATION

I would like to dedicate this culmination of work to my parents Dana and Rhonda Pearson for all their sacrifices during my journey through higher education and their unwavering support of my interests and ambitions. I would also like to dedicate this to all the young children in my family, Riley, Landen, Michael, Tripton, Maddie, and Charli. Higher education has not been commonplace throughout our family history, but that does not preclude us from our personal journey to better ourselves in any way we see fit. I hope that my completion of this long-awaited achievement inspires you to chase the best versions of yourselves in whatever you aspire to be.

ACKNOWLEDGEMENTS

I would first like to thank my major professors, Michael Colvin and David Wise, for taking a chance on a young man with no epidemiology or aquaculture training to his name. I would also like to thank the rest of my committee, Terry Greenway, Matt Griffin, Chuck Mischke, and Ryan Walker for their support throughout this process. I would like to extend a special thank you to Matt Griffin who dealt with a constant barrage of questions, impromptu technical demonstrations, and a wealth of information and opportunities in a range of technical skills. Dr. Walker was a constant point of enthusiasm and fantastic discussions during my pursuit of a Secondary Education minor. I owe a great deal of my continued enjoyment of teaching and teaching research to his enthusiasm and guidance. I also want to give a sincere thank you to the rest of the staff at the Thad Cochran National Warmwater Aquaculture Research Center for all their time and effort they provided over the years. A special thank you goes to Cyndi Ware, Todd Byars, and Monroe Walker for all of their help in the lab and field, as well as Brenda Santucci for her efforts in administrative work that kept this project moving as smoothly as possible and Lester Khoo for his help in procuring historical information from catfish aquaculture in the Mississippi delta and many laughs and conversations.

I want to thank my friends and family all over the country for their support, encouragement, and genuine interest in my research. It was many of these small conversations and the sincere reaction of all of you that helped to continuously spark new questions and ideas through the project.

I would also like to thank the faculty within the College of Forest Resources, particularly those in the Department of Wildlife, Fisheries, and Aquaculture. Whether through mentoring, teaching assistantships, classes, or hallway conversations, each of you have made my experience over the last four years an enjoyable and educational one. I owe a deep level of gratitude to Dr. Ryan Walker and Deb Pounders for allowing me to delve into my love of teaching and help with the environmental education of the Columbus High School students. This was one of my favorite experiences during my doctoral journey and I want to thank the teachers, administrators, and students that were a part of making that happen.

TABLE OF CONTENTS

DEDICATION.....	ii
ACKNOWLEDGEMENTS.....	iii
LIST OF TABLES.....	viii
LIST OF FIGURES	x
CHAPTER	
I. INTRODUCTION.....	1
Objectives	7
II. SPATIAL AND TEMPORAL GENOMIC ANALYSIS OF ATYPICAL AEROMONAS HYDROPHILA ISOLATES COLLECTED FROM AQUACULTURE FARMS OF THE SOUTHEASTERN UNITED STATES.....	9
Introduction.....	9
Materials and Methods	12
Temporal aAh Outbreak Analysis.....	12
Isolate Collection and aAh Confirmation.....	12
Genome Sequencing.....	14
Genomic Comparison	15
Results and Discussion	16
Temporal Outbreak Analysis	16
Spatial and Temporal Haplotype Investigation.....	16
Genomic Comparison	17
Housekeeping Genes.....	18
Type I Fimbrial Pilus.....	18
Type IV Pili Systems	18
Flagella.....	19
Quorum-sensing	19
Type II Secretion System.....	20
Type VI Secretion System	20
Toxins	21
Additional Virulence Factors	21
Discussion and Conclusions	21

III. USING QUANTITATIVE POLYMERASE CHAIN REACTION AND OCCUPANCY MODELS TO ESTIMATE TYPICAL <i>AEROMONAS HYDROPHILA</i> PREVALENCE IN CATFISH	60
Introduction.....	60
Materials and Methods	63
Field and Lab Sampling.....	63
Swab Validation	63
Occupancy Model Sampling	65
qPCR Analysis	65
Statistical Analysis	66
Occupancy Models	67
Results and Discussion	68
Swab Screening Validation.....	68
Swab Field Comparisons	69
Occupancy Models and Prevalence Estimations.....	72
Conclusions.....	74
IV. A COMPARTMENTAL EPIDEMIOLOGY MODEL TO INVESTIGATE ATYPICAL <i>AEROMONAS HYDROPHILA</i> DISEASE DYNAMICS IN CATFISH AQUACULTURE PONDS	82
Introduction.....	82
Materials and Methods	86
Systems model overview and inference	86
Catfish production system model development	87
Medicated Feed	92
Early harvest.....	93
Monitoring pathogen status.....	93
Model simulations	93
Scenario evaluation.....	94
Sensitivity Analysis	94
Results	95
Evaluating pathogen introductions hypotheses.....	95
Scenario evaluation	95
Antibiotic Usage.....	95
Harvest Day.....	96
Routine Monitoring	96
Sensitivity Analysis	98
Discussion and Conclusions	98
REFERENCES	121
APPENDIX	

A. METADATA FOR ALL ISOLATES COLLECTED AND USED IN THE TEMPORAL AND SPATIAL ANALYSIS OF THIS STUDY.....	136
--	-----

LIST OF TABLES

Table 2.1	List of isolates used. Lab indicates which lab originally received the case submission and cultured the isolate occurred. Isolates marked with asterisks (*) are the type-strain isolates for the two haplotypes of atypical <i>A. hydrophila</i> . Strains listed as tAh are typical (non ST-251) <i>A. hydrophila</i>	26
Table 2.2	Primer sequences validated by Griffin et al. (2013) and used for identifying atypical <i>Aeromonas hydrophila</i> (aAh) via polymerase chain reaction (PCR). T_m is the melting temperature of each primer	35
Table 2.3	Temporal outbreak incidence of 2 cooperating catfish aquaculture farms from 2010-2017. Incidences indicate individual pond outbreaks of atypical <i>Aeromonas hydrophila</i> (aAh) (top) or any record of clinical disease (bottom). Contingency tables place aAh outbreaks in current production year along top and outbreaks in previous production year along the side	36
Table 2.4	Number of isolates provided by each diagnostic lab, separated by year. Data excludes the type-strain isolates for the ML09-119 and S14-452 haplotypes.....	37
Table 2.5	Metadata for the 108 genes examined. <i>Group</i> denotes general association between genes. <i>Gene Locus</i> is the coding region within the ATCC 7966 isolate (Accession #: CP000462).	38
Table 3.1	Primer and probe sequences validated by Griffin et al. (2013) and used for quantitative polymerase chain reaction (qPCR).....	76
Table 3.2	Binary responses of all screening tests for fish collected from ponds with active mortalities (N = 296 fish).	76
Table 3.3	Contingency table showing number of PCR-positive and PCR-negative fish based on gill and vent swabs assays from fish collected during field sampling.	77
Table 3.4	Occupancy model prevalence estimates for each pond separated by sampling date. Prevalence estimates were calculated using hierarchical occupancy models with swabs collected from the gills and lower intestine (vent).....	78
Table 3.5	Detection types for atypical <i>Aeromonas hydrophila</i> (aAh) by swab type (N = 526 fish).....	79

Table 4.1 Median profits with 95% and 80% confidence intervals for each scenario evaluated.
For binary variables, 0 is “no”, 1 is “yes”. All profit values are in USD (\$). 105

Table A.1 All isolates used for spatial and temporal analysis of atypical *Aeromonas hydrophila*
in the southeastern U.S. 137

LIST OF FIGURES

Figure 2.1 Electrophoresis gel showing the polymerase-chain reaction (PCR) product bands displayed by the S14-452 and ML09-119 haplotypes.....	47
Figure 2.2 Stacked bar plot showing temporal shift from ML09-119 haplotype to S14-452 haplotype from 2013 to 2018 in the Mississippi Delta region. Data based on diagnostic case submissions from the Thad Cochran National Warmwater Research Center diagnostic lab. Numbers at the top of each column indicate total number of cases included for that year.....	48
Figure 2.3 Heatmap showing nucleotide sequence identity similarity of housekeeping genes in <i>Aeromonas</i> spp. Individual genes are located on the x-axis with each isolate located along the left y-axis. “aAh” and “tAh” designate reference atypical and typical <i>A. hydrophila</i> strains, respectively, acquired from the NCBI database. Green-scale bar along left axis denotes <i>Aeromonas</i> species or <i>Aeromonas hydrophila</i> strain; groups, in descending order, are: <i>A. sobria</i> , <i>A. veronii</i> , reference aAh, ML09-119, S14-452, and reference tAh.	49
Figure 2.4 Heatmap showing nucleotide sequence identity similarity of type I fimbrial (<i>fim</i>) genes in <i>Aeromonas</i> spp. Individual genes are located on the x-axis with each isolate located along the left y-axis. “aAh” and “tAh” designate reference atypical and typical <i>A. hydrophila</i> strains, respectively, acquired from the NCBI database. Green-scale bar along left axis denotes <i>Aeromonas</i> species or <i>Aeromonas hydrophila</i> strain; groups, in descending order, are: <i>A. sobria</i> , <i>A. veronii</i> , reference aAh, ML09-119, S14-452, and reference tAh.	50
Figure 2.5 Heatmap showing nucleotide sequence identity similarity of type IV pilus (<i>flp</i>) genes in <i>Aeromonas</i> spp. Individual genes are located on the x-axis with each isolate located along the left y-axis. “aAh” and “tAh” designate reference atypical and typical <i>A. hydrophila</i> strains, respectively, acquired from the NCBI database. Green-scale bar along left axis denotes <i>Aeromonas</i> species or <i>Aeromonas hydrophila</i> strain; groups, in descending order, are: <i>A. sobria</i> , <i>A. veronii</i> , reference aAh, ML09-119, S14-452, and reference tAh.	51

- Figure 2.6 Heatmap showing nucleotide sequence identity similarity of type IV pilus (*msh*) genes in *Aeromonas* spp. Individual genes are located on the x-axis with each isolate located along the left y-axis. “aAh” and “tAh” designate reference atypical and typical *A. hydrophila* strains, respectively, acquired from the NCBI database. Green-scale bar along left axis denotes *Aeromonas* species or *Aeromonas hydrophila* strain; groups, in descending order, are: *A. sobria*, *A. veronii*, reference aAh, ML09-119, S14-452, and reference tAh.....52
- Figure 2.7 Heatmap showing nucleotide sequence identity similarity of the type IV pili systems (*tap*) genes in *Aeromonas* spp. Individual genes are located on the x-axis with each isolate located along the left y-axis. “aAh” and “tAh” designate reference atypical and typical *A. hydrophila* strains, respectively, acquired from the NCBI database. Green-scale bar along left axis denotes *Aeromonas* species or *Aeromonas hydrophila* strain; groups, in descending order, are: *A. sobria*, *A. veronii*, reference aAh, ML09-119, S14-452, and reference tAh.....53
- Figure 2.8 Heatmap showing nucleotide sequence identity similarity of polar flagellum (*fla*) genes in *Aeromonas* spp. Individual genes are located on the x-axis with each isolate located along the left y-axis. “aAh” and “tAh” designate reference atypical and typical *A. hydrophila* strains, respectively, acquired from the NCBI database. Green-scale bar along left axis denotes *Aeromonas* species or *Aeromonas hydrophila* strain; groups, in descending order, are: *A. sobria*, *A. veronii*, reference aAh, ML09-119, S14-452, and reference tAh.....54
- Figure 2.9 Heatmap showing nucleotide sequence identity similarity of quorum-sensing genes in *Aeromonas* spp. Individual genes are located on the x-axis with each isolate located along the left y-axis. “aAh” and “tAh” designate reference atypical and typical *A. hydrophila* strains, respectively, acquired from the NCBI database. Green-scale bar along left axis denotes *Aeromonas* species or *Aeromonas hydrophila* strain; groups, in descending order, are: *A. sobria*, *A. veronii*, reference aAh, ML09-119, S14-452, and reference tAh.....55
- Figure 2.10 Heatmap showing nucleotide sequence identity similarity of the type II secretion systems (T2SS; *gsp*) genes in *Aeromonas* spp. Individual genes are located on the x-axis with each isolate located along the left y-axis. “aAh” and “tAh” designate reference atypical and typical *A. hydrophila* strains, respectively, acquired from the NCBI database. Green-scale bar along left axis denotes *Aeromonas* species or *Aeromonas hydrophila* strain; groups, in descending order, are: *A. sobria*, *A. veronii*, reference aAh, ML09-119, S14-452, and reference tAh.....56

Figure 2.11 Heatmap showing nucleotide sequence identity similarity of the type VI secretion systems (T6SS) genes in <i>Aeromonas</i> spp. Individual genes are located on the x-axis with each isolate located along the left y-axis. “aAh” and “tAh” designate reference atypical and typical <i>A. hydrophila</i> strains, respectively, acquired from the NCBI database. Green-scale bar along left axis denotes <i>Aeromonas</i> species or <i>Aeromonas hydrophila</i> strain; groups, in descending order, are: <i>A. sobria</i> , <i>A. veronii</i> , aAh (ref), ML09-119, S14-452, tAh (ref).....	57
Figure 2.12 Heatmap showing nucleotide sequence identity similarity of the toxin genes in <i>Aeromonas</i> spp. Individual genes are located on the x-axis with each isolate located along the left y-axis. “aAh” and “tAh” designate reference atypical and typical <i>A. hydrophila</i> strains, respectively, acquired from the NCBI database. Green-scale bar along left axis denotes <i>Aeromonas</i> species or <i>Aeromonas hydrophila</i> strain; groups, in descending order, are: <i>A. sobria</i> , <i>A. veronii</i> , reference aAh, ML09-119, S14-452, and reference tAh	58
Figure 2.13 Heatmap showing nucleotide sequence identity similarity of additional virulence factor genes in <i>Aeromonas</i> spp. Individual genes are located on the x-axis with each isolate located along the left y-axis. “aAh” and “tAh” designate reference atypical and typical <i>A. hydrophila</i> strains, respectively, acquired from the NCBI database. Green-scale bar along left axis denotes <i>Aeromonas</i> species or <i>Aeromonas hydrophila</i> strain; groups, in descending order, are: <i>A. sobria</i> , <i>A. veronii</i> , reference aAh, ML09-119, S14-452, and reference tAh.....	59
Figure 3.1 Diagram of swab analysis using qPCR.....	80
Figure 3.2 Predicted detection probabilities of atypical <i>Aeromonas hydrophila</i> (aAh) in gill and vent swabs, based on the number of replicates in the assay	81
Figure 4.1 Epidemiological (SEIR) model constructed for atypical <i>Aeromonas hydrophila</i> (aAh) disease dynamics.....	113
Figure 4.2 Economics portion of the epidemiological model constructed.....	114
Figure 4.3 Plot of median profit with and without antibiotic usage by harvest day. Solid lines represent no antibiotic usage; dashed lines indicate antibiotic use. Results based on 500 simulations for each scenario. “Abx” = antibiotics	115
Figure 4.4 Simulated median profit by harvest day given the hypothesis of infected fingerlings. The black, solid line shows the median profit with no diagnostic monitoring. Orange and blue lines represent 14- and 30-day intervals in diagnostic monitoring submissions, respectively. Dashed lines represent scenarios with 10 fish submitted per monitoring, solid lines represent cases with 25 fish submitted.....	116

Figure 4.5 Simulated median profit by harvest day given the hypothesis of aAh introduction via birds. The black, solid line shows the median profit with no diagnostic monitoring. Orange and blue lines represent 14- and 30-day intervals in diagnostic monitoring submissions, respectively. Dashed lines represent scenarios with 10 fish submitted per monitoring, solid lines represent cases with 25 fish submitted.....	117
Figure 4.6 Simulated median profit by harvest day given the hypothesis of latent aAh carrier fish. The black, solid line shows the median profit with no diagnostic monitoring. Orange and blue lines represent 14- and 30-day intervals in diagnostic monitoring submissions, respectively. Dashed lines represent scenarios with 10 fish submitted per monitoring, solid lines represent cases with 25 fish submitted.....	118
Figure 4.7 Simulated median profit by harvest day given the hypothesis of aAh as a pond resident. The black, solid line shows the median profit with no diagnostic monitoring. Orange and blue lines represent 14- and 30-day intervals in diagnostic monitoring submissions, respectively. Dashed lines represent scenarios with 10 fish submitted per monitoring, solid lines represent cases with 25 fish submitted.....	119
Figure 4.8 Tornado plot of pond profit sensitivity grouped by hypothesis and disease variable. Plot is color-coded by hypothesis for readability. Hypothesis numbers correspond to modes of pathogen introduction via <i>infected fingerlings</i> , <i>bird vector</i> , <i>latent infections</i> , and <i>pond resident</i> , respectively. Disease variables are transmission rate (β ; beta), progression rate (θ ; theta), and recovery rate (ρ ; rho). Breakeven point is denoted by the hashed vertical line. Sensitivity based on 1000 iterations and each variable was allowed to vary by 20% of the initial values reported by previous studies. All profit values are in thousands of USD and represent the range of values recorded for each analysis.....	120

CHAPTER I

INTRODUCTION

Aquaculture is a global industry pertaining to production of baitfish, crustaceans, food fish, mollusks, ornamental fish, and sport/game fish (USDA 2013a). On an annual basis, global aquaculture returns \$120 billion in revenue (NOAA 2015). Fish produced for human consumption makes up about 46% of fish aquaculture across the world. Asia dominates the global market, producing approximately 88% of aquaculture products (62% from China, alone), while the United States contributes less than 1%, annually (NOAA 2015). China's dominance of the market is reflected in the fact nearly 70% of all aquaculture produced fish are carps originating from China (FAO 2010).

Aquaculture for food has occurred for hundreds or thousands of years, but only began to grow noticeably about 60 years ago. In 1950, less than 1 million tons of fish was produced globally for human consumption; by 2008, the global market was approximately 47 million metric tons (FAO 2010). The aquaculture industry has grown at nearly 8%, annually, over the last 30 years, nearly twice as fast as the livestock industry (FAO 2010). As of 2008, the industry employed nearly 45 million people across the globe, a 167% increase from 1980 (FAO 2010). Freshwater aquaculture comprises most global fish production, both in terms of quantity (59.9%) and value (56.0%, FAO 2010). Of all commodities produced via freshwater aquaculture, fishes dominate the market at over 25 million metric tons produced in 2008; mollusks were the second largest freshwater commodity at nearly 12 million metric tons (FAO 2010).

Food fish farming in the United States began in the 1950s but didn't become established until the early 1980s (FAO 2010). Today, about 65% of the total US aquaculture industry value is held in finfish. The United States generated about \$1.51 billion from all aquaculture products in 2012 (USDA 2018). The US food fish industry generated \$715 million in 2018; with more than \$200 million from aquaculture facilities in Mississippi, nearly half of which was from catfish (USDA 2018). United States catfish production is concentrated primarily in the southeastern states. Mississippi is the leading catfish producer, followed by Alabama and Arkansas (USDA 2013b, 2016, 2018). Nearly 2,500 freshwater farms are located within the US, spanning over 100,000 hectares (USDA 2018). As of 2018, 176 freshwater farms were located in Mississippi, a decline from 224 farms in 2013 (USDA 2013b, 2018). One hundred sixty-one of those 176 farms produce catfish, while the remaining farms produce hybrid striped bass, multiple carp species, or tilapia (USDA 2018).

Commercial fish farming suffers greatly from water-borne diseases and bacterial infections are the most common cause of disease-related issues, particularly in catfish (Sunder et al. 2006). Mass fish kills, defined by Walsh et al. (2004) as any sudden or unexpected mass mortality over a short time, can have widespread ecologic and economic effects. Outbreaks are more likely when the pathogen is coupled with stressed or immunocompromised individuals (Meyer 1970; Wedemeyer 1970). Snieszko (1978) presented the relationship between host, pathogen, and stress as an algebraic equation ($H + P + S^2 = D$); here, the resulting disease (D) is a combination of host characteristics (H; e.g. species, age, susceptibility, etc.), variability in the pathogen (P), and stress (S). Stress is shown as a squared term because it increases more quickly as the tolerance limits of the host are reached (Snieszko 1978). Stress is caused by a variety of biotic and abiotic factors, but is primarily attributed to handling, low dissolved oxygen, increased

ammonia, and overcrowding in ponds. Temperature can serve as a stressor for both host and pathogen. At low temperatures, many fish defenses are inactive, but at lower temperatures bacteria are typically unable to cause disease. However, as temperatures increase bacterial virulence can be enhanced. However, healthy fish can often eliminate bacterial pathogens while weakened individuals become sick and die (Liebmann et al. 1960).

Channel catfish (*Ictalurus punctatus*) of the order Siluriformes are native to North America. They are one of over 40 recognized species in the family Ictaluridae (Page and Lundberg 2007). Other commercially important ictalurids include blue catfish (*I. furcatus*), white catfish (*I. catus*), flathead catfish (*Pylodictis olivaris*), and black, brown, and yellow bullheads (*I. melas*, *I. nebulosus*, and *I. natalis*, respectively) (Wellborn 1988). Channel catfish is the largest aquatic animal commodity in the United States, with Mississippi, Alabama, and Arkansas producing over 95% of all sales (USDA 2016).

Catfish aquaculture facilities are most affected by 4 diseases: Columnaris (Camus et al. 2006; Khoo et al. 2013); Enteric Septicemia of Catfish (ESC), Proliferative Gill Disease (PGD), and Motile Aeromonas Septicemia (MAS; Plumb and Hanson 2010). ESC and Columnaris are bacterial diseases caused by members of the *Edwardsiella* and *Flavobacterium* genera, respectively. Comparably, PGD is a parasitic disease of channel and channel x blue hybrid catfish caused by the myxozoan *Henneguya ictaluri* (Pote et al. 2000; Bosworth et al. 2003; Griffin et al. 2010)

From 1996 to 2001, ESC and Columnaris outbreaks accounted for nearly 60% of all cases reported to the Thad Cochran Warmwater Research Center in Stoneville, MS (Wagner et al. 2002). Bacterial outbreaks are further exacerbated and facilitated by animal behaviors which could increase transmission. Glahn et al. (2002) found Great Blue Herons (*Ardea herodias*) fed

nearly 40x more on ponds infected with ESC than uninfected ponds. Other studies have also shown avian species to be potential vectors for the spread of disease among commercial production ponds (i.e. Jubirt et al. 2015). The behavior of the catfish themselves can also hinder treatment of disease outbreaks since sick fish often decrease feed intake, precluding treatment by medicated feeds (Wise et al. 2004; Wise et al. 2015; Griffin et al. 2017).

MAS is a generic disease used to describe symptoms caused by an array of members of the genus *Aeromonas*, primarily *A. sobria*, *A. caviae*, and *A. hydrophila* (Camus et al. 1998; Plumb and Hanson 2010). *Aeromonas hydrophila* is a gram-negative, rod-shaped bacterium with a single polar flagellum and the capacity to ferment glucose and other select sugars (Plumb and Hanson 2010). Taxonomy and classification within the *Aeromonas* genus have been complicated due to the scale of heterogeneity among isolates in terms of genetics, biochemistry, and serology (Cipriano et al. 1984). *A. hydrophila* has been distinguished from other aeromonads by its ability to hydrolyze esculin, and ferment salicin and arabinose, characteristics not exhibited by other members of the genus (Lallier et al. 1981).

Aeromonads are ubiquitous in freshwater (Cipriano et al. 1984; Camus et al. 1998) but can also be found in brackish and saltwater (Cipriano et al. 1984; Plumb and Hanson 2010). The bacterium is regularly collected from raw sewage and wastewater (Araoju et al. 1991) and is important for self-purification (Schubert 1963, cited in Snieszko 1974). Palumbo et al. (1985) showed members of *Aeromonas* can grow in temperatures ranging from 4-42 °C, with growth of *A. hydrophila* optimized at 25-35 °C; most outbreaks occur in spring and early summer, when temperatures would be expected to fall within this range (Meyer 1970). Cipriano et al. (1984) hypothesized stress caused by winter conditions and dormancy also contributed to spring

outbreaks. Along with fishes, *A. hydrophila* also infects frogs, turtles, alligators, and humans (Cipriano et al. 1984; Pasquale et al. 1994; Camus et al. 1998) and is zoonotic.

Symptoms of MAS are non-specific and often mimic those of other diseases (Camus et al. 1998). *A. hydrophila* can produce chronic, acute, and latent infections (Cipriano et al. 1984; Pasquale et al. 1994). Chronic outbreaks are noted by minimal short-term death but produce hemorrhagic septicemia, ulcers, exophthalmia (bulging eyeballs), reddening/fraying of fins, depigmentation, and abdominal distension (Mitchell and Plumb 1980; Camus et al. 1998; Austin and Austin 2012). Acute outbreaks often produce mass mortalities with survival averaging less than 20% in the absence of treatment (Mitchell and Plumb 1980; Cipriano et al. 1984). Hazen et al. (1982) provided evidence of *Aeromonas* spp. chemotaxis to fish mucus; bacteria were more chemotactic toward healthy fish mucus and slightly repulsive to the mucus of fish already infected with the bacteria. Hazen et al. (1982) suggested this was likely due to antibody secretion from infected fish. Chaudhury et al. (1996) noted *Aeromonas* spp. strains resistant to multiple antibiotics were increasing rapidly, and Mitchell and Plumb (1980) found *A. hydrophila* developed resistance to the antibiotic Furanace (nitrofurazone, $C_6H_6N_4O_4$) in just 48 hours.

Primary pathogenicity has been widely disputed over the years; Hazen et al. (1978) suggested *A. hydrophila* was the primary pathogen of Red Sore Disease (analogous to MAS) with the protozoan *Epistysis* quickly colonizing the epidermal ulcers shortly afterward. However, Camus et al. (1998) suggested *A. hydrophila* is an opportunistic pathogen, requiring weakened fish to successfully proliferate, and the difficulty of immersion challenges in recent studies tend to support this hypothesis. The facultative nature of these bacteria allows them to utilize environmental nutrients in the water, reducing the need for an immediate host (Camus et al. 1998) and increases the window of virulence for *A. hydrophila*. The bacteria have proven

difficult to eradicate due to their ability to reservoir in healthy fish, mud, aquatic plants, and protozoans (Trust et al. 1974; Walters and Plumb 1980; Camus et al. 1998).

Though exact transmission routes are not completely understood, oral entry and epidermal abrasions are likely. Further, *A. hydrophila* has been shown to colonize algae (Kawakami and Hasimoto 1978) and protozoans (Chang and Huang 1981) in the aquatic environment, while Austin and Austin (2012) found the bacteria can be easily spread via accidental abrasions. Moreover, abrasion transmission may be exacerbated because bacterial isolates from infected fish are more virulent than isolates from water samples (De Figueiredo and Plumb 1977); thus, if healthy fish are injured with MAS-infected fish, bacteria shed from infected fish may readily infect open wounds. With the higher stocking rates in today's catfish industry (more than 24,000 fish/ha in many cases; Kumar et al. 2019), crowding issues may also increase the likelihood of accidental wounding during feeding or times of stress.

Gaining a better understanding of the epidemiology and distribution of *A. hydrophila* outbreaks could provide crucial information used to treat, manage, and/or prevent future disease issues and minimize economic losses in the aquaculture industry. Losses attributed to *A. hydrophila* present potential threats to both the economic and social domains of the entire world. Economic losses in the form of lost revenue and increased costs for catfish aquaculture and other global aquaculture species have the potential to impact millions of people directly, while indirect effects may extend to billions. The *A. hydrophila* bacterium is known to occasionally infect humans, but this threat may continue to increase via multi-drug resistant strains continuing to rise and spread globally. Pathogens such as HIV/AIDS, Ebola, SARS, and Avian Flu began as zoonotics but became uncoupled from their animal reservoirs (Wilcox and Colwell 2005) and spread quickly through human populations with little warning.

In 2009, an atypical form of MAS presented itself in catfish ponds of western Alabama. During that production season, a rash of outbreaks caused dramatic economic losses; in some instances, killing over 10,000 kg of market-sized fish in just a few days (Hemstreet 2010). The etiological agent was determined an atypical strain of *Aeromonas hydrophila* (aAh; ML09-119) and over the next 4 years, the pathogen spread to catfish farming operations across Mississippi and Arkansas (Pridgeon and Klesius 2011). In 2014, a new haplotype of aAh (S14-452) was isolated from diseased fish in the Mississippi Delta region. Epizootics attributed to the new strain appeared to be less severe than those caused by the ML09-119 strain. Still, the recurring outbreaks and lack of clinical signs before disease onset continues to cause widespread losses in the catfish industry across the Southeast.

Objectives

This study aimed to determine the overall status of the aAh pathogen in catfish aquaculture of the southeastern United States. There have been two haplotypes identified in this disease, but the ecological significance of this is still unknown. Several studies have characterized the genomes of each haplotype and investigated specific differences in pathogenicity and gene transfer. However, a widespread census of the pathogen has not been conducted to determine the distribution of the two haplotypes in this region.

We used isolates collected from clinical diagnostic cases from geographically unique locations to evaluate the change in prevalence of the two haplotypes since the early onset of aAh. This was considered a crucial step in advancing efforts to mitigate aAh, as vaccine candidates have been identified and immunization strategies are being explored, despite an unknown prevalence of each haplotype. A genomic comparison was also used to further investigate the stability of aAh populations in the southeastern U.S. As vaccines and other management

strategies are explored, a better understanding of the genetic structure of the two haplotypes will facilitate development of more effective vaccines.

The need for a rapid screening method for the aAh pathogen was also deemed important to the aquaculture industry. The aAh pathogen presents few, if any, clinical signs prior to onset disease. As such, an affordable method of screening fish for the bacteria has the potential to save thousands of dollars in lost industry revenue. In addition, a better understanding of disease prevalence within a given pond may allow farmers to use preemptive measures to further minimize losses.

Lastly, a compartmental model was developed to investigate aAh dynamics within a catfish aquaculture system. Information gathered from industry experts, empirical aAh studies, as well as other closely related diseases were used to create a model providing the foundation necessary to evaluate different hypothetical scenarios affecting pond profitability. A variety of management strategies were evaluated to develop a better understanding of aAh dynamics within a pond and throughout the industry.

CHAPTER II

SPATIAL AND TEMPORAL GENOMIC ANALYSIS OF ATYPICAL AEROMONAS
HYDROPHILA ISOLATES COLLECTED FROM AQUACULTURE FARMS
OF THE SOUTHEASTERN UNITED STATES

Introduction

Aeromonas hydrophila is a gram-negative, motile, rod-shaped bacterium common to nearly all freshwater environments (Plumb and Hanson, 2011) and the causative agent of disease in many animal species including fish, birds, reptiles, amphibians, and mammals, including humans (Janda and Abbott 2010; Tomás 2012; Albarral et al. 2016). Though recognized as a disease agent, *A. hydrophila* is typically considered to be a secondary or opportunistic pathogen (Bebak et al. 2015).

In fish aquaculture, *A. hydrophila* is the most common etiological agent of motile *Aeromonas* septicemia (MAS), though septicemia caused by related motile aeromonads is typically grouped under the same umbrella term. MAS has long been recognized in fish culture; however, it has historically been considered a nuisance disease in US catfish aquaculture, and not a disease of major concern (Thune et al. 1993). However, a new clonal group of atypical *A. hydrophila* (aAh), deemed ST251, has emerged as a high-risk pathogen responsible for the MAS outbreaks in China and the southeastern United States (Pang et al. 2015).

The first reported fish kill associated with ST251 outbreaks in cultured fish occurred in the Jiangsu Province of China in 1989, where a strain of aAh, designated as J-1, was recovered

from a diseased carp species (Chen and Lu 1991). A second epidemic of ST251 MAS occurred in China's Guangdong Province, where the ST251 isolate ZC1 was isolated from diseased grass carp (*Ctenopharyngodon idella*) (Deng et al. 2009), while a third outbreak, also in Jiangsu Province occurred in 2010, resulting in the isolation of ST251 strain NJ-35 (Pang et al. 2012).

The first U.S. case of ST251-affiliated MAS occurred in the Delta region of Mississippi in 2004, attributed to aAh isolate S04-690 isolate (Hossain et al., 2014); however, this outbreak was a localized event and did not lead to an epidemic within the industry. As a result, this first occurrence was largely overlooked. In 2009, ST251 aAh isolates were consistently isolated from recurrent MAS outbreaks in channel catfish (*Ictalurus punctatus*) aquaculture ponds in Alabama, U.S. Estimated losses exceeded 1.5 metric tonnes in the first year, with the majority of losses occurring in market-sized fish (Hemstreet 2010). Initially, ST251 aAh outbreaks in Alabama were associated with a highly clonal clade of the US aAh type strain ML09-119 (Hossain et al. 2014). Over the next 4 years, aAh decimated channel catfish farms across Alabama, Mississippi, and Arkansas (Pridgeon and Klesius 2011; Hossain et al. 2014). In 2014, a new strain of ST251 aAh (S14-452) was isolated from diseased channel catfish during a MAS outbreak in the Mississippi Delta region. Anecdotal reports suggested the S14-452 strain displayed different mortality dynamics, with producers reporting less catastrophic losses than those estimated for the ML09-119 strain. Further, the new S14-452 strain demonstrated significant genetic differences from the ML09-119-type cluster from Alabama, specifically in regards to the Type VI Secretion System (T6SS), wherein the S14-452 isolate shared more similarities to the ZC1 isolate from China than the ML09-119 haplotypes linked to catastrophic losses in East Mississippi and West Alabama (Rasmussen-Ivey et al. 2016).

These ST251 aAh isolates from the US and China are hypothesized to share a recent common ancestor (Hossain et al. 2014). Genomic analyses of typical *A. hydrophila* (tAh) and those attributed to ST251 aAh revealed the two groups are genetically distinct (Awan et al., 2018). Some key characters of the ST251 aAh strains include the ability to use *myo*-inositol as a sole carbon source, L-fucose metabolism abilities, and inducible prophages (Hossain et al. 2013, 2014; Pang et al. 2015).

Chronology of the aAh clade shows a new strain appearing about every 5 years. As such, an updated investigation of more recent isolates is warranted to identify plasticity of these clonal groups within U.S. farm-raised catfish. Numerous studies (Liles et al. 2011; Hossain et al. 2013, 2014; Pang et al. 2015; Rasmussen-Ivey et al. 2016; Tekedar et al. 2019) have commented on the highly clonal nature of aAh isolates, but lateral gene transfer has been suggested as a key mechanism for the rapid evolution of this pathogen (Hossain et al. 2013). The aim of the present study was to explain the temporal and geographic dynamics of the two U.S. aAh haplotypes and build on the wealth of information afforded by previous works describing the genomic relationships between typical *A. hydrophila* (tAh) and aAh.

The study chronicled herein explains the distribution dynamics of aAh MAS and prevalence of the two U.S. aAh haplotypes based on diagnostic case submissions from catfish aquaculture in the southeastern U.S. Further, this work investigated the relationships of temporally and geographically discrete aAh strains from the predominant catfish farming regions of Mississippi and Alabama collected from 2010 to 2018.

Materials and Methods

Temporal aAh Outbreak Analysis

Diagnostic records for two geographically distinct, cooperating catfish farms were acquired from the Aquatic Research and Diagnostic Laboratory (ARDL) housed at the Thad Cochran National Warmwater Aquaculture Research Center in Stoneville, MS for 2010 to 2017. Cooperating catfish farms were in the catfish farming region of the Mississippi Delta, defined by Tucker and Hargreaves (2004). Information on pond number, previous disease outbreaks, and current disease outbreaks was provided. Previous and current disease outbreaks were defined as disease outbreaks in the present production year (current outbreak) or the previous production year (previous outbreak). A 2x2 contingency table using current and previous outbreaks was created in the statistical program R (R Core Team 2017) and odds ratios were evaluated using the case control method with a chi-squared (χ^2) test in the *epiR* v1.0-10 package (<https://fvas.unimelb.edu.au/research/groups/veterinary-epidemiology-melbourne>).

Isolate Collection and aAh Confirmation

Bacterial cultures of *Aeromonas hydrophila* cases were collected from 3 diagnostic labs: NWAC, College of Veterinary Medicine at Mississippi State University (Starkville, MS), and College of Veterinary Medicine at Auburn University (Auburn, AL) (Table 1). Isolates were collected from specimen submissions from 2010 to 2018 using standard diagnostic protocols (Hanson et al. 2014). Cryostocks were created by reviving bacterial cultures on Luria-Bertani (L-B; Sigma-Aldrich, Inc., St. Louis, MO) agar plates, followed by expansion in porcine BHI broth (Becton Dickinson, Franklin Lakes, NJ). Glycerol was added at 20% (v/v) and stocks were cryopreserved at -80 °C.

Archived cryostocks were revived onto L-B agar plates and incubated at 28 °C for 24 hours. Individual colonies were removed from the plate and transferred to a clean 1.5 ml Eppendorf tube® (Eppendorf North America, Hauppauge, NY) for aAh haplotype confirmation. Genomic DNA (gDNA) was isolated using the Gentra Purgene Tissue Kit (Qiagen, Germantown, MD) following the manufacturer's suggested protocol for gram-negative bacteria. Primers used for PCR identification of suspect aAh isolates are listed in Table 2. Isolates identified as aAh, were then identified as either ML09-119 or S14-452-like employing the primers described by Rasmussen-Ivey et al. (2016) in a duplex end-point PCR format. Briefly, each 25-µl reaction consisted of 5 µl of sample DNA, 13 µl of EconoTaq PLUS Green 2X Mastermix (Lucigen Corporation, Middleton, WI), 10 pmols of forward and reverse primers for S14-452 and ML09-119 (Eurofins Genomics LLC, Louisville, KY; Table 2), and nuclease-free water to volume. The PCR was performed using a C1000 Touch Thermal Cycler (Bio-Rad Laboratories, Hercules, CA) programmed for an initial denaturation of 3 min at 94°C followed by 35 cycles consisting of a 30 sec denaturation at 95°C, a 30 sec annealing at 58°C, and a 30 second elongation at 72°C, with a final elongation step at 72°C. Aliquots (10 µl) of each reaction and a concurrently run molecular weight marker (Hyperladder 50 bp; BioLine, London, UK) run through 0.75% agarose gels containing 3 ml ethidium bromide (1.5 µg ml⁻¹). Haplotypes were based on the presence of appropriately sized bands (S14-452: 300 bp; ML09-119: 246 bp) (Fig. 2.1). Isolates not amplifying by either ML09-119 or S14-452 primers were ruled out as aAh by qPCR according to Griffin et al. (2013). Identity of isolates not amplifying by either protocol was determined by *gyrB* or 16S sequencing (Lane et al. 1991; Yanez et al. 2003). *GyrB* and 16S amplicons were gel excised and purified using the QIAquick Gel Extraction kit (Qiagen

Bioinformatics, Germantown, MD) and direct sequenced commercially using the same primers employed to generate the amplicons (Eurofins Genomics).

Genome Sequencing

A subset of isolates representing all three diagnostic laboratories and all years available from 2010-2018 were chosen arbitrarily for whole genome sequencing. Isolates were revived from cryopreservation as above and individual colonies were expanded in 9 ml of porcine brain-heart-infusion broth (Becton Dickinson) at 28°C with gentle shaking (20 rpm). Aliquots (3 ml) of expanded culture were concentrated by centrifugation (20,000 x g for 5 min) in a Sorvall RC 6 Plus centrifuge (Thermofisher Scientific). Bacterial DNA was isolated from stock pellets using the Gentra Puregene Tissue Kit (Qiagen Bioinformatics, Germantown, MD) protocol for gram-negative bacteria scaled up 3X.

Following initial gDNA isolation, additional purification was performed to remove impurities carried over from the initial isolation. In short, gDNA was suspended in 195 µl of EB Buffer (Qiagen) and 5 µl of RNase A, 50 µl of 5N NaCl, and 75 µl of 100% ethanol (ETOH) was added to each suspension. Samples were placed on a rotomixer (about 20 rpm) for 10 minutes. Impurities were pelleted for 20 minutes at 20,000 x g and the supernatant decanted into a clean 1.5 ml Eppendorf tube®. To precipitate the DNA, 425 µl of 100% ETOH was added to the tube, mixed by gentle inversion, incubated at -80 °C for 1 hour and gDNA pelleted by centrifugation at 20,000 x g for 3 minutes. The supernatant was removed by decanting and the pellet washed with 300 µl of 70% ETOH, centrifuged at 20,000 x g for 3 minutes, supernatant decanted, and gDNA pellet air dried for 15 minutes before resuspension in 50 µl EB Buffer. Template purity was evaluated spectrophotometrically (NanoDrop 2000; Thermo Fisher

Scientific Inc, Waltham, MA) targeting a 260/280 ratio ranging from 1.8-2.0 and 260/230 ratios from 1.6-2.2.

Draft genomes were obtained for chosen isolates by Oxford Nanopore Technology (ONT) using the ONT Rapid Barcoding Kit (SQK-RBK004; Oxford Nanopore, Oxford, UK). Barcoded sequencing products were loaded on the MinION Flow Cell (v9.4.1; Oxford Nanopore Technologies, Oxford, UK) as per manufacturer's recommendations and sequencing performed on a GridION X5 (Oxford Nanopore Technologies, Oxford, UK). Obtained Fastq files were trimmed using NanoFilt (<https://github.com/wdecoster/nanofilt>) to remove 100 bp from each end and filtered to remove all reads <1000 bp and <Q7. Genomic contigs were assembled from filtered reads using Canu v1.8 (Koren et al. 2017) and consensus sequence errors corrected using Medaka (<https://github.com/nanoporetech/medaka>). Validation of circularized genomes, when applicable, was performed by removing overlapping sequences at the contig ends and 1 Mb at the end of the genomic contig was moved to the 5' end. Long reads were then realigned to the contig with minimap2 (<https://github.com/lh3/minimap2/blob/master/cookbook.md>). The alignments were visualized in Integrated Genomics Viewer (Thorvaldsdottir et al. 2013) to validate continual read coverage across the junction. As a quality control check, one isolate (S13-597) was isolated and sequenced independently on different flow cells to confirm sequencing accuracy.

Genomic Comparison

The presence/homology of known *A. hydrophila* virulence factors (T6SS, quorum sensing, etc.) within the sequenced aAh genomes was determined in Geneious Prime® v2020.0.4 software program (Biomatters Ltd.). Representative gene sequences for select housekeeping genes (Martino et al. 2011) and known virulence factors (Rasmussen-Ivey et al. 2016; Awan et

al. 2018) were obtained from the genome of *A. hydrophila* isolate ATCC 7966 (GenBank Accession# CP000462) deposited in the National Center for Biotechnology Information (NCBI). Localized BLAST searches (Megablast) of sequenced aAh genomes were performed in Geneious Prime. Target gene sequences identified by Megablast search were aligned using MUSCLE (Edgar 2004). The calculated identity distances (% similarity) for all isolates against the tAh type strain (ATCC 7966) for all genes were exported as individual CSV files and a heatmap created from identity distances using the *gplots* package (v3.0.1.1; Warnes et al. 2019) in the statistical program R (R Core Team 2017).

Results and Discussion

Temporal Outbreak Analysis

Evaluation of clinical records from 53 observations from 2013 to 2017 showed in 1 instance, a pond produced an aAh outbreak in back-to-back production cycles. Two cases occurred in ponds with no record of aAh the previous year and 4 cases showed in ponds with an outbreak the previous year but with no record of aAh in the following season (Table 3). This resulted in a mean odds ratio of 5.75 (0.42 - 78.10, 95% Wald confidence limits). This odds ratio was not statistically significant from 1 ($\chi^2 = 2.126$, $p = 0.145$). The odds ratio is relatively large, but large confidence limits and a small sample size suggest additional data could further confirm these results.

Spatial and Temporal Haplotype Investigation

Viable clinical isolates (252) were provided by the 3 cooperating diagnostic labs (35 from Alabama, 112 from East Mississippi, 105 from the Mississippi Delta) including the two US aAh type strains, ML09-119 and S14-452 (Rasmussen-Ivey et al. 2016) (Table 4). Of these, PCR

identified 157 of the isolates (62.8%) belonged to the S14-452 haplotype, 75 isolates (30.0%) were ML09-119, 16 (6.4%) were typical *A. hydrophila* (tAh), 2 (0.8%) were identified as *A. sobria*, and 2 (0.8%) were *A. veronii*.

Isolates collected in Alabama were almost exclusively (88.5%; 31 of 35) the ML09-119 haplotype. For East Mississippi, isolates were only available for 2016 and 2018. In the 2016 East Mississippi cases, 56 of the 70 isolates (80%) were identified as the S14-452 haplotype, 11 (15.7%) were ML09-119, and 3 (4.2%) were tAh. This trend continued in 2018, where 35 of 42 isolates (83.3%) were S14-452, 1 ML09-119 (2.3%), and 6 were tAh (14.2%) (Table 2.4). Isolates from the Mississippi Delta were provided for all years from 2013 to 2018 which showed a notable haplotype shift, consistent with results from East Mississippi (Fig. 2.2). In 2013, all 17 isolates from the Mississippi Delta were the ML09-119 haplotype. The following year, 4 of the 14 case isolates (28.6%) were from the S14-452 haplotype with 1 isolate identified as tAh. In 2015, the S14-452 group was responsible for 81.8% of cases with the remainder being ML09-119. The trend continued in 2016, where 16 of the 22 (72.7%) recovered isolates were S14-452, 2 were ML09-119 (9.1%), and 4 were tAh (18.2%). Finally, in 2017 and 2018, the ML09-119 haplotype was not identified from disease case submissions from the Mississippi Delta, as 28 of the 30 isolates (93.3%) belonged to the S14-452 haplotype, with 2 isolates identified as *A. sobria* (Table 2.4).

Genomic Comparison

A subset of 40 isolates were arbitrarily chosen from the pool of 252 confirmed isolates. Efforts were made to encompass all represented years and geographic regions in the subset of isolates used for sequencing. The selected isolates consisted of 16 ML09-119 isolates, 20 S14-452 isolates, 1 *A. sobria*, and 1 *A. veronii* to serve as known outgroups. All isolates used

originated from catfish tissues (*Ictalurus* spp.) in West Mississippi, East Mississippi or West Alabama. In addition, 4 reference aAh genomes, and 2 reference tAh genomes were downloaded from NCBI and included in the genomic analysis. Whole genomes from the nanopore sequenced genomes averaged 5.1 Mb with a C-G% of 60.7%. Individual genes (115) were investigated; however, only genes present in the ATCC 7966 strain (108 genes; Table 2.5) are presented here.

Housekeeping Genes

Investigation of multiple housekeeping genes and revealed Ah isolates were essentially identical in all scenarios, with consistent differences present with respect to non-aAh isolates (Fig. 2.3). The tAh isolates was similar to the ATCC reference nucleotide sequence; however, larger dissimilarities were present in *A. sobria* and *A. veronii*. Still, nearly all gene identities exceeded 90% similarity, evincing strong intrageneric conservation of among these select genes.

Type I Fimbrial Pilus

Fimbriae genes were similar across all aAh isolates with noticeable differences found in tAh, *A. sobria*, and *A. veronii*. Analysis of the type I fimbriae revealed all *fim* components were present in tAh but *fimE* was missing from both *A. sobria*, *A. veronii*, and all aAh isolates. The *fimF* homologue was also missing from *A. veronii* (Fig. 2.4). The biological and ecological significance of the missing *fimE* gene is still unclear.

Type IV Pili Systems

The *flp* pili system was consistent (>95% homology) across all aAh isolates (Fig. 2.5); however, all four of the investigated components were absent in the fish-related tAh (AL06-06), *A. sobria*, and *A. veronii*.

Thirteen components of the mannose-sensitive hemagglutinin (*msh*) type IV pilus were investigated. This group is also known as the “bundle-forming pili” (*bfp*) in Aeromonads (Kirov et al. 1999; Boyd et al. 2008). Sequence identities were relatively stable between the two aAh haplotypes with no noticeable pattern between them (Fig. 2.6). The *mshA* gene was the most dissimilar among aAh isolates being 85.5% similar to the reference sequence. Overall, pairwise similarity was also consistent in tAh, however, *A. sobria* and *A. veronii* showed increased dissimilarity from the reference sequence. Six components were absent from the *A. veronii* isolate with 2 additional components showing <80% similarity to the reference sequence. *A. sobria* possessed all *msh* components but showed more dissimilarity in nearly all cases, compared to the aAh isolates.

The genes encoding the type IV Aeromonas pilus (*tap*) were present in all tAh and aAh isolates (Fig. 2.7). Identity similarities were relatively stable across all aAh and non-aAh isolates; however, *tapA* was absent from *A. veronii* and shared a higher similarity across all other isolates than the other 3 genes.

Flagella

Of the 5 genes examined from the polar flagellum operon, only *flaA* was present in all *A. hydrophila* isolates; *flaB*, *flaG*, *flaH*, and *flaJ* were completely absent from all aAh isolates, as well as *A. veronii* (Fig. 2.8). Interestingly, all 5 genes were present in tAh.

Quorum-sensing

Of the 5 quorum-sensing genes analyzed, very little variation was found between the two aAh haplotypes (Fig. 2.9). Typical *A. hydrophila* and *A. sobria* also showed strong similarity to the reference sequence with all five components possessing similarities of ≥90%. *A. veronii*

showed the largest deviation from the reference sequence with the highest similarity being 91.8% in the *luxS* gene, which encodes for extracellular signaling. The *ahyI*, *ahyR*, and *qseC* genes were the most dissimilar with values of 81.2%, 83.4%, and 82.6%, respectively.

Type II Secretion System

Ten genes from the type II secretion system (T2SS) were included in the analysis and revealed consistent similarities across all isolates except *A. veronii* (Fig. 2.10). *A. hydrophila* and *A. sobria* were nearly identical across all 10 genes with *gspG* being the most similar to the reference sequence for all isolates. The *gspB* gene was the most dissimilar in all isolates, including *A. veronii*. This was one of 6 T2SS genes in *A. veronii* to display similarity values of less than 90% to the reference.

Type VI Secretion System

Twenty components associated with the type VI secretion system (T6SS) were investigated, with only 4 components (*hcp2*, *tssI*, *vgrG2*, and *vgrG3*) present in all *A. hydrophila* isolates except for *A. veronii*, and these components showed similarity values $\geq 90\%$. However, the S14-452 haplotype possessed all 20 components of the T6SS, while ML09-119 haplotypes and the tAh isolate possessed only the four previously mentioned. Both haplotypes possess the genes encoding for the needle-like tip (*vgrG2* and *vgrG3*), the shaft (tail) of the “needle” (*hcp2*), a portion of the baseplate (*tssI*), but the ML09-119 haplotype is missing key components such as the contractile sheath (*tssBC*), numerous baseplate components (*tssEFGK*), a trans-membrane complex (*tssMLJ*), the plate locking to the anchor (*tssA*), ATPase-associations (*clpBV*), and transcriptional regulators (*vasAFHK*).

Toxins

This study included 11 toxin-related genes, with all nucleotide sequences consistently similar across all aAh isolates (Fig. 2.12). The *rtxA* (RTX toxin), which causes gastrointestinal diseases in humans (Suarez et al., 2012), was only present in aAh isolates but similarity did not differ between haplotypes. This toxin was also absent from both non-*A. hydrophila* species. *A. veronii* was also missing the *aerA*, *ast*, *hemolysin*, and both RTX toxin genes while *A. sobria* was missing only the two RTX genes.

Additional Virulence Factors

An additional 10 virulence-related genes were included in the analysis as they have been investigated in previous studies (Fig. 2.13). There were no notable differences in similarity values across any *A. hydrophila* isolates. One gene (*tonB-dependent receptor I*) was absent from *A. veronii* but all other genes were present in all isolates. Similarity values were similar to the reference sequence across *A. hydrophila* and *A. sobria* isolates for most genes. *A. veronii* was consistently the most dissimilar of any isolate with the *tonB*-dependent hemoglobin receptor with one version of the gene missing and the other with a similarity value of 80.6%.

Discussion and Conclusions

Several recent studies have characterized atypical *Aeromonas hydrophila* has being highly clonal (Pang et al. 2015; Rasmussen-Ivey et al. 2016; Awan et al. 2018). The results of this study indicated the clonal nature of aAh continues between the ML09-119 and S14-452 haplotype groups. Few differences in similarity were identified in the 106 genes examined. The most notable difference between the two haplotypes, is the presence of a type VI secretion system in the S14-452 group (Fig. 2.13). Rasmussen-Ivey et al. (2016) and Baumgartner et al.

(2018) showed most mandatory genes for the T6SS were present in the S14-452 haplotype while nearly all were missing from ML09-119. The results of the present study expand on this, showing additional T6SS genes are also present, while most of this system is absent from tAh, *A. sobria*, and *A. veronii* isolates. The absence of T6SS from other *Aeromonas* spp. and Ah haplotypes provides additional evidence lateral gene transfer is the likely mechanism giving rise to aAh, as suggested by Hossain et al. (2013). This work also supports reports by Awan et al. (2018), who showed variation in the presence of virulence factors in ST-251 isolates (aAh) and other Ah ST groups (tAh). Here, we investigated many of the same virulence factors with corresponding heatmaps to better understand the similarity in the different haplotypes.

It has been hypothesized the ML09-119 strain should be more efficient at evading the host immune system since it is lacking the majority of the T6SS genes (Rasmussen-Ivey et al. 2016). Comparably, a potentially functional T6SS in the S14-452 haplotype might also increase virulence. In the lab, isolates from both lineages display typical opportunistic behavior, with infection only occurring in compromised fish (Zhang et al. 2016). The two haplotypes also display similar mortality rates in the lab (Hossain et al. 2014; Rasmussen-Ivey et al. 2016), so the presence or absence of a functional T6SS does not appear to have a direct impact on pathogenicity. However, the ability for the S14-452 to utilize the T6SS to deliver effector proteins to competitors, including members of the ML09-119 haplotype, likely provide it with a competitive advantage in the environment or when co-infections occur.

Schwarz et al. (2001) commented the T6SS may be useful in protecting bacteria from simple eukaryotic cells and/or other bacteria. This may lead to increased survival of aAh belonging to the S14-452 haplotype within the host during latency. The ability to combat the host immune system may lead to long persistence at low densities within the host between outbreak

events. The T6SS has also been reported to have additional functions possibly increasing the fitness of the S14-452 group. Namely, it has been shown the T6SS can secrete effector proteins increasing the acquisition of nutrients and metals, such as iron (Wang et al. 2015; Si et al. 2017a,b). When nutrients are limited, the ability to use these effectors could also provide a competitive advantage over other organisms not possessing the T6SS. It is hypothesized that in addition to within-host survival, possessing a secretion system used to fend off simple and more complex cellular types may provide S14-452 haplotypes with increased survivability within earthen ponds. The anti-eukaryotic nature of the T6SS provides additional defenses against amoeba predation and fungi species (Hachani et al. 2016; Bayer-Santos et al. 2018; Trunk et al. 2018).

The repeat-in-toxin (Rtx) and similar operons have been identified as an important virulence factor in the environmental *A. hydrophila* type-strain, ATCC 7966 (Seshadri et al. 2006), as well as *Vibrio* spp. (Lin et al. 1999; Lee et al. 2008). The first gene of the operon (*rtxA*) codes for an exotoxin activated by proteins coded by other genes in the group. Interestingly, while *rtxA* was identified in aAh isolates, the gene was absent from tAh isolate AL06-06, which was isolated from a diseased goldfish (Tekedar et al. 2015). Before the emergence of aAh, *A. hydrophila* infections in catfish aquaculture were not considered a serious threat and the absence of *rtxA* suggests other tAh fish pathogens may be missing this virulence factor as well and could provide reasoning for the increased virulence of aAh in fish compared to the typical haplotypes. *RtxA* has been cited as having multiple functions. In *V. cholerae*, *rtxA* increased survival of the pathogen by resisting phagocytosis by the host (Lo et al. 2011) and aided in *V. cholerae* and *V. vulnificus* reaching the host bloodstream by causing apoptotic death of the intestinal epithelial cells (Kim et al. 2008; Lee et al. 2008). Peatman et al. (2018) reported catfish fed to satiation

before aAh challenge showed increased susceptibility to the disease. This suggests aAh is able to benefit from a synergistic interaction of *rtxA* and the stretched/engorged stomach and intestines of recently fed fish. Voracious feeding may cause micro-tears in the intestine and stomach, while *rtxA* increases epithelial cell death leading to an easier translocation into the bloodstream of the host. A recent study (Richardson et al. in review) showed aAh was present in low densities (approximately 100 cells) within the lower intestine of approximately 10% of catfish from seemingly healthy ponds (i.e. no overt signs of disease, normal feeding, etc.). If the pathogen is already present within the host, this could also increase the likelihood of it taking advantage of any available route to the bloodstream.

From 2013 to 2017, the S14-452 group completely supplanted the ML09-119 haplotype in the Mississippi Delta. This pattern may also be occurring in East Mississippi and West Alabama, although more recent isolates are needed from these locations to validate these claims. This haplotype shift raises many intriguing questions, particularly, what selective pressures allow the S14-452 group to outcompete the ML09-119 strain. The data presented here may provide some important clues to the proliferation of this aAh haplotype.

Unfortunately, the sample size of case data was too small to make concrete determinations of the increased likelihood of an aAh outbreak when an outbreak occurred in the previous year. The data shows a potentially higher risk of an aAh outbreak in ponds with a history of previous outbreaks; however, the large confidence interval ($p=0.145$) showed no statistically significant change. Additional data is needed to determine whether aAh outbreaks are more likely to occur in ponds with previous outbreaks. The confirmation of this increased risk has significant management implications, as it suggests aAh remains in the pond system for an extended time and may over-winter there. Cai et al. (2019) showed *Aeromonas* sp. densities in

biofilms and sediments of catfish ponds increased throughout the production season, particularly after August. The late summer and early fall are critical periods during production as water temperatures, fish size, and feeding rates typically peak and farmers prepare to harvest fish and stock new fingerlings. Additionally, Cai and Arias (2017) showed *A. hydrophila* can easily adhere to and colonize a range of substrates such as polyethylene liners, PVC, and nylon. All these materials are commonplace in catfish aquaculture suggesting the ability to easily translocate the *A. hydrophila* pathogen among ponds and farm operations.

Calcium (Ca^{2+}) has also been shown to significantly increased biofilm formation of both tAh and aAh strains, though tAh showed a stronger effect (Cai and Arias 2017). Biofilms serve as a mechanism in which the *A. hydrophila* bacterium can alter the environment to increase survival. The ability to sustain life in a sessile fashion reduces external factors (Van Acker et al. 2014). To date, the exact reservoir of aAh in catfish aquaculture is still unknown. Recent work (Richardson et al. in review) has shown asymptomatic carrier fish can harbor the pathogen for extended periods in a pond at low concentrations. However, another mechanism may be the formation of biofilms on the sediments, vegetation, dissolved oxygen (DO) probes, etc. within the ponds. These biofilms likely also increase the resistance to disinfectants and antibiotics (Jahid and Ha 2014); thus, they may show decreased susceptibility to foodborne antibiotics (i.e. flurofenicol) leeching from uneaten feed pellets during fish treatment. The presence of *flp* genes in the aAh genome may partially explain the increased virulence compared to tAh isolates collected from fish hosts (e.g. AL06-06). The ability to form pili structures likely increases biofilm formation in aAh making it more resistant to stressors and increasing survival within the environment and/or the fish host.

Table 2.1 List of isolates used. Lab indicates which lab originally received the case submission and cultured the isolate occurred. Isolates marked with asterisks (*) are the type-strain isolates for the two haplotypes of atypical *A. hydrophila*. Strains listed as tAh are typical (non ST-251) *A. hydrophila*.

Isolate	Lab	Year	Strain	Isolate	Lab	Year	Strain
*ML09-119	Auburn	2009	ML09-119	A18-035	MSU	2018	tAh
*S14-452	NWAC	2014	S14-452	A18-160	MSU	2018	S14-452
ALG10-167	Auburn	2010	ML09-119	A18-117	MSU	2018	S14-452
ALG10-197	Auburn	2010	<i>A. veronii</i>	A18-071	MSU	2018	tAh
ML10-115 F2	Auburn	2010	ML09-119	A18-198	MSU	2018	S14-452
ALG10-160 F1	Auburn	2010	ML09-119	A18-115	MSU	2018	S14-452
ML10-113	Auburn	2010	ML09-119	A18-180-1	MSU	2018	S14-452
ML10-115 F3	Auburn	2010	ML09-119	A18-165	MSU	2018	S14-452
ML10-052	Auburn	2010	ML09-119	A18-189	MSU	2018	S14-452
ALG10-064-2	Auburn	2010	ML09-119	A18-063-1	MSU	2018	tAh
ALG10-064	Auburn	2010	ML09-119	A18-118	MSU	2018	S14-452
ML10-191 F1	Auburn	2010	ML09-119	A18-202	MSU	2018	tAh
ALG10-123	Auburn	2010	ML09-119	A18-116	MSU	2018	S14-452
ALG10-196	Auburn	2010	<i>A. veronii</i>	A18-126	MSU	2018	S14-452

Table 2.1 (continued)

Isolate	Lab	Year	Strain	Isolate	Lab	Year	Strain
ALG10-144	Auburn	2010	ML09-119	A18-213	MSU	2018	S14-452
ALG10-161 F1	Auburn	2010	ML09-119	A18-014	MSU	2018	S14-452
ALG10-161 F2	Auburn	2010	ML09-119	A18-170-1	MSU	2018	S14-452
ALG10-194 F2	Auburn	2010	tAh	A18-093	MSU	2018	S14-452
ALG10-126	Auburn	2010	tAh	A18-162	MSU	2018	S14-452
ALG10-140	Auburn	2010	ML09-119	A18-181	MSU	2018	S14-452
ALG10-163 F2	Auburn	2010	ML09-119	A18-141	MSU	2018	S14-452
ALG10-064	Auburn	2010	ML09-119	A18-142	MSU	2018	S14-452
ALG10-064-1	Auburn	2010	ML09-119	S13-597	NWAC	2013	ML09-119
ML12-061	Auburn	2012	ML09-119	S13-612A	NWAC	2013	ML09-119
ML12-069	Auburn	2012	ML09-119	S13-612B	NWAC	2013	ML09-119
ML12-063	Auburn	2012	ML09-119	S13-613A	NWAC	2013	ML09-119
ML12-062	Auburn	2012	ML09-119	S13-613B	NWAC	2013	ML09-119
ML12-076	Auburn	2012	ML09-119	S13-614A	NWAC	2013	ML09-119
IRPS15-28	Auburn	2015	ML09-119	S13-614B	NWAC	2013	ML09-119

Table 2.1 (continued)

Isolate	Lab	Year	Strain	Isolate	Lab	Year	Strain
IPRS15-009A	Auburn	2015	ML09-119	S13-615A	NWAC	2013	ML09-119
ML15-159 B1	Auburn	2015	ML09-119	S13-615B	NWAC	2013	ML09-119
IPRS15-30	Auburn	2015	ML09-119	S13-615C	NWAC	2013	ML09-119
IPRS15-034	Auburn	2015	ML09-119	S13-633	NWAC	2013	ML09-119
IPRS15-031	Auburn	2015	ML09-119	S13-634	NWAC	2013	ML09-119
AL15-079	Auburn	2015	ML09-119	S13-656	NWAC	2013	ML09-119
ML15-022-1630	Auburn	2015	ML09-119	S13-657	NWAC	2013	ML09-119
C16-00231	MSU	2016	S14-452	S13-658	NWAC	2013	ML09-119
C16-12824-1	MSU	2016	S14-452	S13-660	NWAC	2013	ML09-119
C16-12825	MSU	2016	S14-452	S13-700	NWAC	2013	ML09-119
C16-12827	MSU	2016	S14-452	S14-230	NWAC	2014	tAh
C16-13322	MSU	2016	S14-452	S14-296	NWAC	2014	ML09-119
C16-13421-1	MSU	2016	S14-452	S14-448A	NWAC	2014	ML09-119
C16-13422-1	MSU	2016	ML09-119	S14-448B	NWAC	2014	ML09-119
C16-13424-1	MSU	2016	ML09-119	S14-451	NWAC	2014	S14-452

Table 2.1 (continued)

Isolate	Lab	Year	Strain	Isolate	Lab	Year	Strain
C16-13426-1	MSU	2016	tAh	S14-455	NWAC	2014	S14-452
C16-13569	MSU	2016	S14-452	S14-458	NWAC	2014	S14-452
C16-13688	MSU	2016	ML09-119	S14-533	NWAC	2014	ML09-119
C16-13689	MSU	2016	S14-452	S14-603	NWAC	2014	ML09-119
C16-13690	MSU	2016	S14-452	S14-604	NWAC	2014	ML09-119
C16-13760	MSU	2016	S14-452	S14-605	NWAC	2014	ML09-119
C16-13763	MSU	2016	S14-452	S14-606	NWAC	2014	ML09-119
C16-14080A	MSU	2016	S14-452	S14-699	NWAC	2014	ML09-119
C16-14080B	MSU	2016	S14-452	PB15-921-1	NWAC	2015	ML09-119
C16-14082	MSU	2016	S14-452	PB15-921-2	NWAC	2015	ML09-119
C16-14202	MSU	2016	S14-452	S15-016	NWAC	2015	S14-452
C16-14204	MSU	2016	S14-452	S15-130	NWAC	2015	S14-452
C16-14297	MSU	2016	S14-452	S15-246	NWAC	2015	S14-452
C16-14375	MSU	2016	S14-452	S15-247	NWAC	2015	S14-452
C16-14530	MSU	2016	ML09-119	S15-265	NWAC	2015	S14-452

Table 2.1 (continued)

Isolate	Lab	Year	Strain	Isolate	Lab	Year	Strain
C16-14930A	MSU	2016	S14-452	S15-266A	NWAC	2015	S14-452
C16-14930B	MSU	2016	ML09-119	S15-266B	NWAC	2015	S14-452
C16-14959	MSU	2016	S14-452	S15-267	NWAC	2015	S14-452
C16-14961	MSU	2016	S14-452	S15-268	NWAC	2015	S14-452
C16-15077	MSU	2016	ML09-119	S15-269	NWAC	2015	ML09-119
C16-15148	MSU	2016	S14-452	S15-272	NWAC	2015	S14-452
C16-15175A	MSU	2016	S14-452	S15-295	NWAC	2015	ML09-119
C16-15175B	MSU	2016	ML09-119	S15-308	NWAC	2015	S14-452
C16-15207	MSU	2016	tAh	S15-309	NWAC	2015	S14-452
C16-15245	MSU	2016	S14-452	S15-400	NWAC	2015	S14-452
C16-16046	MSU	2016	ML09-119	S15-401	NWAC	2015	S14-452
C16-16047-1	MSU	2016	ML09-119	S15-451	NWAC	2015	S14-452
C16-16153-1	MSU	2016	S14-452	S15-452	NWAC	2015	S14-452
C16-16154	MSU	2016	S14-452	S15-591A	NWAC	2015	S14-452
C16-16432B	MSU	2016	S14-452	S15-591B	NWAC	2015	S14-452

Table 2.1 (continued)

Isolate	Lab	Year	Strain	Isolate	Lab	Year	Strain
C16-16434A	MSU	2016	S14-452	S16-004	NWAC	2016	S14-452
C16-16581	MSU	2016	S14-452	S16-070	NWAC	2016	S14-452
C16-16582	MSU	2016	S14-452	S16-219A	NWAC	2016	S14-452
C16-16748	MSU	2016	S14-452	S16-219B	NWAC	2016	S14-452
C16-16952	MSU	2016	S14-452	S16-220A	NWAC	2016	S14-452
C16-17033	MSU	2016	S14-452	S16-220B	NWAC	2016	S14-452
C16-17034	MSU	2016	S14-452	S16-229	NWAC	2016	S14-452
C16-17064	MSU	2016	S14-452	S16-232	NWAC	2016	S14-452
C16-17538	MSU	2016	ML09-119	S16-345	NWAC	2016	tAh
C16-17585	MSU	2016	S14-452	S16-346	NWAC	2016	tAh
C16-17588	MSU	2016	S14-452	S16-349	NWAC	2016	S14-452
C16-17589	MSU	2016	tAh	S16-367	NWAC	2016	S14-452
C16-17637A	MSU	2016	ML09-119	S16-415	NWAC	2016	S14-452
C16-17637B	MSU	2016	S14-452	S16-456	NWAC	2016	S14-452
C16-17638	MSU	2016	S14-452	S16-535	NWAC	2016	S14-452

Table 2.1 (continued)

Isolate	Lab	Year	Strain	Isolate	Lab	Year	Strain
C16-17734	MSU	2016	S14-452	S16-539A	NWAC	2016	S14-452
C16-17830	MSU	2016	S14-452	S16-539B	NWAC	2016	S14-452
C16-18206-1	MSU	2016	S14-452	S16-546	NWAC	2016	ML09-119
C16-18254	MSU	2016	S14-452	S16-547	NWAC	2016	ML09-119
C16-18256	MSU	2016	S14-452	S16-548	NWAC	2016	tAh
C16-18316	MSU	2016	S14-452	S16-549	NWAC	2016	tAh
C16-18317	MSU	2016	S14-452	S16-704	NWAC	2016	S14-452
C16-18324	MSU	2016	S14-452	S17-131	NWAC	2017	S14-452
C16-19094	MSU	2016	S14-452	S17-151	NWAC	2017	S14-452
C16-19100	MSU	2016	S14-452	S17-177	NWAC	2017	S14-452
C16-19102	MSU	2016	S14-452	S17-196	NWAC	2017	S14-452
C16-19147	MSU	2016	S14-452	S17-221	NWAC	2017	S14-452
C16-19712	MSU	2016	S14-452	S17-278	NWAC	2017	S14-452
C16-19713	MSU	2016	S14-452	S17-286	NWAC	2017	S14-452
C16-19755	MSU	2016	S14-452	S17-293	NWAC	2017	S14-452

Table 2.1 (continued)

Isolate	Lab	Year	Strain	Isolate	Lab	Year	Strain
C16-20267	MSU	2016	S14-452	S17-299	NWAC	2017	S14-452
C16-20657	MSU	2016	S14-452	S17-343	NWAC	2017	S14-452
A18-190	MSU	2018	S14-452	S17-344	NWAC	2017	S14-452
A18-092	MSU	2018	S14-452	S17-380	NWAC	2017	S14-452
A18-139	MSU	2018	S14-452	S17-401	NWAC	2017	S14-452
A18-126-2	MSU	2018	S14-452	S17-406	NWAC	2017	S14-452
A18-201	MSU	2018	tAh	S17-494	NWAC	2017	S14-452
A18-136	MSU	2018	S14-452	S17-859	NWAC	2017	S14-452
A18-189	MSU	2018	S14-452	S17-886	NWAC	2017	S14-452
A18-166	MSU	2018	S14-452	S17-888	NWAC	2017	S14-452
A18-179-1	MSU	2018	S14-452	S18-167	NWAC	2018	A. sobria
A18-126	MSU	2018	S14-452	S18-316	NWAC	2018	A. sobria
A18-128	MSU	2018	S14-452	S18-331	NWAC	2018	S14-452
A18-206	MSU	2018	S14-452	S18-400	NWAC	2018	S14-452
A18-088-2	MSU	2018	tAh	S18-404	NWAC	2018	S14-452

Table 2.1 (continued)

Isolate	Lab	Year	Strain	Isolate	Lab	Year	Strain
A18-096	MSU	2018	ML09-119	S18-567	NWAC	2018	S14-452
A18-157	MSU	2018	S14-452	S18-568	NWAC	2018	S14-452
A18-197	MSU	2018	S14-452	S18-569	NWAC	2018	S14-452
A18-163	MSU	2018	S14-452	S18-570	NWAC	2018	S14-452
A18-135	MSU	2018	S14-452	S18-571	NWAC	2018	S14-452
A18-186	MSU	2018	S14-452	S18-607	NWAC	2018	S14-452
A18-140	MSU	2018	S14-452	S18-641	NWAC	2018	S14-452

Table 2.2 Primer sequences validated by Griffin et al. (2013) and used for identifying atypical *Aeromonas hydrophila* (aAh) via polymerase chain reaction (PCR). T_m is the melting temperature of each primer

PCR Primer	Sequence (5'-3')	T_m (°C)
ML09-119F	GTTCCGTTCCATCTGTTCGTGA	62.7
ML09-119R	CAACCATCTGGTCGCAATC	60.4
S14-452F	CAGAACGTGCTGCAGAGATTGA	62.7
S14-452R	TCCGAGAATTGATGACGAAGG	62.7
<i>gyrB</i> 3F	TCCGGCGGTCTGCACGGCGT	
<i>gyrB</i> 14R	TTGTCCGGGTTGTACTCGTC	
16S 27F	AGAGTTTGATCCTGGCTCAG	
16S 1492R	GGTTACCTTGTACGACTT	
16S 1525R	AAGGAGGTGATCCAGCC	

Table 2.3 Temporal outbreak incidence of 2 cooperating catfish aquaculture farms from 2010-2017. Incidences indicate individual pond outbreaks of atypical *Aeromonas hydrophila* (aAh) (top) or any record of clinical disease (bottom). Contingency tables place aAh outbreaks in current production year along top and outbreaks in previous production year along the side

		Current aAh outbreak		$p = 0.145$
		Yes	No	
Previous aAh outbreak	Yes	1	4	
	No	2	46	

Table 2.4 Number of isolates provided by each diagnostic lab, separated by year. Data excludes the type-strain isolates for the ML09-119 and S14-452 haplotypes.

	NWAC	MSU	Auburn
2009		1	
2010			21
2011			
2012			5
2013	17		
2014	14		
2015	22		8
2016	22	70	
2017	18		
2018	12	42	
Total	105	113	34

Table 2.5 Metadata for the 108 genes examined. *Group* denotes general association between genes. *Gene Locus* is the coding region within the ATCC 7966 isolate (Accession #: CP000462).

Group	Gene	Gene Locus	Product/Function
Flagella	flaA	1858995-1859901	flagellin
	flaB	1860482-1861387	flagellin
	flaG	1861426-1861862	filament length control
	flaH	1861902-1863292	HAP2
	flaJ	1863328-1863750	chaperone DNA topoisomerase (ATP-
Housekeeping	gyrB	3883-6294	hydrolyzing) subunit B
	groL	924310-925944	chaperonin groEL
	gltA	2098162-2099448	citrate synthase
	metG	2464976-2467009	methionine--tRNA ligase
	ppsA	3005995-3008373	phosphoenolpyruvate synthase
	recA	4147646-4148710	recombinase

Table 2.5 (continued)

Group	Gene	Gene Locus	Product/Function
Misc. Virulence Factors	gyrA	2576258-2579005	DNA topoisomerase (ATP-hydrolyzing) subunit A
	atpD	4718188-4719576	F0F1 ATP synthase subunit beta
	dnaJ	3356344-3357486	molecular chaperone
	dnaK	3357741-3359669	molecular chaperone
	mdh	707075-708010	malate dehydrogenase
	radA	4108941-4110305	DNA repair protein
	rpoB	4466890-4470918	DNA-directed RNA polymerase subunit beta
	rpoD	895108-896973	RNA polymerase sigma factor
	tsf	1272267-1273148	elongation factor Ts
	zipA	1337458-1338570	cell division protein
	eprAI	3047455-3049246	extracellular protease
	iron uptake regulator	1677303-1677731	iron uptake

Table 2.5 (continued)

Group	Gene	Gene Locus	Product/Function
Quorum-sensing	galE	4547328-4548341	UDP-galactose-4-epimerase protein
	tonB dependent receptor 1	2161351-2163324	tonB-dependent receptor
	tonB dependent receptor 2	3861765-3864320	tonB-dependent receptor
	Phospholipase C	115445-117501	phospholipid cleavage
	Phospholipase A	4472317-4473018	phospholipase A glucose inhibited division protein A,
	gidA	4727222-4729111	cell division, gene regulator glucose inhibited division protein B,
	gidB	4726575-4727201	cell division
	eno	882795-884486	phosphopyruvate hydratase
	elastase	913816-914355	elastase
	dam	3597382-3598254	DNA adenine methyltransferase
Quorum-sensing	qseB	3638429-3639118	response regulator
	qseC	3639115-3640554	sensor histidine kinase

Table 2.5 (continued)

Group	Gene	Gene Locus	Product/Function
Type II Secretion System	luxS	748411-748920	luxS
	ahyR	591318-592103	transctional activator
	ahyI	590632-591255	autoinducer synthase
Type II Secretion System			
(T2SS)	gspB	4214412-4215095	localization/assembly complex
	gspD	603731-605764	channel-/pore-forming protein
	gspE	605764-607269	ATP binding and hydrolysis
	gspF	607272-608487	IM platform complex
	gspG	608607-609038	pseudopilus
	gspH	609213-609753	pseudopilin
	gspI	609751-610109	pseudopilin
	gspJ	610194-610805	pseudopilin
	gspK	610897-611922	pseudopilin
	gspN	613776-614531	transporter protein

Table 2.5 (continued)

Group	Gene	Gene Locus	Product/Function
	ascR	1511877-1511948	inner membrane ring complex
Type VI Secretion System			
(T6SS)	VgrG2	1212752-1214648	T6SS tip protein vgrG
	hcp2	1211755-1212273	hcp-2 hemolysin-coregulated protein
			ATPase-associate (many cellular
	clpB	2007876-2010518	activities)
	vasH	2010521-2012059	transcriptional regulator
			accessory protein for translocation of
	vasK	2014151-2017636	effector into eukaryotic cell
			accessory protein for translocation of
	vasF	2007145-2007855	effector into eukaryotic cell
	vasA	2001166-2002932	virulence-associated secretion
	VgrG3	2019669-2021679	effector protein of T6SS
	tssI	1212752-1215535	T6SS tip protein vgrG

Table 2.5 (continued)

Group	Gene	Gene Locus	Product/Function
	tssC	1870227-1871198	T6SS contractile sheath
	tssE	2000731-2001162	T6SS baseplate subunit
	tssG/F	2002897-2003894	T6SS baseplate subunit
	tssK	2005719-2007053	T6SS baseplate subunit
	tssL/dotU	2007145-2007855	dotU family T4SS/T6SS protein
	tssH	2007876-2010450	T6SS ATPase
	tagO	2010521-2012059	T6SS-associated protein
	tssA	2012673-2014109	T6SS protein
	tssM	2014151-2017636	T6SS membrane subunit
	lysozyme	2000731-2001162	lysozyme
	tssJ	2003951-2005201	T6SS membrane subunit
	tagH	2005201-2005716	ATP-binding protein
	tagA	1058502-1060880	toxR-regulated lipoprotein

Table 2.5 (continued)

Group	Gene	Gene Locus	Product/Function
Toxins			beta-barrel pore-forming toxin
	aerA	466510-467991	aerolysin
	alt	116473-117573	cytotoxic enterotoxin gene
			alkyl hydroperoxide reductase subunit
	ahpF	1894849-1896429	F
	ahpC	1896523-1897089	peroxiredoxin
			3-phosphohikimate 1-
	aroA	2172785-2174068	carboxyvinlytransferase
	rtxA	1479789-1493846	RTX holotoxin
	hylB	1606672-1607775	hyaluronidase, putative
	hemolysin III	3932893-3933524	hemolysin
	ast	861793-863439	thermostable cytotoxic enterotoxin
	ahh1	1652272-1654137	hemolysin
	act	467288-467687	cytotoxic enterotoxin

Table 2.5 (continued)

Group	Gene	Gene Locus	Product/Function
Type I Fimbriae	fimA	552789-553331	type I fimbrial protein
	fimB	553358-553820	type I fimbrial protein
	fimC	553888-556422	fimbrial assembly protein
	fimD	556433-557149	molecular chaperone
	fimE	557618-558203	fimbrial protein
	fimF	558215-558766	fimbrial protein
Type IV Pilus	tapA	4297901-4298001	type IV prepilin
	tapB	4298386-4300092	pilus biogenesis
	tapC	4300208-4301434	pilus biogenesis
			type IV prepilin
	tapD	4301496-4302344	peptidase/methyltransferase
	flpL	1594459-1595841	pilus assembly
	flpK	1593952-1594458	pilus assembly
	flpJ	1593515-1593955	pilus assembly

Table 2.5 (continued)

Group	Gene	Gene Locus	Product/Function
	flpD	1587934-1588482	pilus assembly
	mshA	415673-416051	msha biogenesis
	mshB	414987-415658	msha biogenesis
	mshI	404926-405776	msha biogenesis
	mshI-1	405890-406483	msha biogenesis
	mshJ	406483-407130	msha biogenesis
	mshK	407123-407449	msha biogenesis
	mshL	407520-409193	msha biogenesis
	mshM	409271-410161	msha biogenesis
	mshC	416165-416649	msha biogenesis
	mshD	416636-417199	msha biogenesis
	mshO	417199-418020	msha biogenesis
	mshP	418010-418480	msha biogenesis
	mshQ	418480-421396	msha biogenesis

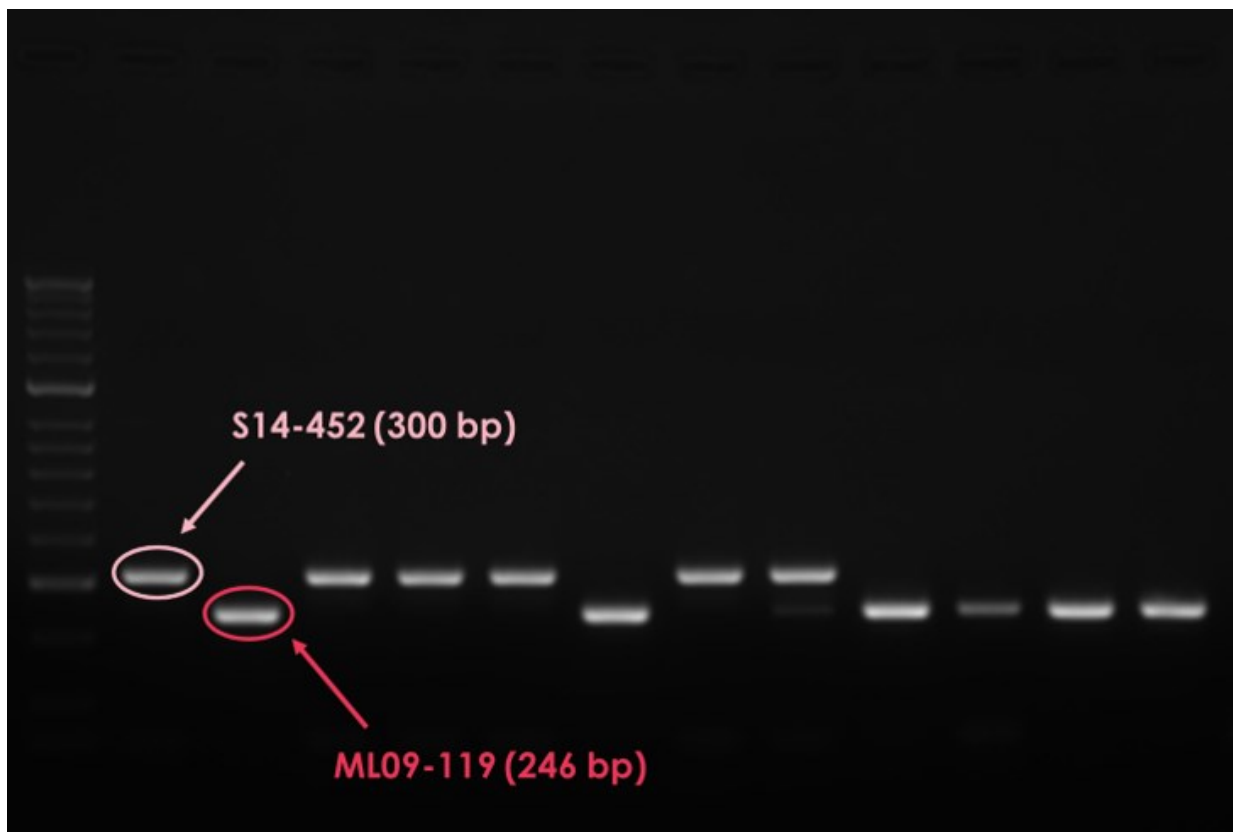


Figure 2.1 Electrophoresis gel showing the polymerase-chain reaction (PCR) product bands displayed by the S14-452 and ML09-119 haplotypes.

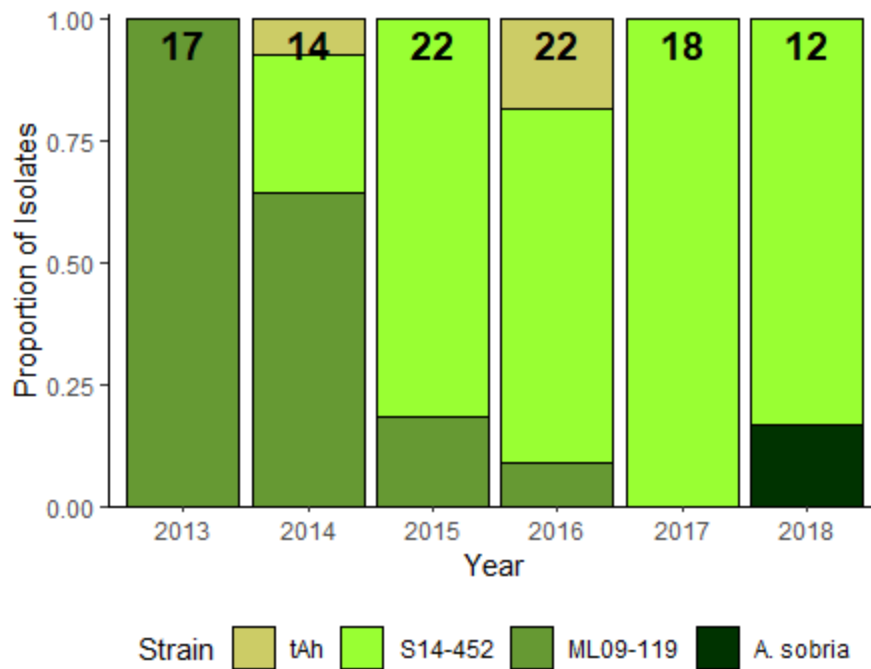


Figure 2.2 Stacked bar plot showing temporal shift from ML09-119 haplotype to S14-452 haplotype from 2013 to 2018 in the Mississippi Delta region. Data based on diagnostic case submissions from the Thad Cochran National Warmwater Research Center diagnostic lab. Numbers at the top of each column indicate total number of cases included for that year.

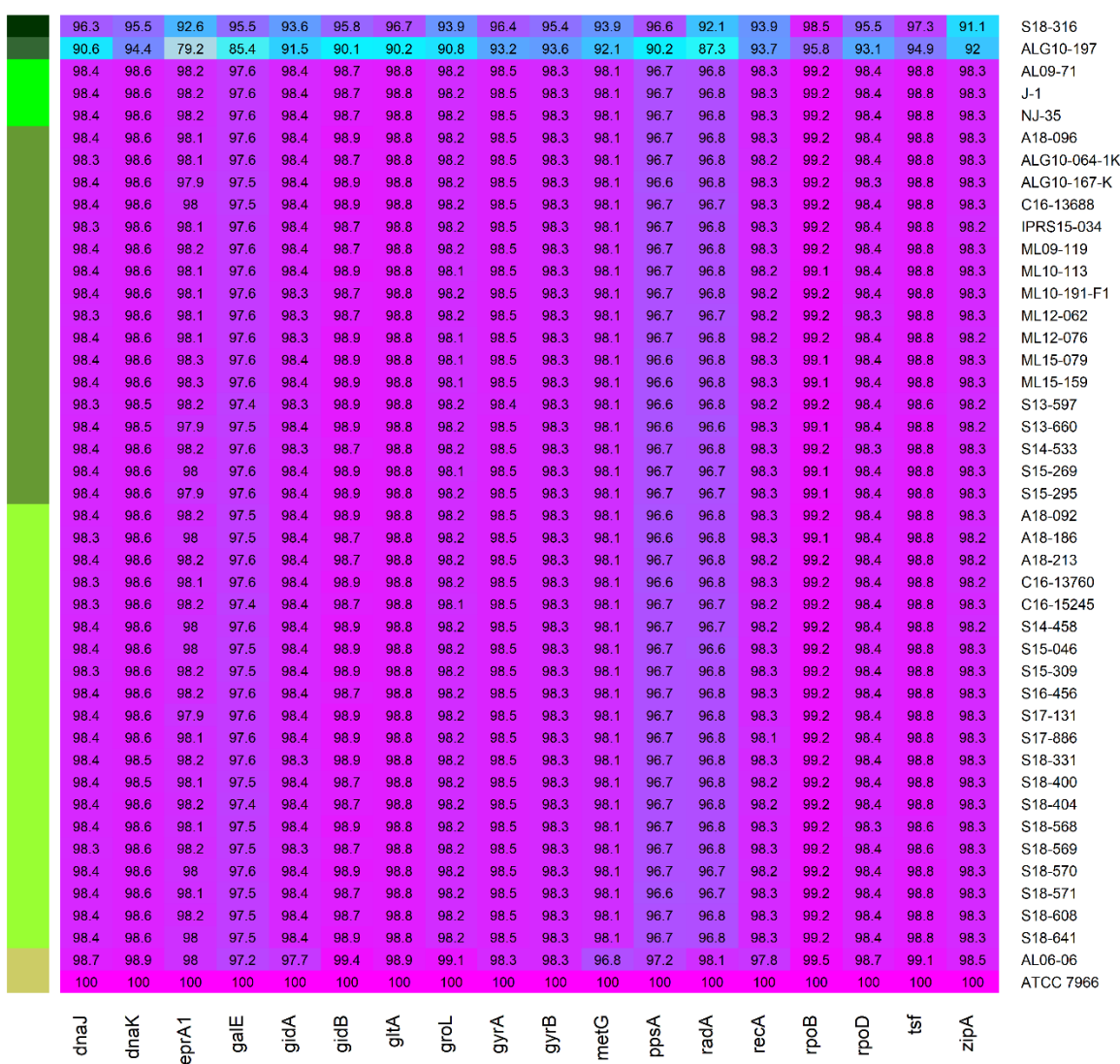


Figure 2.3 Heatmap showing nucleotide sequence identity similarity of housekeeping genes in *Aeromonas* spp. Individual genes are located on the x-axis with each isolate located along the left y-axis. “aAh” and “tAh” designate reference atypical and typical *A. hydrophila* strains, respectively, acquired from the NCBI database. Green-scale bar along left axis denotes *Aeromonas* species or *Aeromonas hydrophila* strain; groups, in descending order, are: *A. sobria*, *A. veronii*, reference aAh, ML09-119, S14-452, and reference tAh.

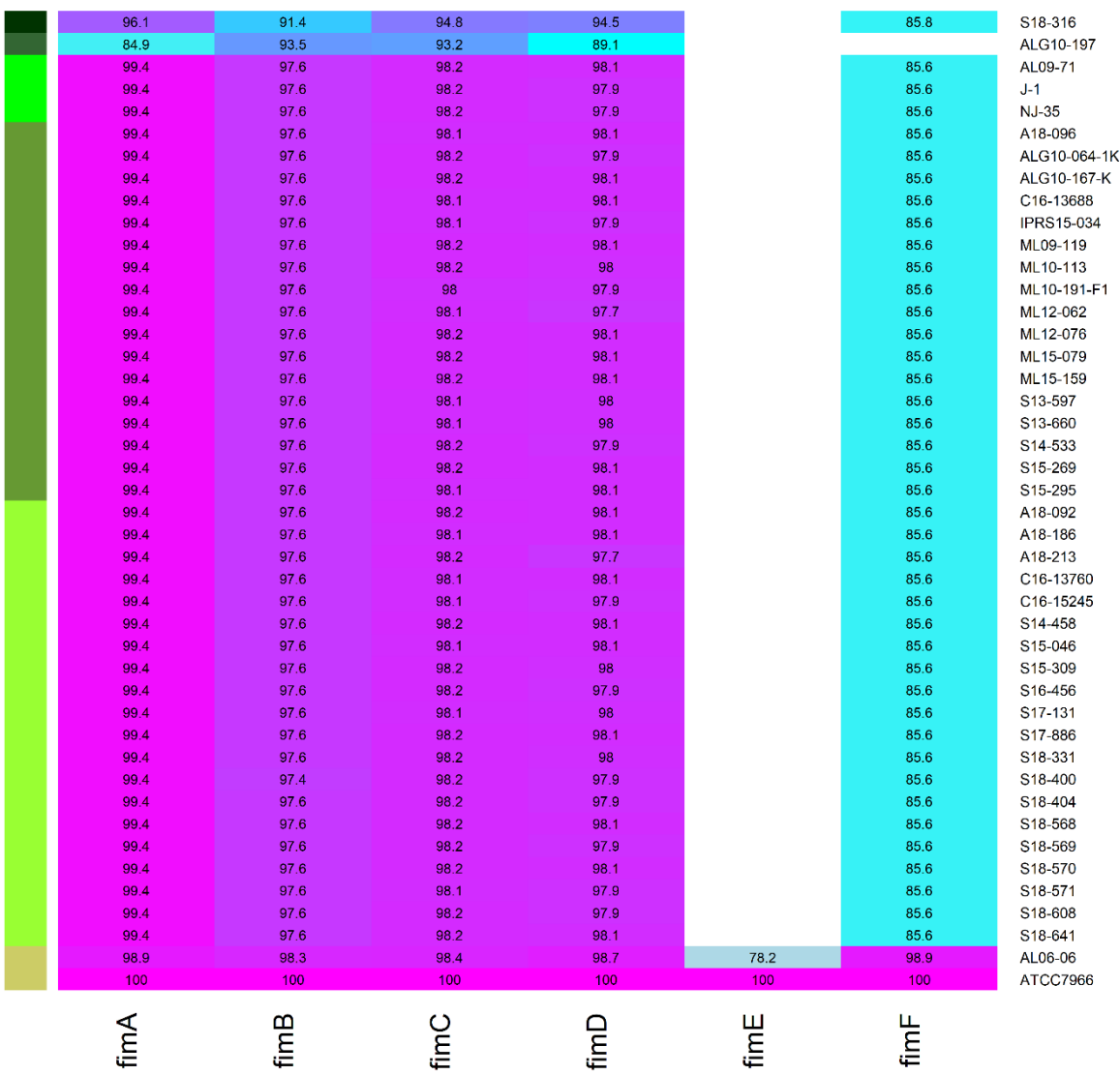


Figure 2.4 Heatmap showing nucleotide sequence identity similarity of type I fimbrial (*fim*) genes in *Aeromonas* spp. Individual genes are located on the x-axis with each isolate located along the left y-axis. “aAh” and “tAh” designate reference atypical and typical *A. hydrophila* strains, respectively, acquired from the NCBI database. Green-scale bar along left axis denotes *Aeromonas* species or *Aeromonas hydrophila* strain; groups, in descending order, are: *A. sobria*, *A. veronii*, reference aAh, ML09-119, S14-452, and reference tAh.

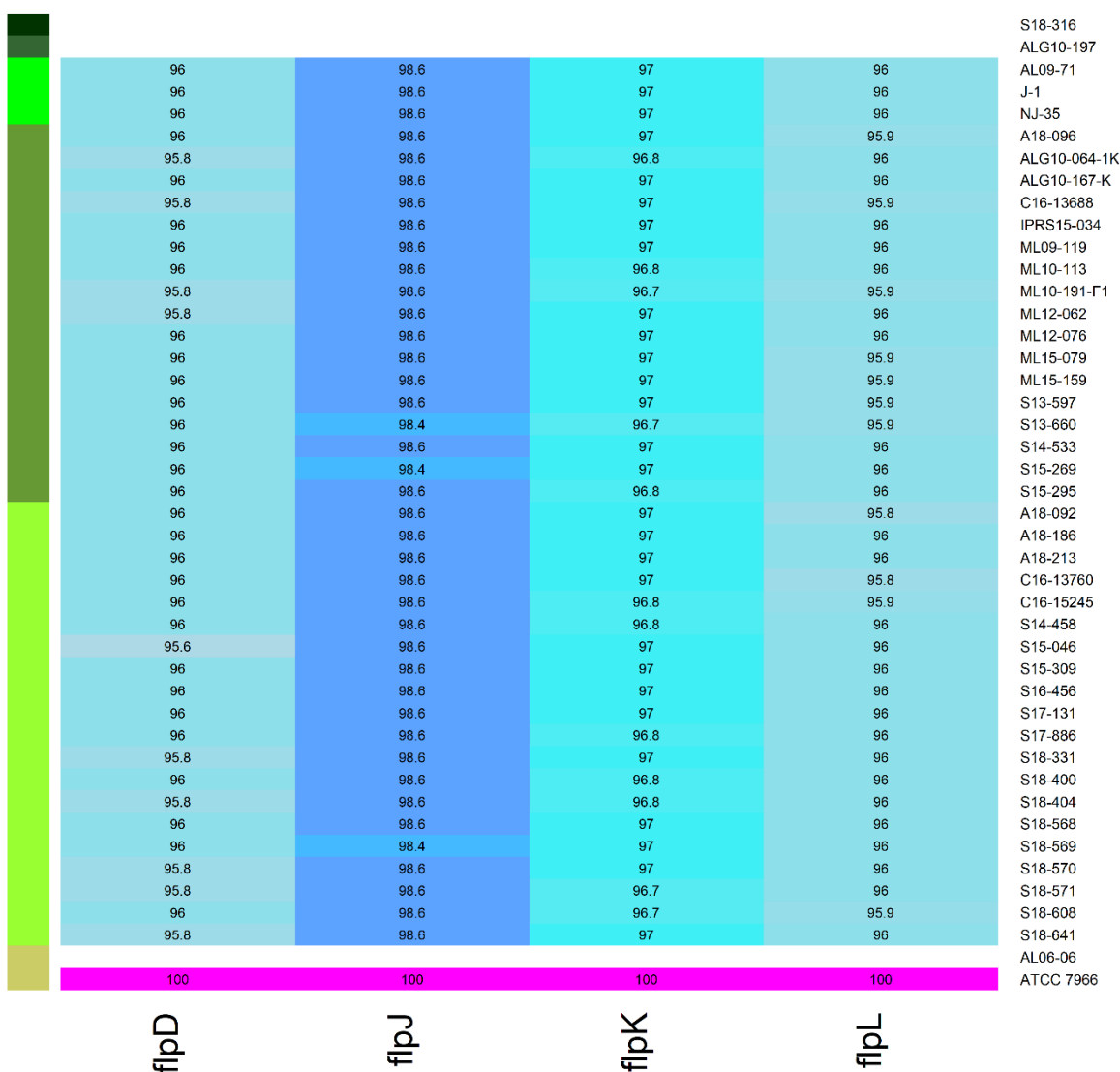


Figure 2.5 Heatmap showing nucleotide sequence identity similarity of type IV pilus (*fip*) genes in *Aeromonas* spp. Individual genes are located on the x-axis with each isolate located along the left y-axis. “aAh” and “tAh” designate reference atypical and typical *A. hydrophila* strains, respectively, acquired from the NCBI database. Green-scale bar along left axis denotes *Aeromonas* species or *Aeromonas hydrophila* strain; groups, in descending order, are: *A. sobria*, *A. veronii*, reference aAh, ML09-119, S14-452, and reference tAh.

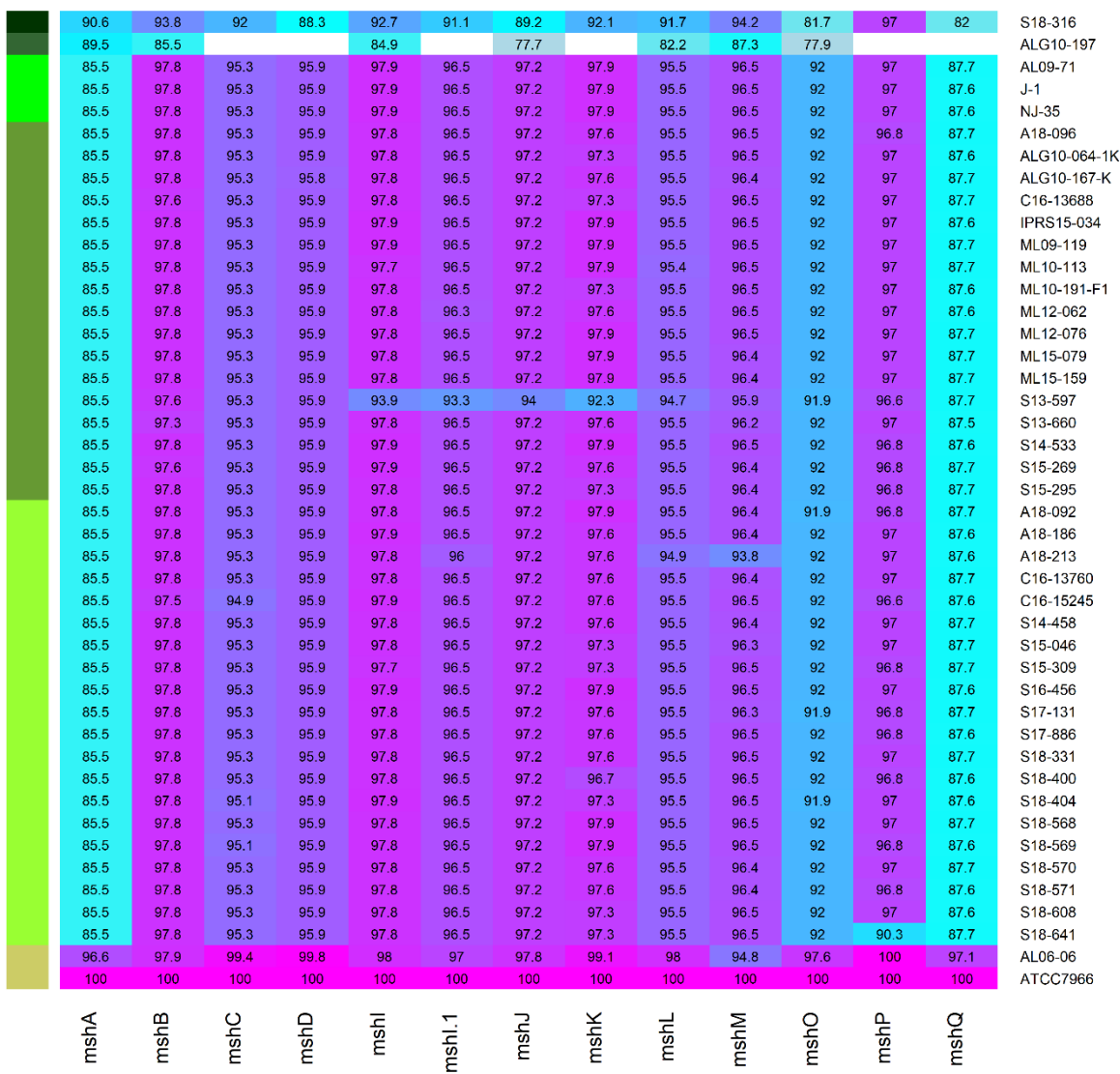


Figure 2.6 Heatmap showing nucleotide sequence identity similarity of type IV pilus (*msh*) genes in *Aeromonas* spp. Individual genes are located on the x-axis with each isolate located along the left y-axis. “aAh” and “tAh” designate reference atypical and typical *A. hydrophila* strains, respectively, acquired from the NCBI database. Green-scale bar along left axis denotes *Aeromonas* species or *Aeromonas hydrophila* strain; groups, in descending order, are: *A. sobria*, *A. veronii*, reference aAh, ML09-119, S14-452, and reference tAh.

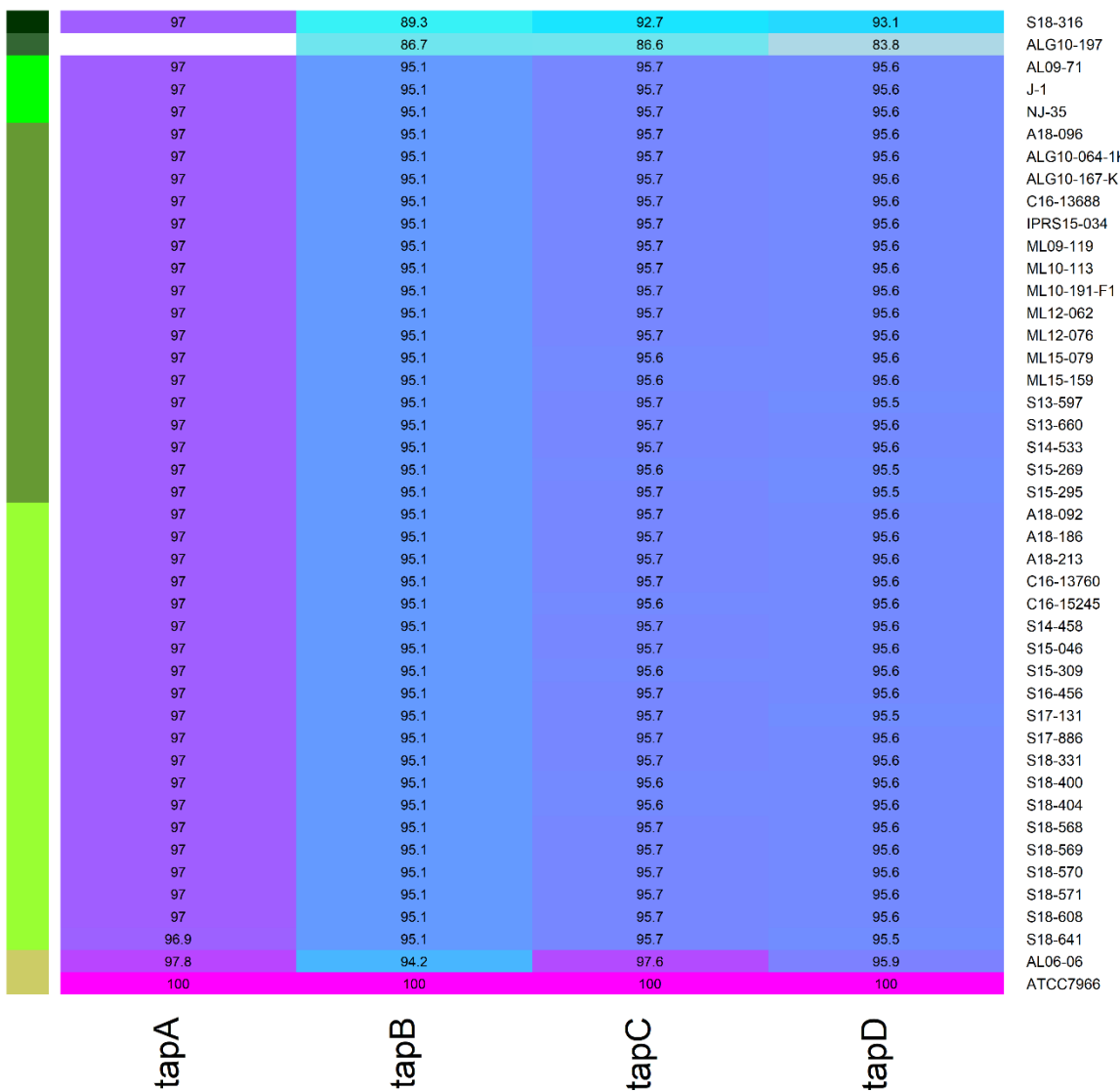


Figure 2.7 Heatmap showing nucleotide sequence identity similarity of the type IV pilus systems (*tap*) genes in *Aeromonas* spp. Individual genes are located on the x-axis with each isolate located along the left y-axis. “aAh” and “tAh” designate reference atypical and typical *A. hydrophila* strains, respectively, acquired from the NCBI database. Green-scale bar along left axis denotes *Aeromonas* species or *Aeromonas hydrophila* strain; groups, in descending order, are: *A. sobria*, *A. veronii*, reference aAh, ML09-119, S14-452, and reference tAh.

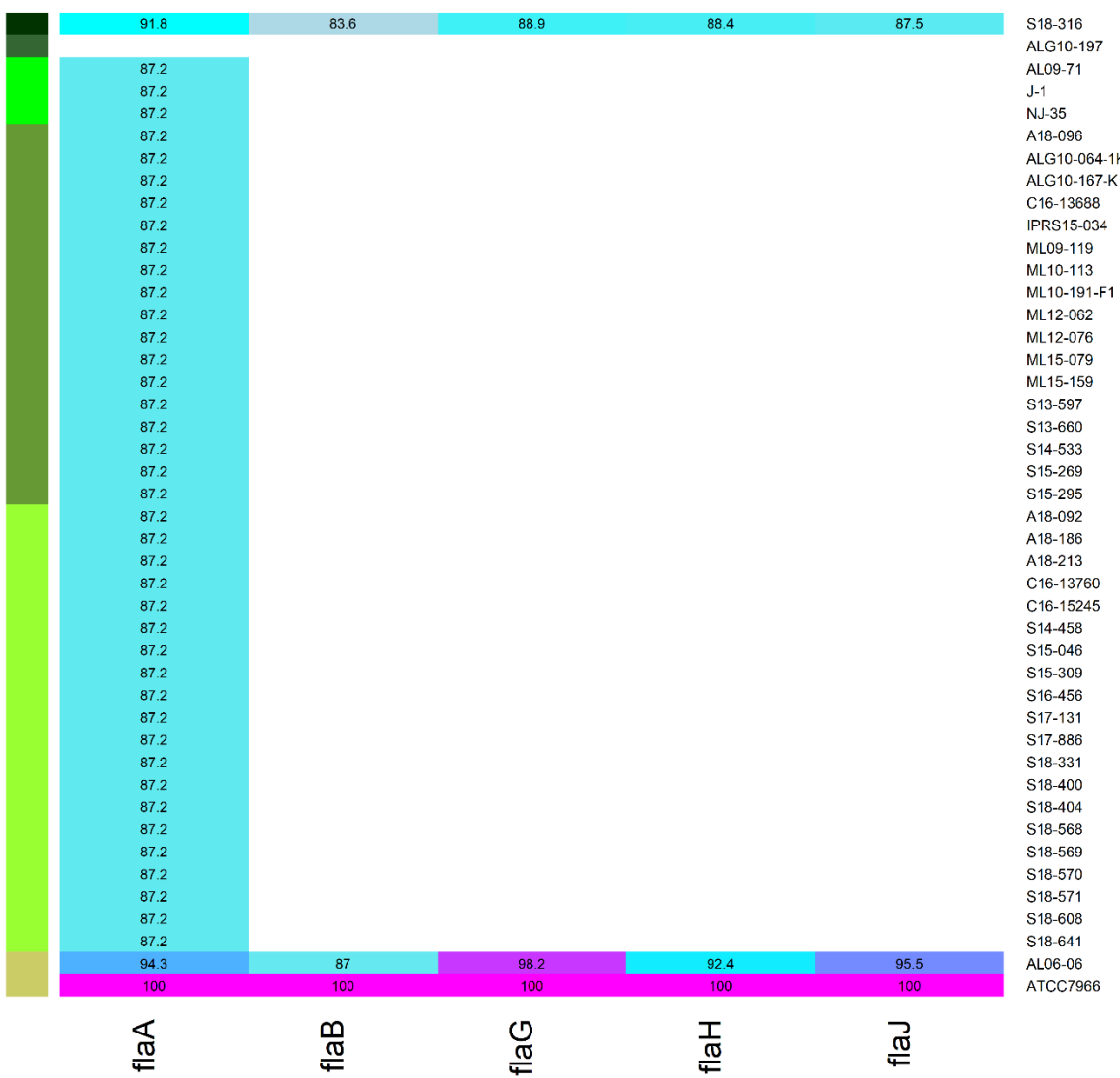


Figure 2.8 Heatmap showing nucleotide sequence identity similarity of polar flagellum (*fla*) genes in *Aeromonas* spp. Individual genes are located on the x-axis with each isolate located along the left y-axis. “aAh” and “tAh” designate reference atypical and typical *A. hydrophila* strains, respectively, acquired from the NCBI database. Green-scale bar along left axis denotes *Aeromonas* species or *Aeromonas hydrophila* strain; groups, in descending order, are: *A. sobria*, *A. veronii*, reference aAh, ML09-119, S14-452, and reference tAh.

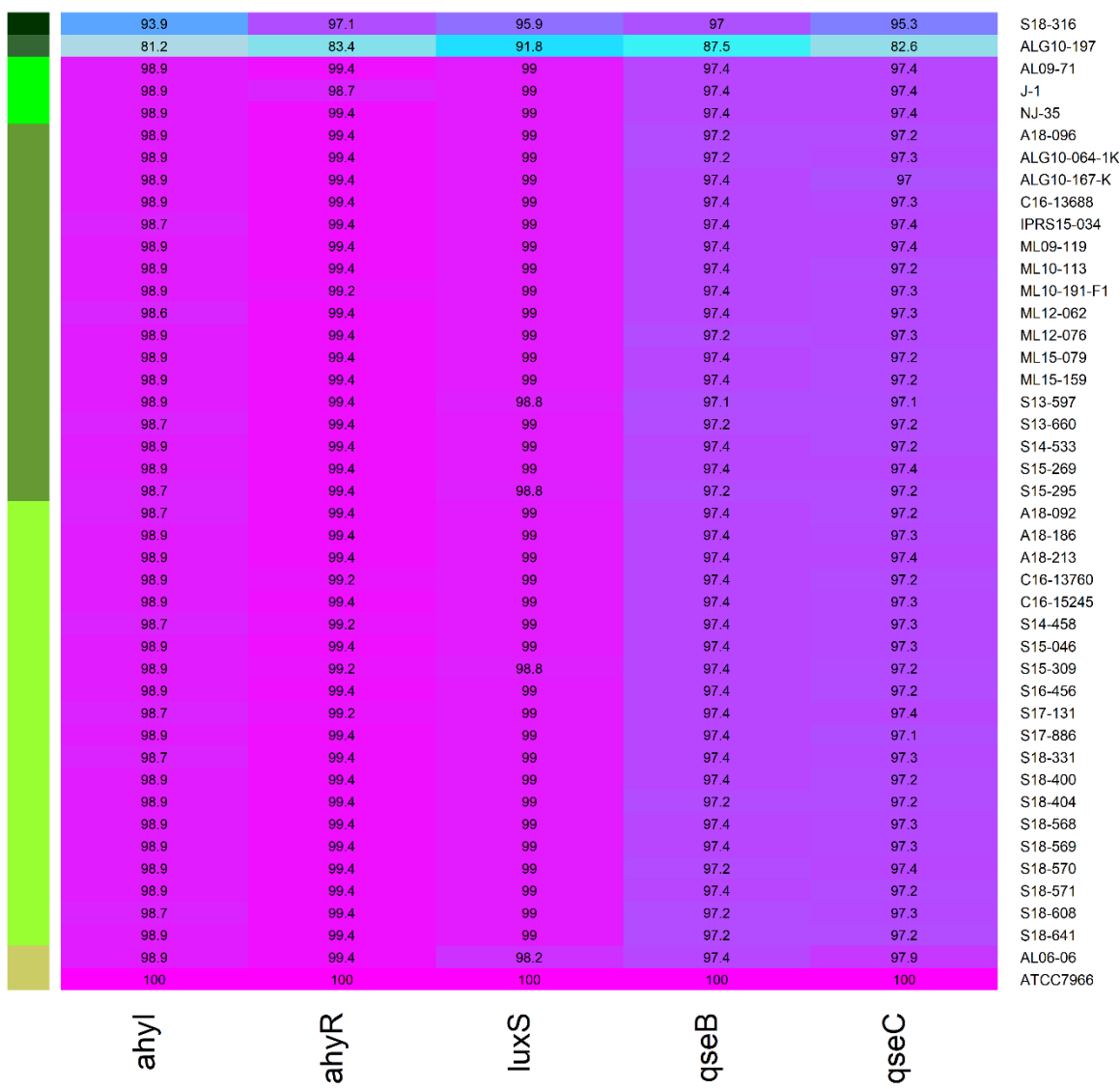


Figure 2.9 Heatmap showing nucleotide sequence identity similarity of quorum-sensing genes in *Aeromonas* spp. Individual genes are located on the x-axis with each isolate located along the left y-axis. “aAh” and “tAh” designate reference atypical and typical *A. hydrophila* strains, respectively, acquired from the NCBI database. Green-scale bar along left axis denotes *Aeromonas* species or *Aeromonas hydrophila* strain; groups, in descending order, are: *A. sobria*, *A. veronii*, reference aAh, ML09-119, S14-452, and reference tAh.

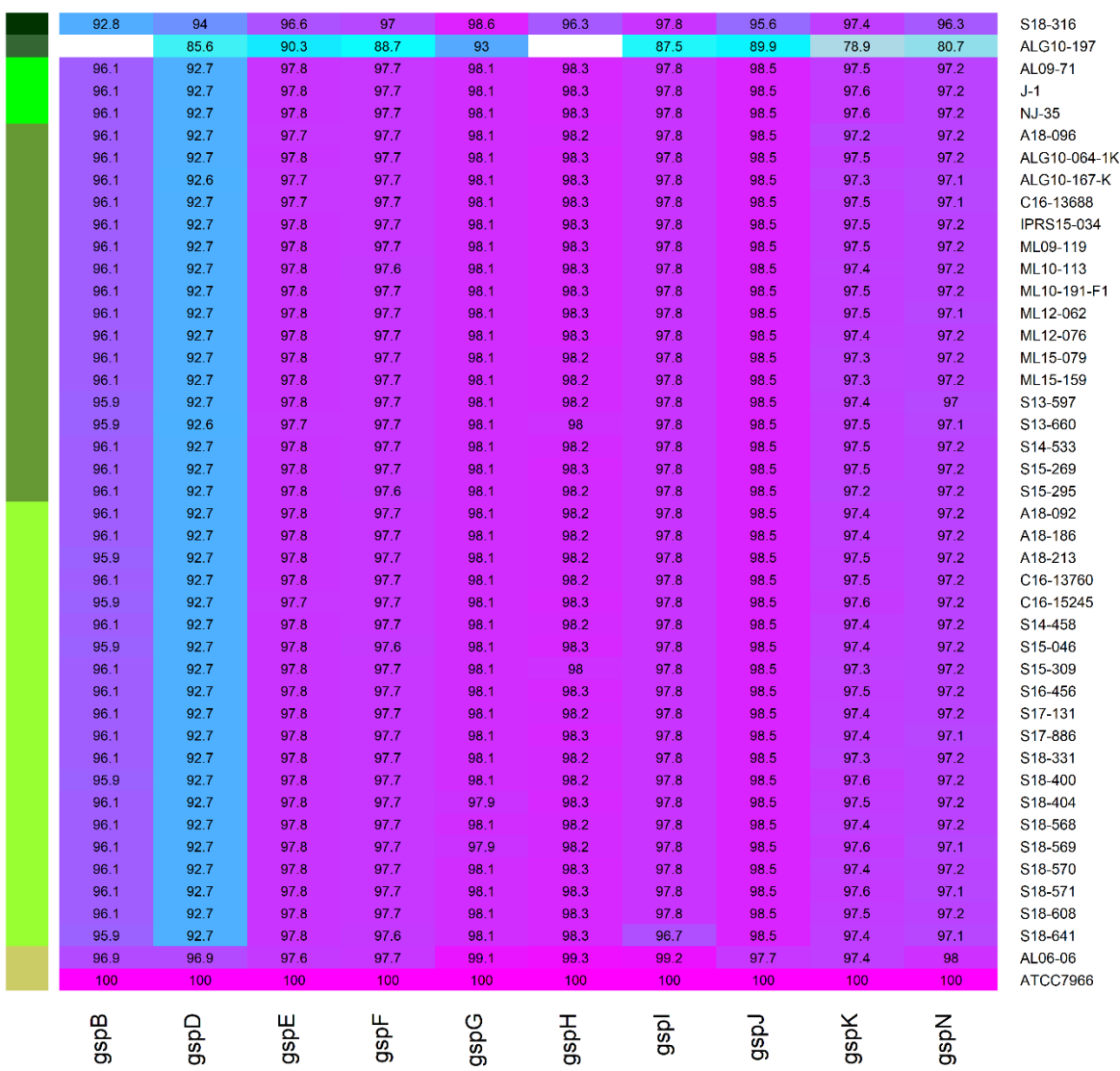
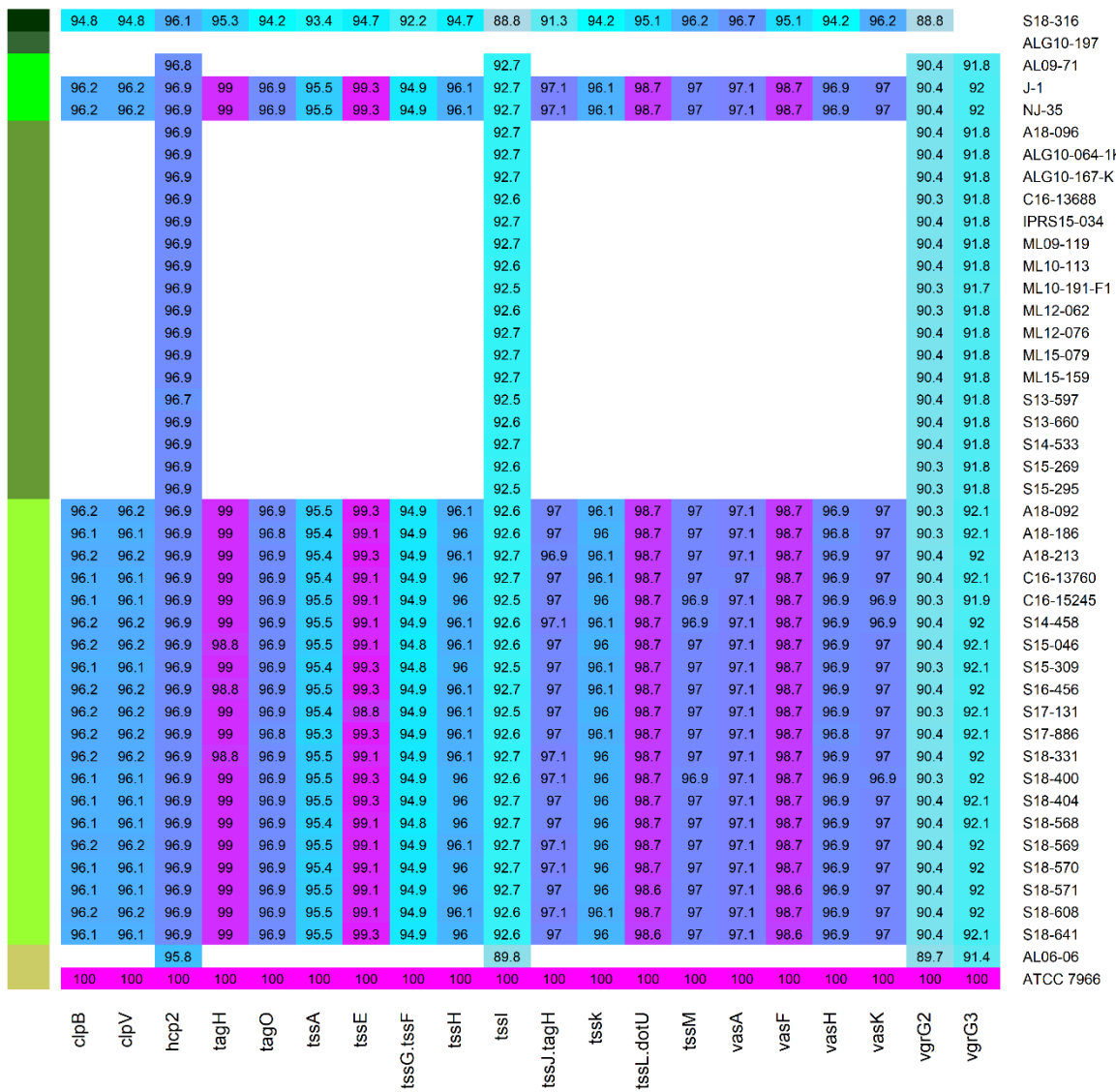


Figure 2.10 Heatmap showing nucleotide sequence identity similarity of the type II secretion systems (T2SS; gsp) genes in *Aeromonas* spp. Individual genes are located on the x-axis with each isolate located along the left y-axis. “aAh” and “tAh” designate reference atypical and typical *A. hydrophila* strains, respectively, acquired from the NCBI database. Green-scale bar along left axis denotes *Aeromonas* species or *Aeromonas hydrophila* strain; groups, in descending order, are: *A. sobria*, *A. veronii*, reference aAh, ML09-119, S14-452, and reference tAh.



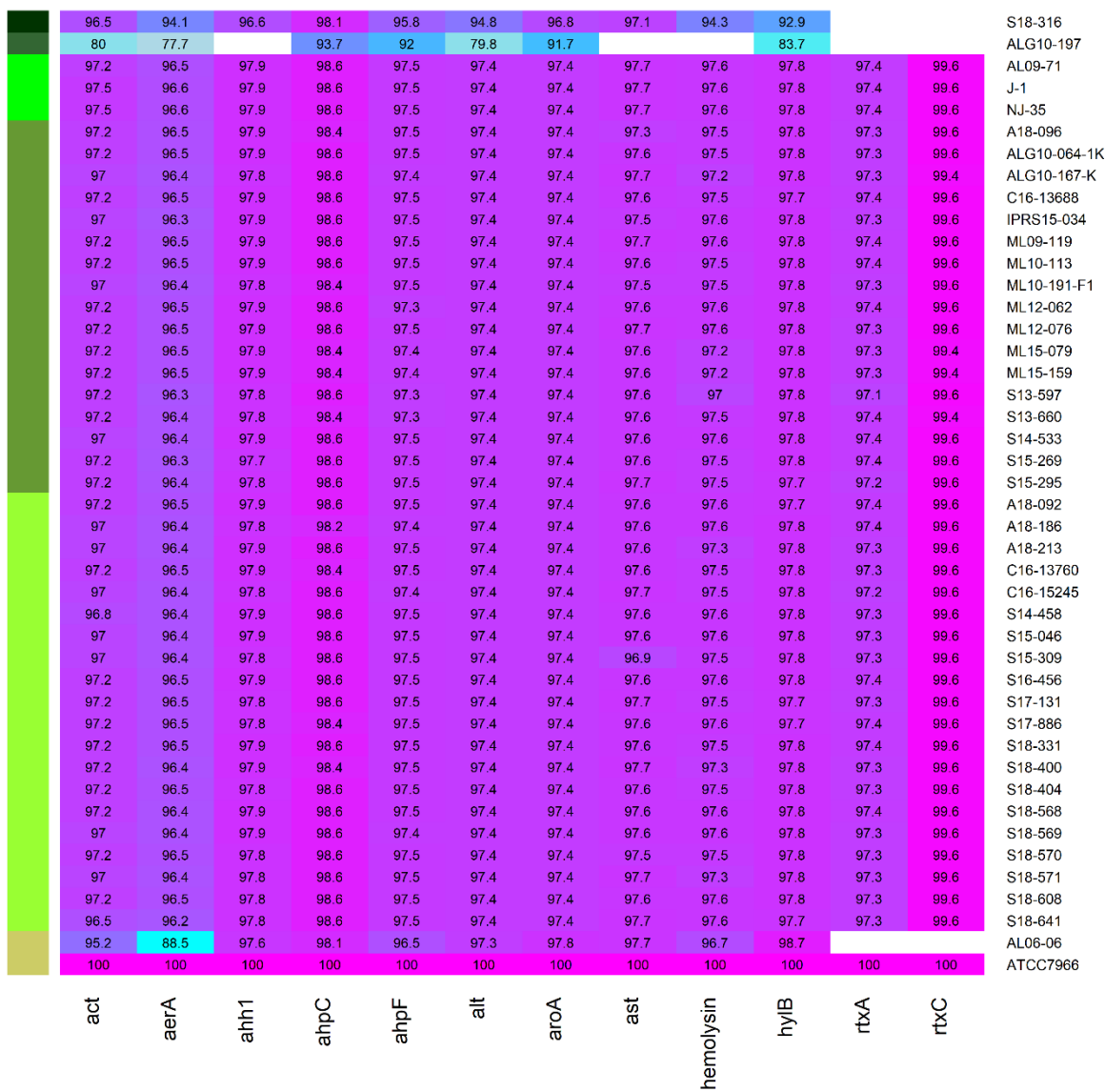


Figure 2.12 Heatmap showing nucleotide sequence identity similarity of the toxin genes in *Aeromonas* spp. Individual genes are located on the x-axis with each isolate located along the left y-axis. “aAh” and “tAh” designate reference atypical and typical *A. hydrophila* strains, respectively, acquired from the NCBI database. Green-scale bar along left axis denotes *Aeromonas* species or *Aeromonas hydrophila* strain; groups, in descending order, are: *A. sobria*, *A. veronii*, reference aAh, ML09-119, S14-452, and reference tAh.

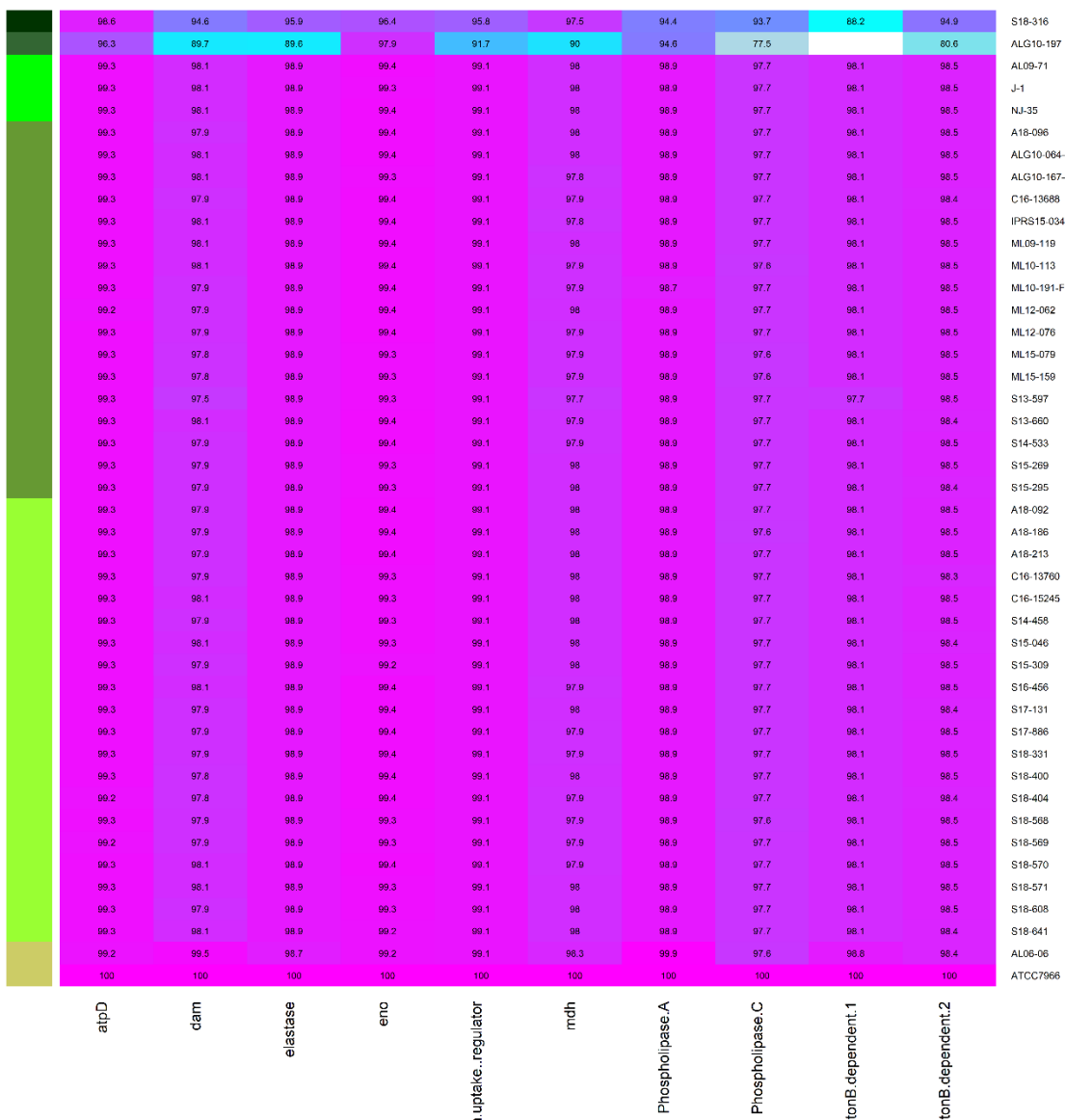


Figure 2.13 Heatmap showing nucleotide sequence identity similarity of additional virulence factor genes in *Aeromonas* spp. Individual genes are located on the x-axis with each isolate located along the left y-axis. “aAh” and “tAh” designate reference atypical and typical *A. hydrophila* strains, respectively, acquired from the NCBI database. Green-scale bar along left axis denotes *Aeromonas* species or *Aeromonas hydrophila* strain; groups, in descending order, are: *A. sobria*, *A. veronii*, reference aAh, ML09-119, S14-452, and reference tAh.

CHAPTER III

USING QUANTITATIVE POLYMERASE CHAIN REACTION AND OCCUPANCY MODELS TO ESTIMATE TYPICAL AEROMONAS HYDROPHILA PREVALENCE IN CATFISH

Introduction

Aeromonas hydrophila is a versatile Gram-negative bacterium, often manifesting as an opportunistic pathogen in many vertebrate species (Janda and Abbott 2010) including fish (Ansary et al. 1992, Radu et al. 2003, Sunder et al. 2006), reptiles (Pasquale et al. 1994), and humans (Davis et al. 1978, Hazen et al. 1978). The bacterium is ubiquitous (Araoju et al. 1991). Since 2009, an emergent strain of *A. hydrophila* with increased pathogenicity (hereafter, atypical *A. hydrophila*; aAh) has been plaguing catfish farms of the southeastern United States (Pridgeon and Klesius 2011). In 2009, the Alabama catfish industry experienced significant mortality events in channel catfish *Ictalurus punctatus* farm ponds caused by aAh (Hemstreet 2010). Since then, aAh has spread and been detected in the catfish farming regions of Mississippi and Arkansas.

With aAh seemingly acting as a primary pathogen, accurate diagnosis and early detection are critical to facilitate appropriate treatment protocols and to minimize fish loss. The quantitative polymerase chain reaction (qPCR) method has proven useful in pathogen detection in a variety of sample matrices, including fish tissues, fish and piscivorous fecal material, and the environment (Brinkman et al. 2003, Hallett and Bartholomew 2006; Griffin et al. 2008). In line

with similar assays targeting other catfish pathogens (Griffin et al. 2009, 2010, 2011; Reichley et al. 2015), a qPCR assay for detection and quantification of aAh has been validated (Griffin et al. 2013). Collecting aAh from tissues for qPCR analysis is often performed in the lab where cultures from the liver, spleen, and/or kidney are grown on selective media then re-isolated for confirmatory diagnosis (Zhang et al. 2014). Given the abrupt onset of disease, a rapid field-based detection method would be beneficial to researchers and aquaculture managers. Present diagnostic techniques are reactive and rely on morbidity and mortality to begin before a problem is recognized and fish are submitted for diagnostic assessment. Moreover, the dynamics of aAh outbreaks and accelerated onset of mortality often precludes collection of moribund or freshly dead fish suitable for diagnostic assessment. As a result, it can be difficult to get an accurate diagnosis. Furthermore, post-mortem fish autolysis can complicate diagnostic evaluations. A field-based method has the potential to increase sample sizes and provide earlier detection of aAh through regular screening and improve diagnostic resolution and reliability.

In most cases of bacterial disease, fish will reduce feed intake during the initial outbreak, which can serve as an early indication to farm managers diagnostic assessment is needed, and medicated treatments may be necessary. However, with aAh epizootics, pond populations tend to continue feeding at normal rates until catastrophic mortality occurs, leaving farm managers with few signs of disease until significant losses have occurred. Given the extremely short incubation and rapid disease progression of aAh (Rasmussen-Ivey et al. 2016; Zhang et al. 2016; Peatman et al. 2018), once mortality begins, the efficacy and feasibility of medicated feed can be greatly reduced as susceptible individuals often die from aAh before treatments can be initiated. In addition, most clinical signs of disease associate with aAh are non-descript and can be found in a variety of other diseases, which makes initial diagnosis even more difficult and highlights the

need for a more proactive screening method for the pathogen before an epizootic. Thus, developing a pond-level view of infection in the absence of outward disease signs could help farmers better prepare for and prevent impending outbreaks.

Estimated disease prevalence in a population in a pond is usually negatively biased because diagnostic assays are imperfect (i.e., sensitivity < 100%). Typically, sensitivity is estimated by comparing a rapid diagnostic tool against a highly sensitive benchmark diagnostic tool to estimate sensitivity, i.e., the probability of detecting the pathogen given it is present. Occupancy models are commonly used in ecological studies to estimate detection probability and can be used in disease studies to estimate assay sensitivity using replicated detections (i.e., detected-not detected) within a host. Data for occupancy models can be in four states: present and detected (State 1), present but not detected (State 2), not present but detected (State 3), not present and not detected (State 4). States 2 and 3 represent Type II (false negatives) and Type I (false positives) errors, respectively. These two states provide information on the sensitivity (State 2) and specificity (State 3) of the assay. By including these data in the analysis, the occupancy models can estimate the probability of each state, correct the naïve pathogen prevalence estimates, and estimate assay sensitivity. Using an occupancy framework, a better understanding of pond-level disease dynamics can be obtained by sampling a subset of the population. Estimated assay sensitivities can then be used to guide how many fish are needed to sample and minimize the risk of missing the pathogen within and among hosts. In this context it is important to make an explicit distinction between a “carrier” state and an “infected” state. Throughout this manuscript, the “carrier state” represents asymptomatic fish harboring the pathogenic bacteria based on qPCR analysis. Conversely, “infected” is used to represent fish in

the infectious disease state in which gross lesions may or may not be present and the pathogenic bacteria is successfully cultured from the kidney or other organs.

It was hypothesized qPCR analysis of fish swabs could serve as a rapid alternative to gross inspection, necropsy, aerobic tissue culture and phenotypic testing for identifying aAh in resident fish populations. The objectives of this study were to i) evaluated the potential of gill and lower intestinal swabs as a field-based screening method for rapid, non-lethal detection of aAh in catfish ponds during epizootic events and from seemingly healthy ponds, ii) evaluate swab screening methods against other common diagnostic tools (lesions, bacterial plate cultures for identifying carrier states within a pond population, and iii) use qPCR replicates of gill and vent swabs in an occupancy framework to estimate pond-level aAh pathogen dynamics and estimate pond-level prevalence.

Materials and Methods

Field and Lab Sampling

All fish handling procedures were performed in compliance with the Mississippi State University Institutional Animal Care and Use Committee. Fish were collected by hook and line or seine during the summer and fall of 2016 from cooperating catfish farms with a history of aAh disease outbreaks in the Delta Region of western Mississippi, USA.

Swab Validation

From August to October 2016, fish were collected from 7 ponds, representing 2 separate farm operations, using standard industry cut seining practices (Tucker and Robinson 1990). All seining activities were conducted by crews employed or contracted by each respective farm. All ponds were displaying active mortalities consistent with aAh outbreaks at sampling, with

estimated total losses per pond ranging from 5,000 to 20,000 kg. The number of fish collected from each pond was constrained by availability. Collected fish were stored, in aggregate, on ice in pond-specific 142-liter coolers and transported to the Fish Health Laboratory at the Thad Cochran National Warmwater Aquaculture Center in Stoneville, MS, for processing.

Fish were euthanized by an overdose of tricaine methanesulfonate (MS-222, >300 mg/l; Western Chemical Inc., Pentair, Cary, NC) and measured to the nearest 1 cm. Fish were aseptically necropsied and designated as aAh positive or negative based on examination of the viscera; in particular, diffuse hemorrhage of the internal organs was used as the primary sign of infection (Baumgartner et al. 2017). Posterior kidney cultures were inoculated onto tryptic soy agar (TSA; Becton, Dickinson, and Co., Franklin Lakes, NJ) plates supplemented with 5% sheep blood. Cultures were incubated at 28°C for 24 hours, inspected for growth, and evaluated as presence-absence of colonies consistent with aAh (Hanson et al. 2014).

Additionally, swabs were collected from the gills and lower intestine of all fish, using sterile cotton swabs, to determine the relationship between internal lesions and kidney culture with qPCR analysis. Gill swabs consisted of lifting the operculum and swabbing the gill chamber and lamellae. Intestinal swabs (“vent swabs” hereafter) were collected by inserting the cotton swab into the lower intestine via the vent. The swab was then gently rotated while being moved longitudinally (approx. 0.5 cm) along the lower intestinal tract. Separate cotton swabs were used for each organ culture and swabs were placed directly into PowerSoil® Bead Tubes (Qiagen, Hilden, Germany). One swab was collected from each location per fish. Isolation of aAh genetic material was performed using the PowerSoil® DNA Isolation Kit following the manufacturer’s protocol for wet samples.

Occupancy Model Sampling

To estimate prevalence using occupancy estimators, we collected fish from a block of 21 ponds on a commercial catfish operation in western Mississippi, USA. Sampling occurred monthly from May through July, with a final sampling in September 2016. Fish were not sampled in August. Ponds were sampled based on availability of fish and all ponds were sampled a minimum of two times in successive months. During daily feeding, 6 to 9 fish were collected from each pond using heavy-action snagging rods equipped with a treble hook and placed in a holding tank containing pond water. Immediately after sampling, fish were transported to a centralized location on the farm and euthanized by immersion bath in MS-222 (>300 mg/l). Gill and vent swabs were collected in the field following the same protocol outlined in the previous section. PowerSoil® tubes containing the swab cultures were transported back to the lab for DNA isolation.

qPCR Analysis

All quantitative polymerase chain reactions (qPCR) were performed using aAh primers and probes validated by Griffin et al. (2013). Reactions were carried out on a C1000 Touch Thermal Cycler (Bio-Rad Laboratories, Hercules, CA) programmed for an initial denaturation of 15 min at 95°C followed by 40 cycles consisting of a 15 sec denaturation at 95°C and a 1 min annealing/elongation at 60°C. Data was collected at the end of the annealing/elongation step of each cycle. Analysis on each swab was performed in triplicate (i.e., DNA extracted from a given swab was used in three replicate wells on a single qPCR plate) and included the SPUD internal positive control (IPC) to test for potential inhibition (Nolan et al. 2006). Each 20-μl reaction consisted of 5 μl of sample DNA, 9.5 μl of TaqMan Environmental Mastermix v2.0 (Applied Biosystems, Carlsbad, CA), 10 pmols each of the aAh forward and reverse primers (Table 3.1), 1

pmols of 6-Carboxyfluorescein (FAM) labeled aAh probe, 500 copies of IPC target DNA, 5 pmols each of the SPUD forward and reverse primers, 1 pmols of hexachlorofluorescein (HEX) labeled SPUD probe and TE buffer (10 mM Tris, 1mM EDTA, pH 7-8) to volume. Three no template controls and 5 serially diluted aAh standards ($1.0 \times 10^2 - 1.0 \times 10^6$ genome equivalents) were included in each reaction plate. If sample IPC signal differed from mean standard IPC signal by more than 1 standard deviation, inhibited samples were diluted five-fold using TE buffer and analysis repeated.

Statistical Analysis

All PCRs were performed in triplicate resulting in 6 quantity readings per fish (Fig. 3.1). For each swab, the average of the 3 readings was used for all analyses. To assess the agreement of the two culture locations (gill vs. vent), a fish was considered aAh-positive if 2 or more of the technical replicates for each respective swab type were positive for aAh. For bacterial pathogen load, estimated genome equivalents were averaged across replicates for each swab type. The detection limit for the assay used is about 100 CFU/sample (Griffin et al. 2013) corresponding to a quantification cycle (Cq) of about 37 or 38; thus, as a conservative estimate any replicate expressing a Cq value ≥ 37 was considered “negative” (non-infected) for aAh, due to a lack of reliability in this range.

Contingency tables were created to compare internal lesions, plate cultures, and swab types. McNemar’s Test (paired χ^2) and Cohen’s kappa (k) were used to evaluate agreement between all pairwise comparisons. For pathogen load analysis, all calculated genome equivalents from qPCR analysis were discretized to integers and differences in bacterial pathogen loads between swab types were compared using the nonparametric Wilcoxon Rank Sum Test.

Probabilities < 0.05 were considered statistically significant in all cases. All statistics were performed using R statistical software (R Core Team 2017).

Occupancy Models

A hierarchical occupancy model structure adapted from Colvin et al. (2015) was used to estimate pond-level prevalence accounting for imperfect pathogen detection. Briefly, the model estimates the prevalence (P ; probability the aAh pathogen is present in the pond), the conditional fish prevalence rate (Ψ ; probability the pathogen is detected in the fish given it is present in the pond), the conditional organ prevalence rate (φ ; probability the pathogen is present in the gill or vent, given it is present in the fish), and the detection probability of each swab type (s ; probability the pathogen is detected in the swab given it is present in the fish). The model uses a Bayesian approach to estimate the state of individuals within the entire population using the observed data from a subset plus sampling uncertainty.

The hierarchical occupancy model was fit using Markov Chain Monte Carlo (MCMC) in WinBUGS 2.14 (Lunn et al. 2000) and the 95% Bayesian credible intervals were used to estimate occupancy. Each model used diffuse priors with 25,000 iterations and 5,000 burn-in samples (i.e. first 5,000 iterations were discarded). All chains were thinned by 2 to minimize autocorrelation. Models were evaluated for viability by inspecting traceplots and ensuring Rhat statistics for each variable were about 1.0 (Gelman and Rubin 1992). Detection probability was simulated for 1 to 10 replicates of each swab type to evaluate differences in probability of detection. The R programming environment and the JAGS package were used for all analyses (Plummer 2003; R Core Team 2017).

Results and Discussion

Throughout this study, mean qPCR efficiencies (E) were 99.0 % and 98.8 % for vent and gill swabs, respectively, within the acceptable ranges for qPCR analysis (Taylor et al. 2010; Griffin et al. 2013). Fish (296) were collected from ponds with active aAh outbreaks between August and October 2016. Forty fish were collected from 5 ponds, 23 fish from one pond, and 73 fish from another. Fish ranged from 17 to 55 cm (mean = 37.4 cm).

Swab Screening Validation

Despite being collected during active aAh mortality events, aAh was only recovered from 47 of 296 fish (15.9%) using kidney cultures on blood agar plates. About half the fish were aAh-positive based on qPCR analysis of vent (143 fish, 48.3%) and gill (186 fish, 62.8%) swabs (Table 3.2). The low number of culture-positive fish collected during active aAh fish-kills supports anecdotal reports from the industry moribund fish are rare, and fish tend to be found in one of two states, healthy or dead. As mentioned previously, this complicates diagnostic assessments as collecting fish suitable for necropsy can be difficult in the absence of a moribund disease state.

To better understand the wide breath of disagreement found in the previous analyses, the detection probability estimates of carrier states were compared between screening methods. As noted previously, the carrier state represents fish without symptoms harboring the pathogen and represent a potential source of future infection. Since gill swabs identified the largest proportion of fish as aAh-positive, we used gill swabs when building the contingency tables. We also compared vent swabs and bacterial growth. Lastly, we used the composite information of gill and vent swabs to compare to kidney culture results. In this last instance, a fish was considered PCR-positive if the aAh target was amplified from either gill or vent swabs. McNemar's test showed

significant disagreement between all screening methods (all $p < 0.001$). Gill and vent swabs agreed on aAh in 217 of 296 (73.3%) fish. In 61 cases (20.6%) fish were PCR-positive at the gills, but negative at the vent. Comparably, 18 fish were PCR-positive in the vent while gill swabs were negative.

Gill swabs agreed with kidney cultures in aAh in only 137 fish (46.3%). Gill swabs detected aAh in 149 culture negative fish (50.3%). Conversely, 10 culture positive fish (3.4%) had negative gill swabs. Vent qPCR and kidney cultures agreed in 150 fish (50.6%). Vent swabs detected aAh in 121 culture negative fish (40.9%), while 25 fish (8.4%) were culture positive but PCR negative at the vent.

Composite results of the gill and vent swabs revealed the two methods (PCR vs. culture) only agreed in 41.6% of cases, with swabs (gills or vent) detecting aAh in 165 culture negative fish (55.7%). Concurrently, 8 fish (2.7%) were culture positive yet PCR-negative at both swab sites. The large number of cases in which fish were PCR-positive while kidney-culture negative emphasizes the need for a more sensitive screening method. In nearly 50% of fish collected from active outbreaks, swabs revealed aAh DNA in the gills and/or intestine in the absence of systemic infection. Though gill and vent swabs disagreed in 27% of fish, aAh was detected by qPCR in more than 40% of culture negative fish. This implies both swab types are potentially viable screening methods for detecting carrier states of aAh in catfish ponds.

Swab Field Comparisons

To evaluate the efficacy of gill and vent swabs as monitoring methods, fish were collected monthly from ponds to estimate aAh prevalence. Of the 526 individuals collected from seemingly healthy ponds, gill and vent swabs agreed in 519 (98.7 %) cases, meaning both swab types agreed on the presence, or absence, of aAh within the fish. Cohen's kappa showed

moderate agreement with relatively high variability (0.58 ± 0.16 ; $k \pm SE$) between observed and expected probabilities. Based on qPCR analysis, 514 individuals (97.8 %) showed no aAh in either swab type while 5 (0.95 %) showed aAh DNA in both swab types. The remaining 7 individuals (1.3 %) only showed aAh to be present in vent swabs. Comparably no individuals showed aAh present in gill swabs only (Table 3.3). The disagreement between swab types was significant (McNemar's $\chi^2 = 5.14$, d.f. = 1, $p = 0.023$) with vent swabs detecting aAh more often than gill swabs. Pond prevalence estimates were also higher in vent swabs (2.2%) compared to gill swabs (0.95%). If monitoring ponds using swabs were implemented on a farm, it is likely the number of swabs and/or fish sampled would be limited by cost constraints and therefore, vent swabs should provide a better estimate of aAh prevalence.

The Wilcoxon rank sum test found no statistical difference in pathogen loads, estimated by qPCR analysis, between gill and vent swabs. The Wilcoxon test returned values of $W = 139,961$ and $p = 0.25$ indicating neither swab type outperformed the other in relation to the cell concentration equivalents. Taken with the binary response results, the pathogen load results were of great interest. The field results suggest aAh concentrations are not necessarily higher in the lower intestine of infected fish, but if aAh is present, it is more likely to be detected in the lower intestine than in the gills. These findings may provide information on the primary mode of entry for aAh. Atypical *A. hydrophila* studies exploring waterborne challenge methods for channel catfish have been largely unsuccessful (Xu et al. 2012) without simulated injuries such as adipose fin clipping (Zhang et al. 2016) or other manipulation (Peatman et al. 2018). Without some physical barrier disruption, the vent and lower intestinal tract of channel catfish may provide the best location for the pathogen while also providing nutrients and growth resources. It is still unclear whether the aAh bacteria must be ingested to reach the colon, or if entry through

the vent is also plausible. The lower intestine may also provide a refuge for the aAh bacterial cells. Cells contacting the gills are likely at greater risk of being sloughed off in the mucous, but those in the lower intestine may avoid this defense mechanism.

Since qPCR is detecting bacterial DNA, rather than actual cells, it is possible the differences in sensitivity between gill and vent swabs is because of increased mucous replenishment in the gills. Mucous in the gills and on the dermis is continually sloughed and replaced, so extended retention of bacterial DNA is unlikely, especially if the bacteria are external. Also, aAh on the gills may be a function of the bacteria in the water since the gills are exposed to the external environment, whereas isolating aAh from the lower intestine may be more indicative of bacterial colonization in the fish, even if the host is without symptoms. This is supported by our study where fish were collected from active mortality ponds; gill swabs were more likely to diagnose fish as aAh-positive than vent swabs (Table 3.2). During an active outbreak, the number of hosts shedding the bacteria should increase the concentration of waterborne aAh, which should lead to increased prevalence in environmental exposed surfaces. In contrast, during sampling, vent swabs diagnosed more fish as aAh-positive, which likely indicates these fish were predominately asymptomatic hosts and bacterial concentrations in the environment were low (Table 3.3).

The fact atypical *A. hydrophila* densities were not different between swab locations may result from wide variation among individual swabs or may suggest the bacteria remain at relatively low densities in the lower intestine until conditions are favorable for entry into the bloodstream, leading to an epizootic. If a portal of entry is required for aAh to infect the host, then any scenario resulting in hemorrhaging could serve as the disease trigger; this could include any enteritis, proliferative gill disease (PGD), or abrasions. Also, Peatman et al. (2018) found

feeding channel catfish to satiation before a challenge increased susceptibility to aAh infection. Feeding to satiation may cause micro-abrasions in the stomach and intestines allowing aAh to enter the bloodstream and cause systemic disease. Anecdotal accounts also lend support to the importance of feeding in aAh infections. In 2018, a lack of processor demand within the catfish industry forced one catfish farm in western Mississippi to hold market-sized catfish in ponds for an extended time until they could be marketed. The fish were fed a maintenance ration (feeding 2-3 times per week) throughout summer production, rather than the standard daily feedings. This farm had frequent aAh outbreaks across several ponds in each of the five previous years from 2013-2017; however, no aAh outbreaks occurred on this farm while being fed the maintenance ration in 2018 (B. M. Richardson, personal observation). Whether due to stress, micro-abrasions, or another unknown source, feeding appears to play some role in the susceptibility of catfish to disease caused by aAh.

Occupancy Models and Prevalence Estimations

Pathogen prevalence varied at the pond- and fish-levels, pond-level prevalence (0.10 – 90.7%) encompassed fish-level prevalence (0.50 – 86.3%). Mean prevalence estimates from the occupancy model were higher in vent swabs (9.8%) than gill swabs (6.6%) and showed considerable increase from the naïve prevalence estimates of 2.2% and 0.95%, respectively, calculated based on initial presence-absence data from qPCR. On two occasions (Table 3.4), the models estimated aAh was present in >50% (58% and 72%) of the fish population of a given pond, but showed no outward signs of disease (i.e. lack of feeding activity, increased mortality, or gross lesions) during sampling.

The probability of detecting aAh in a fish (i.e., sensitivity) increased with the number of technical replicates assayed for both gill and vent samples (Fig. 3.2). Sensitivity was always

higher for vent samples. We performed our assays in triplicate yielding a detection probability of 0.93 for vent swabs and about 0.73 for gill swabs. The probability of detecting aAh given it is present in the lower intestine using qPCR results from vent swabs was 0.97 for 4 or more technical replicates but gill swabs required 8 or more replicates to reach the same level of sensitivity. Taken in conjunction with previously mentioned results finding no PCR-positive in the gills while PCR negative in the vent, these results indicate vent swabs are more reliable and should be preferred over gill swabs if only one swab location can be sampled. This intimation gains additional support when technical replicates must be limited. Even with only a single PCR well, vent swabs showed a sensitivity of 0.60, compared to a 0.35 detection probability for gill swabs (Fig. 3.1).

Comparing the detections within the dataset ($n = 526$), imperfect detection (i.e., a combination of 0s and 1s between PCR assay replicates) accounted for 2.5% and 2.3% of observed detections in vent and gill swabs, respectively (Table 3.5). Seven more non-detections were found in gill swabs than in vent swabs, accounting for 1.3% of total detections. Imperfect pathogen detection can occur based on pathogen abundance and distribution within a host. The proportion of imperfect detections was similar between the two sites sampled within the fish indicating the pathogen is likely to infiltrate both areas above detection limits. However, vent swabs showed higher rates of positive samples which may indicate this location allows for faster growth and replication which would cause the bacteria to reach detectable concentrations more quickly. Additionally, PCR-positive results of the gills may be more influenced by bacterial load in the water, resulting in a more transient result due to filtration rather than colonization.

Conclusions

These data show gill and intestinal swabs can be used to collect field-based bacterial samples for use in qPCR analysis. During active mortality events, gill swabs showed higher sensitivity to aAh than vent swabs. In contrast, gill and intestinal swabs agreed on diagnosis of > 95% of fish in field sampling, however, all discrepancies favored vent swabs in detection of the aAh bacterium. This could be due to increased bacterial concentrations being shed into the surrounding environment during outbreak events and lower concentrations when no outbreak is present. Detection of aAh using vent swabs may be more indicative of bacterial colonization within the host and increased disease risk than gill swabs. Therefore, if resources are limited and only one swab type can be collected, results indicate vent swabs will provide a better estimation of disease risk monitoring; however, sampling multiple locations and replicates within locations allows for increased opportunities for pathogen detection.

Current protocols for acquiring a veterinary feed directive for antibiotic treatment requires submission of multiple moribund fish with evident gross lesions, often followed by a minimum 24-hours to verify aAh by aerobic isolation culture and phenotypic confirmation. Given the rapid progression of the disease and the accelerated time to death (<24 hr) once fish break with an infection, collection of moribund or sick fish suitable for diagnostic evaluation is challenging. With the proposed protocol, fish can be sampled from seemingly healthy ponds when aAh is prevalent, and a simple outbreak risk assessment made. Furthermore, these protocols lend themselves to systematic pond monitoring throughout production. While these results may not satisfy regulatory requirements for VFD prescription, proactive monitoring has the potential to save farm managers money by reducing the cost of diagnosis, as well as limiting fish losses by increasing preparedness for impending outbreaks. Rather than serving as a

diagnostic for prescription acquisition, this monitoring protocol has the potential to be an early warning for farm managers, identifying which ponds are at risk of aAh.

The sensitivity and specificity values from this study are important for comparison but must be evaluated with care as they are affected not only by the efficiency of each respective screening method but also the sensitivity and specificity of the method being designated as the benchmark. The sensitivity and specificity of any method is also dependent on disease load. Weak infections will likely lead to a lower sensitivity and specificity compared to a strong epizootic. Internal lesions were only present in about 10% of the sample population while bacteria were cultured from ~16% of kidneys and DNA of the pathogenic bacterium was detected in >47% of individuals using vent and gill swabs. Culture-positive fish represent active disease states in which fish health is compromised, whereas qPCR-positive fish may represent carrier states serving as a potential source of future disease. Both gill and vent swabs detected more incidences of aAh in catfish than did internal lesions or kidney cultures. In 90-95% of aAh-positive qPCR assays, calculated cell equivalents were at low levels (<1000 cells/sample) likely representing a reservoir population.

Perhaps most importantly, the pond survey suggests the resident fish population can be aAh-positive with no outward signs of disease at the pond level. This implies additional unknown conditions are at play and aAh in the pond is not the sole contributing factor to disease. The environmental triggers initiating catastrophic fish kills associated with aAh remain elusive. The applications of these techniques in future epidemiological studies will assist in identifying putative environmental triggers associated with disease outbreaks and better clarify the mechanisms and dynamics of aAh infection.

Table 3.1 Primer and probe sequences validated by Griffin et al. (2013) and used for quantitative polymerase chain reaction (qPCR).

qPCR/Primer	Sequence (5'-3')	Tm (°C)*
2968F	CTATTACTGCCCTCGTTC	58.7
2968R	ATTGAGCGGTATGCTGTCG	59.8
2968P	TCAAGCGTTCATAAAGTG CCGAGTCA	69.6

* Represents the melting temperature of each primer or probe.

Table 3.2 Binary responses of all screening tests for fish collected from ponds with active mortalities (N = 296 fish).

	Test Result*	
	Negative	Positive
Kidney Culture	249	47
Gill Swab	110	186
Vent Swab	153	143
Composite Swabs	92	204
Total [†]	604	580

* Results from swab samples are derived from triplicate quantitative polymerase chain reaction (qPCR) results and designated as “positive” or “negative” based on simple majority from the three technical replicates per fish.

† Total values are sums from all assays pooled and were used as the benchmark.

Table 3.3 Contingency table showing number of PCR-positive and PCR-negative fish based on gill and vent swabs assays from fish collected during field sampling.

		Vent Swabs		
		Negative	*Positive	Total
Gill Swabs	Negative	514	7	521
	*Positive	†0	5	5
	Total	514	12	526

* Positive results occurred when 2 or more of the qPCR replicates of a given swab type showed detectable quantities of atypical *Aeromonas hydrophila* DNA.

† No fish showed a PCR-positive result in gill swabs only.

NOTE: Disagreement was significant based on McNemar's paired Chi-squared (χ^2) test ($p < 0.05$).

Table 3.4 Occupancy model prevalence estimates for each pond separated by sampling date. Prevalence estimates were calculated using hierarchical occupancy models with swabs collected from the gills and lower intestine (vent).

Pond	Sampling Occasion			
	24-May-16	23-Jun-16	27-Jul-16	8-Sep-16
1	0.003	0.003		
2	0.012	0.013	0.276	
3	0.291	0.028	0.282	
4	0.002	0.001	0.001	0.001
5	0.014	0.187	0.013	
6	0.284	0.019		
7	0.002	0.002	0.002	
8	0.002	0.002	0.002	
9	0.002	0.002	0.002	
10	0.002	0.002	0.002	
11	0.004	0.003		
12	0.009	0.009	0.009	0.287
13	0.002	0.002	0.002	
14	0.002	0.002	0.002	
15	0.277	0.019		
16	0.013	0.013	0.21	
17	0.003	0.003		
18	0.003	0.005		
19	0.907	0.013	0.013	
20	0.012	0.576	0.013	
21	0.724	0.027	0.28	

NOTE: The only pond showing active mortality during sampling was Pond 19 on 24-May-16, but fish suitable for diagnostic assessment could not be collected and cause of mortality was never determined. No other ponds showed increased mortality, clinical signs, or were diagnosed with aAh throughout sampling.

Table 3.5 Detection types for atypical *Aeromonas hydrophila* (aAh) by swab type (N = 526 fish).

	Non-detection	Imperfect Detection	Perfect Detection
Vent Swabs	506	13	7
Gill Swabs	513	12	1

NOTE: Non-detection was designated as all PCR assay replicates showed negative (i.e. 000). Perfect detection represents fish where all replicates were positive (i.e. 111). Imperfect detection represents fish where aAh was not detected in all replicates (i.e. 001, 010, 100, 011, 101, 110).

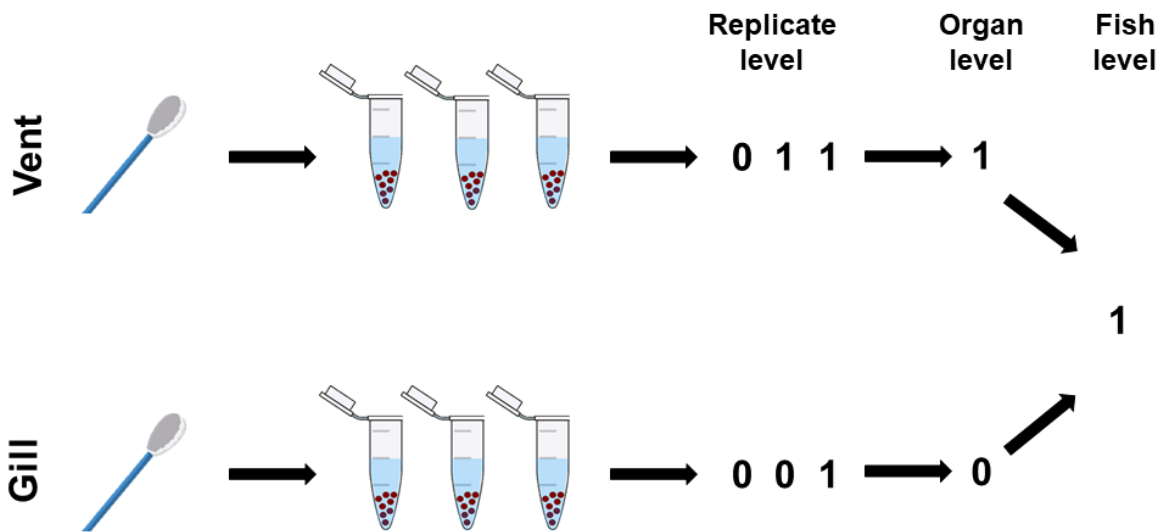


Figure 3.1 Diagram of swab analysis using qPCR.

NOTE: One swab was collected from each of 2 locations on a fish, three replicate reactions on a qPCR plate included 5 µl of DNA extracted from a given swab, quantitation cycle (Cq) results from each of the replicate wells was converted to a binary response, then the binary response was used to designate a fish as positive or negative for aAh based on simple majority.

NOTE: For the binary response, a “1” (PCR-positive) represents a technical replicate with a Cq value of < 37, while a “0” (PCR-negative) represents a technical replicate showing no fluorescence or resulted in a Cq value ≥ 37 .

NOTE: The Cq value of 37 corresponds to an approximate concentration of 100 aAh cell equivalents per sample, which is the detection limit of this assay; therefore, any replicate with a Cq value larger than this was considered a negative result.

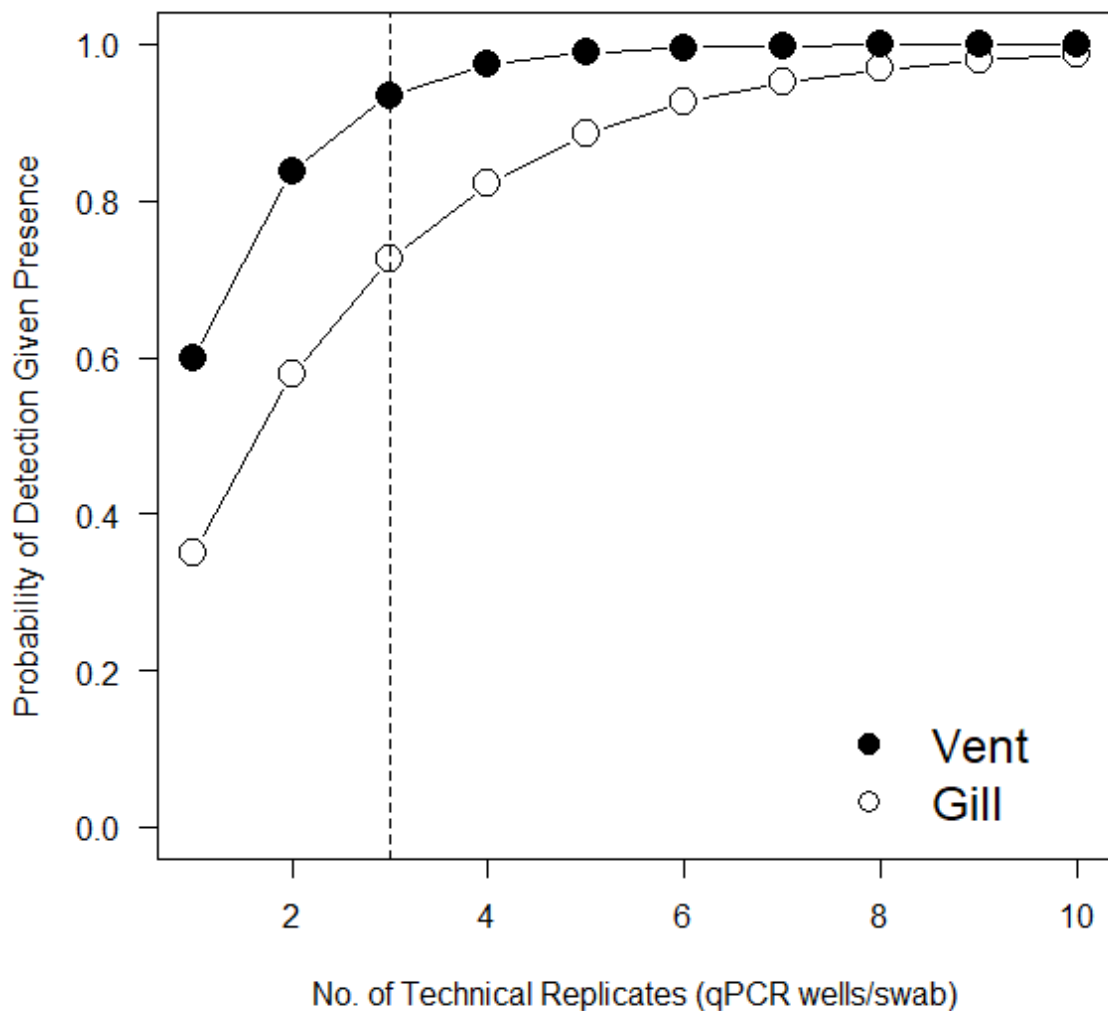


Figure 3.2 Predicted detection probabilities of atypical Aeromonas hydrophila (aAh) in gill and vent swabs, based on the number of replicates in the assay.

NOTE: Dashed line represents samples assayed in triplicate.

CHAPTER IV

A COMPARTMENTAL EPIDEMIOLOGY MODEL TO INVESTIGATE ATYPICAL *AEROMONAS HYDROPHILA* DISEASE DYNAMICS IN CATFISH AQUACULTURE PONDS

Introduction

Catfish aquaculture, like most agriculture industries, is in a constant state of maximizing per-unit production and minimizing losses due to biotic and abiotic stressors. A primary reason for lost income in catfish aquaculture is disease (Sunder et al. 2016). The U.S. catfish aquaculture industry has seen impressive technological and operational advances in its relatively short lifespan, beginning in the 1960s and flourishing approximately 20 years later (FAO 2010). The shift from vast, extensive pond culture with low stocking rates and little anthropogenic input has now become intensive culture with high stocking densities, use of hybrid species, precise aeration regimes, and multi-batch systems (Tucker and Robinson 1990). All these advances work to increase the production per unit area, but they also provide opportunities for pathogens to proliferate when abiotic and biotic conditions are favorable for pathogen outbreaks.

Epidemiology, the study of disease occurrence, is a multi-faceted discipline with influences from ecology, economics, culture, geography, and biotic and abiotic variables, as well as many others (Hethcote 1989); however, even looking at disease from a strictly ecological viewpoint is complex. Snieszko (1974) provided an eloquent representation of the issue, using a 3-ringed Venn diagram to demonstrate the interrelationship of the host, pathogen, and

environment on the outbreak of disease, with disease only occurring if all three conditions were favorable. Snieszko (1978) would later expand on this in the form of an equation ($H+P+S^2=D$) emphasizing disease (D) occurs when the proper conditions of the host (H ; species, age, susceptibility, etc.), pathogen (P), and environmental stress (S) are present. Stress was represented as a squared term because it can have a magnifying effect, thus creating increasing the probability of disease outbreak more rapidly. Increased stocking densities and nutrient inputs are typically offset by reducing stress by using intensive aeration and water quality management (Boyd et al. 2018); however, disease is still a major threat to the profitability to any catfish operation.

Pathogen introduction to a pond can take many forms and may be influenced by biotic and abiotic processes as well as normal operating practices. For instance, birds are known to be susceptible to many of the same diseases infecting humans and other vertebrates (Benskin et al. 2009). Piscivorous birds, particularly the American white pelican (*Pelecanus erythrorhynchos*) and double-crested cormorant (*Phalacrocorax auritus*), are frequently found on commercial ponds (Glahn and King 2004) and are able to harbor and shed a variety of diseases (Overstreet et al. 2002; Doffitt et al. 2009; Cunningham et al. 2018; Rosser et al. 2018). Parasites can also be shed from several invertebrate hosts found in catfish ponds such as *Henneguya ictaluri*, the causative agent of proliferative gill disease (PGD), shed by the *Dero digitata* oligochaete (Pote et al. 2000) or *Bolbophorus damnificus*, a parasite shed by the marsh rams horn snail (*Planorbella trivolvis*) (Overstreet et al. 2002; Levy et al. 2002). Lastly, farm operations may inadvertently introduce pathogens to susceptible populations through normal seining and stocking practices. Sharing seining equipment, such as nets and boats, among ponds has the potential to translocate pathogens and/or infected hosts (Garrett et al. 2008). In multi-batch systems where a single pond

is partially harvested and subsequently understocked in a continuous cycle, the chance of introducing new pathogens from any of these sources is likely increased.

Channel catfish (*Ictalurus punctatus*) has been the predominate species cultured in the U.S., though hybrid catfish (channel catfish (♀) x blue catfish *I. furcatus* (♂)) has increased in popularity among catfish producers since the late 2000s (USDA 2018). The hybrid catfish has increased feeding rates and growth, less variable size distribution at harvest, increased tolerance of crowding and low dissolved oxygen, and improved disease resistance compared to channel catfish (Dunham et al. 1983; Bosworth et al. 2004; Li et al. 2004; Kumar et al. 2019). Unfortunately, intensive culture practices continue to result in detrimental impacts of disease for both production species.

The U.S. catfish industry production and economics is most heavily impacted by diseases. Bacterial diseases like columnaris, caused by *Flavobacter columnare*; motile aeromonas septicemia (MAS), which has multiple etiological agents but is primarily attributed to *Aeromonas hydrophila*; enteric septicemia of catfish (ESC), caused by *Edwardsiella ictaluri*, and a related bacterial disease, *E. piscicida* are commonly encountered in catfish production (Plumb and Hanson 2010). The myxozoan *Henneguya ictaluri* is the causative agent of proliferative gill disease (PGD) in channel and hybrid catfish (Pote et al. 2000; Griffin et al. 2010; Rosser et al. 2018) and can also negatively affect catfish production (Wise et al. 2004). As noted, 4 of the 5 most common diseases are caused by bacteria, making their control and understanding important to the success of catfish operations.

In 2009, an atypical form of MAS was recorded in repeated disease outbreaks in catfish ponds of west Alabama (Hemstreet 2010) consistent with the global clonal subgroup ST251 (Rasmussen-Ivey et al. 2016). The causative agent was an atypical strain of *A. hydrophila* (aAh),

which displayed sudden onset of disease and acute mortality (Rasmussen-Ivey et al. 2016; Zhang et al. 2016; Peatman et al. 2016). As of 2014, aAh had caused an estimated \$12 million in losses to the industry (Hossain et al. 2014). Several studies have investigated aAh, evaluating comparative genomics (Liles et al. 2011; Hossain et al. 2014; Rasmussen-Ivey et al. 2016, Tekedar et al. 2019), pathogenicity (Rasmussen-Ivey et al. 2016; Zhang et al. 2016; Peatman et al. 2018), and potential transmission vectors (Jubirt et al. 2015; Cunningham et al. 2018), but little attention has been paid to the epidemiology of aAh in the production systems.

Compartmental epidemiology models have been used to investigate the dynamics of other aquaculture diseases such as furunculosis (Ogut et al. 2004, 2005; Ogut and Bishop 2007), which is caused by a non-motile aeromonad – *Aeromonas salmonicida*. Modeling aAh dynamics in the catfish production system could be an important tool for identifying risk factors (de Jong et al. 1995), improving disease dynamics understanding, and evaluating management strategies.

Epidemiological models are pivotal to understanding the transmission mechanisms and interactions of a disease in a population (Hethcote 1989). In these models, the population is divided into discrete compartments based on an individual's disease status (Kermack and McKendrick 1927). Kermack and McKendrick (1927) used this compartmentalization to describe the simplest of the epidemiological models which consists of individuals in 3 states: susceptible to the disease (S), infected (I), or recovered (R) (SIR model). This basic model has since been adapted to include an additional latent state as the “susceptible-latent-infected-recovered” (SLIR; Fig. 4.1) model (Ogut and Bishop 2007). This variant includes adding a latent state where an individual is actively carrying the pathogen but is not yet infectious to others and is typically asymptomatic (Ogut and Bishop 2007).

We constructed a compartmental SLIR model to better understand the disease dynamics of aAh in catfish ponds, evaluate potential management actions, and to highlight important areas of future research. The presented model combines empirical information, expert elicitation, and stochasticity to investigate changes in disease dynamics in a variety of settings. The model also evaluates the characteristics of four pathogen reservoir hypotheses. The objectives of this study were to 1) develop and variableize a SLIR model for aAh, and 2) evaluate disease management scenarios using medicated feeding, early harvest, and pond monitoring over the production season to minimize production losses and maximize profits.

Materials and Methods

Systems model overview and inference

Catfish aquaculture in the southeastern U.S. primarily uses earthen ponds filled with well water. Broodstock are allowed to randomly mate in brood ponds using spawning pots. Fertilized eggs are then collected and moved to a fish hatchery. Once hatched, fry are reared in the hatchery for a short time before being transferred to nursery ponds and grown to fingerling size throughout the summer. Fingerlings are stocked into growout ponds during the autumn or winter and grown to market size and harvested the following summer or autumn when they reach approximately 0.5-1.0 kg. During final growout, fish are typically fed once daily at a rate of 1.5-2.0% bodyweight. Fish growout can be performed in single-batch systems, where a single cohort of fish are stocked into a pond and all fish are harvested at once, or multi-batch systems, where a pond is partially harvested and new fish are stocked into the pond to replace those removed. Single-batch systems are more common in hybrid catfish production while multi-batch systems are typical in the production of channel catfish.

The epidemiological model constructed here assumes the population is divided into non-overlapping classes of disease state (susceptible, infected, recovered) and an individual may only belong to one state at any time (t). Additionally, it is assumed the operation is a single-batch system, thus the population is closed over the simulation of additions, and N (population size) is only effected by removal via mortality, harvest, and samples removed for disease diagnosis, with no effect of new introductions through birth or any other method. The model also assumes homogenous mixing is occurring within the population (Hethcote 1989). This model is based on a single hypothetical pond within a farm but could be expanded to investigate farm-level scenarios using the base model.

Laboratory studies of aAh have shown challenge via intraperitoneal (IP) injection (Hossain et al. 2014; Zhang et al. 2014, Rasmussen-Ivey et al. 2016) and water bath with adipose fin clip (Zhang et al. 2016) result in acute mortality typically occurring within 48 hours. This would suggest a simpler SIR model may suffice; however, the SLIR model was used due to the recent identification of a carrier (exposed, latent) state in commercial catfish farms (Richardson et al. *in review*). With little empirical data on aAh dynamics in aquaculture, much of this model variableization relies on anecdotal information from catfish farmers and researchers.

Catfish production system model development

The SLIR model (Fig. 4.1) was constructed with a graphical interface in the web-based application Insight Maker (insightmaker.com). The basic flowchart of the model is presented in Fig. 4.1 where rectangles (stocks) represent the state of an individual in the populations and arrows (flows) represent the movement of individuals between states. The flow of individuals from the recovered to the susceptible state indicates surviving infection provides temporary

protection (via antigen presentation or other mechanism) and wanes at some given rate (Leung et al. 2018).

Variable annotations and equations were derived from Ogut and Bishop (2007) The equation representing the dynamics of susceptible fish (\dot{S}) was:

$$\dot{S} = -\beta \cdot S \cdot I - \rho \cdot S - \gamma \cdot S \quad (4.1)$$

where, β is the contact rate between individuals and represents the rate of individuals moving from susceptible to exposed state, S is the number of susceptible individuals, I is the number of infected individuals, ρ is the treatment rate, and γ is the natural mortality rate. The dynamics for the exposed fish (\dot{L}) was:

$$\dot{L} = \beta \cdot I \cdot S - \alpha \cdot L - \rho \cdot L - \gamma \cdot L \quad (4.2)$$

where, L is the number of latent individuals, α is the disease-specific mortality rate, and additional variables are as previously defined. The dynamics for the infected fish (\dot{I}) was:

$$\dot{I} = \theta \cdot L - \alpha \cdot I - \rho \cdot I - \gamma \cdot I \quad (4.3)$$

where, θ is the progression variable indicating the rate of individuals moving from latent to infectious and additional variables are as previously defined. Dynamics of the recovered individuals (\dot{R}) was:

$$\dot{R} = \alpha \cdot I - \rho \cdot R - \gamma \cdot R \quad (4.4)$$

where R is the number of recovered individuals and all additional variables are as previously defined. Pond profits (\dot{P}) were calculated using the equation:

$$\dot{P} = (F - C) \cdot W \cdot (S + L + I + R) \quad (4.5)$$

where P is the pond profit, F is the dollar value per pound of fish, W is the total weight of fish harvested (converted to lbs), C is the seining cost per pound of fish, and all other variables are as previously defined.

Variable values for the present model were estimated using empirical estimations from aAh, as well as a closely related fish pathogen, *A. salmonicida* and anecdotal evidence from catfish aquaculture experts. To date, no experiments or observational studies have been conducted to estimate the infection rate (β) of aAh and any estimates of disease-specific removal rate (α) taken from Zhang et al. (2016) would be >0.75 infected ind. day $^{-1}$, so initial values of these two variables, were taken from Ogut et al. (2004) and used in a random uniform distribution with min/max values representing $\pm 20\%$ of the calculated rate. Since Ogut et al. (2004) used an SIR model and no estimate of the progression rate (θ , movement from exposed to infectious), this variable was given an initial value of 0.20, equal to the inverse of the approximate mean duration (5 days) of untreated outbreaks occurring in commercial catfish ponds and was allowed to vary from the arbitrary values of 0.14 to 0.33 representing potential outbreak durations of 3 to 7 days.

Structural uncertainty: evaluating alternate pathogen introduction hypotheses

Management decisions to minimize production loss and consequent economic losses due to aAh may be influenced by the mode of pathogen introduction to the system which is uncertain. We evaluated four hypotheses representing common hypotheses of aAh vectors/reservoirs in catfish aquaculture. Each hypothesis is explained in more detail below. Hypothesis 1 (H_1) was carrier-state fry are purchased and later stocked into the ponds as fingerlings, providing a point of subsequent pathogen spread. Hypothesis 2 (H_2) represents the hypothesis of birds as a potential vector of introduction. Hypothesis 3 (H_3) encompasses the presence of a carrier state within adult fish transferring the pathogen to naïve cohorts in each new production year. Finally, hypothesis 4 (H_4) assumes the pathogen is ever-present in the environment and the probability of a new individual being infected is function of time, with the probability of 1/30, indicating infections from the surrounding environment are relatively rare and one new infection occurs, on average, every 30 days.

The distribution of fry is an important bottleneck in the potential spread of aAh across the southeastern U.S. Hypothesis 1 has yet to be tested, but movement and supplanting patterns of the S14-452 pathotype of the disease (Ch. 2) appear to show infected fry (H_1) as a potentially viable hypothesis. This model was constructed with a focus on catfish growout operations (fish grown from fingerlings or stocker sizes to market-size) and so the dynamics simulated assuming this hypothesis would constitute the dynamics potentially displayed by infected fingerlings.

Piscivorous birds are common on catfish aquaculture farms and cause substantial losses to the industry through direct predation (Glahn and King 2004; Dorr et al. 2012). Piscivorous birds are commonly attributed with the spread of bacterial diseases in fish (Taylor 1992) and work by Jubirt et al. (2015) and Cunningham et al. (2018) showed this to be possible for aAh.

Under hypothesis 2, the presence of the pathogen (number of additional exposed fish) is based on a random binomial distribution with a probability of 0.165. Jubirt et al. (2015) showed four of six great egrets (*Ardea alba*) fed aAh-infected fish shed the bacteria in their feces for no more than 4 days following the last feeding; thus, our pathogen presence probability for H_2 was calculated as (1/maximum number of shedding days)*(proportion of birds shedding the maximum number of days), or 0.25*0.66 to give an approximate probability of 0.165. At the start of the simulation, there are no exposed or infected individuals, and all are assumed to be susceptible.

Exposed fish have been shown to comprise as much as 60% of a pond population (Ch. 3) with no clinical signs of disease (i.e., carrier fish); however, aAh genetic material was typically detected in approximately 10% of the population. For H_3 , we used an initial exposed population of 1 to maintain minimal starting conditions comparable to other hypotheses, some of which began with no exposed or infected individuals. Carrier fish could pass between cohorts in a single-batch system if a fish escapes the seine during harvest (Steeby and Lovshin 1993) and the pond is not drained before being placed back into production with a new cohort of fish. The initial conditions of this hypothesis provide a conservative starting point to evaluate this scenario.

Several studies have shown aAh presence in catfish ponds over a long time. The pathogen is typically found in biofilms (Cai et al. 2019) and/or the pond sediments (Cai and Arias 2017; Cai et al. 2019). So, we included a hypothesis (H_4) representing a scenario where the aAh pathogen is a continuous pond resident. In this hypothesis, all fish in the population are considered susceptible and there are no exposed or infected individuals at the start of the simulation. Once exposed, progression of the disease within the population continues as in other scenarios. Disease outbreaks occurred at random, with a probability of 0.033, equating to an

average of 1 outbreak per month. Because the exact trigger of an aAh outbreak is still unknown, the random occurrence was used match observed outbreak frequencies.

Disease management scenarios

The model was used to evaluate varying scenarios occurring on a catfish aquaculture operation and potentially manage aAh and other diseases. Using medicated feed, various harvest timing scenarios, and routine diagnostic monitoring were all evaluated to determine their effects on potential pond profits. In total, 75 unique scenarios were evaluated, and median net profits were determined for each.

Medicated Feed

Using medicated feed is a common and effective method for disease treatment. For aAh, florfenicol or other antibiotics are administered orally through prepared feed mixes. Feed costs can constitute more than 50% of the annual production budget (Kumar and Engle 2017) so additional costs incurred through medicated feed has the potential to decrease profitability. Using medicated feed was triggered by a random number between 500 and 1000 aAh mortalities in a given day or if at least 1 infected fish was submitted to the diagnostic lab during routine monitoring scenarios. This was done to account for farm managers more cautious (500 mortalities) and those more hesitant to react (1000 mortalities) (D. Wise, pers. obs.). Treatment efficiency was assumed to be 70% of the population receiving a therapeutic dose, and feed price increasing from \$360 to \$850 per ton for a 10-day regimen during treatment. And a 15-day withdrawal period before any potential harvest was used, which is standard for florfenicol usage (FWS.gov). Fish receiving medicated feed moved to the recovered state but lost the protective

antibiotic effects and transitioned back into the susceptible state at a constant rate of 0.07, representing a maximum of 15 days of protection after the last day of treatment.

Early harvest

To meet consumer demand, fish are harvested and sold to processing plants year-round (Engle 2003) and delaying fish harvest can also incur substantial costs due to increased feed usage and reduced value of larger fish. To evaluate the timing of fish harvest on the economics of aAh risk, three harvest periods were selected to simulate an early (day 260), normal (day 300), and late harvest (day 450).

Monitoring pathogen status

Lastly, the efficacy of routine monitoring was evaluated as a proactive management strategy for aAh. Both monitoring frequency (14 vs. 30 submission intervals) and number of fish submitted (10 vs. 25 fish) were used to evaluate potential changes in profitability. Fish were randomly “sampled” from the entire population of susceptible, exposed, infected, and recovered individuals at each submission timepoint. Routine submission occurred every 14 or 30 days. Each submission case cost \$50, the current price for fish diagnostics at the Aquatic Research and Diagnostic Laboratory (Stoneville, MS).

Model analysis and evaluation

Model simulations

For all model simulations the size of the initial population (N_0) was at 50,000 individuals, a typical pond population in catfish aquaculture. Feeding rate was 2% mean body weight per day. As a baseline, simulations were run to determine median per-pond profit for harvesting at day 260, 300, and 450 in the absence of the aAh pathogen. Each hypothesis was selected at the start

of the simulations and performed with 500 replications for each harvest day to evaluate uncertainty. Final median net profit was calculated based on each 500-replicate run.

Scenario evaluation

Each of the four hypotheses and management scenarios were evaluated to determine the potential net profit of a given pond. All stochastic variables had initial values chosen from a random distribution and then were held at the initial value for the duration of the simulation. Sensitivity analysis was performed using 500 simulations and returning the median profit and the 80% and 95% confidence region of pond profit. Results were analyzed by comparing median profits.

Sensitivity Analysis

The sensitivity of estimated pond profits to perturbations of the disease variables (β , θ , and ρ) were evaluated using an identical model developed using STELLA modeling software (STELLA v10.0.2, isee Systems, Inc.; iseesystems.com). To investigate the sensitivity of the model, all management actions (e.g. medicated feed, routine monitoring, etc.) were removed to determine baseline changes in pond profit. For each proposed hypothesis, each disease variable was allowed to vary +/- 20% from the initial value previously described resulting in 12 sensitivity estimates. Each variable was given an initial value at the start of each simulation and held constant for the duration of the individual run. All sensitivity analyses consisted of 1000 iterations and a tornado plot was created using the difference between minimum and maximum profit values.

Results

Seventy-five scenarios were investigated using the model created. Median profits in the absence of aAh were \$39,211.89, \$40,310.03, and \$33,765.20 for harvesting at day 260, 300, and 450, respectively, and provided a baseline to which all other scenarios were compared (Table 4.1).

Evaluating pathogen introductions hypotheses

All hypotheses of pathogen introduction resulted in a significant profit reduction. Hypothesis 1 (infected fingerlings) in the absence of any management actions yielded median profits of \$22,874.75, \$23,207.08, and \$18,019.52 when harvested at day 260, 300, and 450, respectively, nearly a 50% profit reduction compared to baseline simulations. Hypothesis 2 (bird vector) also showed reduced profits at the early, typical, and late harvest days producing \$24,306.64, \$25,099.10, and \$20,267.20, a reduction of approximately 40% from baseline aAh-free simulations. Latent infections (hypothesis 3) showed profit reductions like the bird vector hypothesis. Median profits were \$23,432.46, \$24,094.99, and \$19,228.19 for the successive harvest dates. Finally, the pond resident hypothesis also showed similar declines to the previous 2 hypotheses, netting median profits of \$24,365.81, \$25,776.37, and \$20,765.74 at days 260, 300, and 450, respectively. Results showed the infected fingerling hypothesis showed the most substantial decrease in potential profit compared to the other three hypotheses (Table 4.1).

Scenario evaluation

Antibiotic Usage

Using antibiotics to treat aAh consistently increased median profits regardless of the hypothesis operating. With antibiotics, hypotheses 2, 3 and 4 showed nearly identical median

profits when harvested on day 300 and 450 (Fig. 4.3); however, hypothesis 1 also showed the lowest profit among the different hypotheses, regardless of antibiotic usage. Results showed using antibiotic treatments could increase profits between \$4000 and \$6000 per pond. Antibiotic feed incurs a substantial cost to the farmer, but assuming a 70% treatment efficiency as in the present model, this additional cost appears to be outweighed by the reduction in fish loss due to an aAh outbreak.

Harvest Day

Harvesting at day 300 consistently yielded the highest profit, followed by day 260 and, finally, 450 in all scenarios (Fig. 4.3 to 4.7). The difference in profit between day 260 and 300 was least pronounced in the infected fingerling hypothesis (H1; Fig. 4.4) where values differed by less than \$2000. Interestingly, the profit difference in harvesting at these two times was most noticeable for the latent infection hypothesis (H3; Fig. 4.6). Harvesting at day 450 always yielded the lowest median profit, typically declining by \$4000 to \$6000 from day 300. This suggests day 300 provides a balance between maximum fish growth with minimal risk of fish loss to disease outbreaks and additional feed costs. Day 260 shares similar characteristics, but the additional 40 days of growth allowed for more profit per fish as weight increased.

Routine Monitoring

The decision to perform routine monitoring reduced profitability in most scenarios, particularly as time-to-harvest increased. The frequency of submissions showed minimal effect on median profits (Fig. 4.4-4.7) as 14- and 30-day intervals were nearly indistinguishable. Small differences could be seen in hypotheses 1 (Fig. 4.4) and 3 (Fig. 4.6) in which 14-day intervals were more profitable if harvest occurred at day 260. Alternatively, in the case of hypothesis 4

(Fig. 4.7), 30-day submission intervals were more profitable, and was similar to the outcome of no monitoring, if harvest did not occur until day 450.

Profits declined substantially as the number of fish submitted increased from 10 to 25 (Fig. 4.4-4.7). Diagnostic submissions of 25 fish reduced profit by approximately \$6000, on average. In most cases, submitting 10 fish per case also did not reduce simulated profits below scenarios with no monitoring by any appreciable amount. Unsurprisingly, submitting in 30-day intervals was always more profitable when 25 fish were submitted at a time. Regardless of the monitoring routine chosen, all profit values followed a similar pattern of optimal harvest at day 300, followed by harvesting at day 260, and the lowest profit at day 450.

Based on simulation results of 75 scenarios, certain policies were optimal across all introduction hypotheses evaluated. Medicated feed usage, based on visual inspection of mortalities, and harvesting at day 300 consistently yielded the highest median profit regardless of aAh hypothesis (Table 4.1). Conversely, all other policies showed some variability in the optimal scenarios based on the hypothesis being evaluated. For the infected fingerling hypothesis, monitoring in 14-day intervals with 10 fish per submission was the optimal scenario yielding a median profit of \$28,643.60. Meanwhile, the highest median profit for the bird vector hypothesis was \$29,836.70 which occurred with no monitoring. The optimal management strategy for the latent infection hypothesis was similar to hypothesis 1 where monitoring occurred every 14 days and 10 fish were submitted; this scenario resulted in a median profit of \$29,259.40. Lastly, the optimal policy for the pond resident hypothesis was also with no monitoring regime, yielding a simulated median profit of \$29,905.70. As previously mentioned, in all scenarios where the aAh was present, using medicated feed and harvesting at day 300 were part of the optimal scenario.

Sensitivity Analysis

Twelve sensitivity results were returned, examining the effects of different pathogen introduction hypotheses and disease dynamics variables (Fig. 4.8). Pond profit was relatively robust to disease variable changes. All model variants (hypothesis and fluctuating variable) showed differences of approximately \$50,000 between the minimum and maximum values returned during the analysis. All models have similar maxima since 50,000 fish was the maximum that could be harvest and sold. In 3 of the 4 hypotheses (H1, H2, and H4), the model was least sensitive to the recovery rate (smallest difference between minimum and maximum values); however, in H3 (*latent infections*) the model was least sensitive to the progression rate (Fig. 4.8). This could be because the pond system is already primed with infected fish from the start, so the transmission rate and recovery rate have a stronger influence on disease dynamics within the population. Also, H1 (*infected fingerlings*) and H4 (*pond resident*) were most sensitive to the progression rate showing a greater impact of fish moving from the latent state to infectious state on disease dynamics. Hypotheses H2 (*bird vector*) and H3 were most sensitive to transmission rate where fish moving between the susceptible state and latent state had the largest impact on pond profit estimates. Hypothesis 3 showed minimal change in sensitivity between disease variable.

Discussion and Conclusions

Here, the disease dynamics of aAh was modeled using a stochastic dynamic model. The aim of the model was to evaluate unknown aAh dynamics, such as the reservoir/vector and their potential impacts on the economics of the disease. In addition, we aimed to evaluate the effects of different modes of pathogen introduction on the potential profit of a catfish aquaculture pond. Disease management is a key aspect of maintaining profitability in catfish aquaculture (Wise et

al. 2008) so the ability to minimize pathogen impacts can provide increased profit in the long term. To date, no studies have evaluated these aspects of the disease, partially due to difficulties with waterborne lab challenges (Zhang et al. 2016). The model also included variables of feed and harvest economics to evaluate the direct impact of aAh timing and severity on the profitability of a farm pond. Based on simulation results, reactionary use of medicated feed and a typical harvest time provide the optimal profitability for a catfish operation.

Relatively little epidemiological knowledge of aAh at the commercial scale is known. Studies have confirmed acute epizootic cases with losses exceeding 10,000 kg of fish (Hemstreet 2010), with estimates indicating atypical strains are more than 200-times more virulent to channel catfish than other catfish (Pridgeon and Klesius 2011). The potential for birds to serve as vectors between farms and ponds has also been shown (Jubirt et al. 2015; Cunningham et al. 2018). However, due to the rapid onset of disease and subsequent mortality in lab studies (Hossain et al. 2013; Zhang et al. 2015), estimates of disease transmission variables are lacking and, as a result, a basic understanding of the disease dynamics at the commercial scale. In this model, the initial values of the progression coefficient (σ) and recovery rate (γ) were deliberately selected based on anecdotal (estimated fish mortalities) and empirical data (mean proportion of exposed fish in a pond; see Ch. 2) of aAh disease to emulate observed dynamics. Several aspects of our preliminary model are based on anecdotal reports and estimates from industry farmers, but we believe these anecdotal and observed data provide an adequate starting point for developing an epidemiological model of this disease. Additional sensitivity analyses could be used to evaluate the effect of these variables on system dynamics.

In controlled infectivity trials, nearly all mortality occurring as a result of aAh challenge occur within 48 hours post-challenge (Rasmussen-Ivey et al. 2016, Zhang et al. 2016a,b;

Abdelhamed et al. 2017). As challenge models are improved and lab studies more closely resemble commercial outbreaks, the infectious period of aAh would be a valuable research direction. Ogut (2001) determined the latency for *A. salmonicida* to be approximately 3 days in chinook salmon (*Oncorhynchus tshawytscha*) and the fish were infectious for just 2 days before succumbing to the disease. This short timeframe may also be found in aAh infections, but additional research is needed to begin evaluating the transmission variables more explicitly.

Simulation results differed based on the introduction hypothesis selected. The infected fingerling hypothesis resulted in the greatest loss of profit for the pond, reducing potential profits by nearly 50% over non-aAh simulations. The present model is based on a single-batch production system, but infected fingerlings have the potential to provide a consistent influx of aAh to a pond in multi-batch systems, which are more common in channel catfish production than single-batch variants. The hypothesis also has the potential to introduce a large number of carrier hosts into the system at a given time. Our model used a single carrier host at the beginning of the simulation to make results comparable to other hypotheses with no exposed/infected individuals to start (bird vector and pond resident hypotheses); however, a single stocking of 15,000 fry at 1% prevalence would provide 150 starting points for the proliferation of the disease.

The bird vector hypothesis raises many important questions. Cunningham et al. (2018) showed different bird species fed aAh-infected fish shed in inconsistent patterns for up to 10 days after switching to non-infected prey. In the present model we assume a bird sheds aAh for a maximum of 4 days and only 66% of birds will be shedding by day 4, as was shown in egrets (Jubirt et al. 2015). This model also consciously reduces the complexity of including an animal vector in an epidemiological model (see Eisen and Eisen 2014). The aim of this model was not to

evaluate or explain the dynamics of an animal vector, but rather to explore the potential implications on disease dynamics if aAh were reliant on a bird (or other animal) to introduce the pathogen to the population. *Aeromonas hydrophila* is a known pathogen of a variety of species commonly found near/in commercial ponds including frogs, turtles, and mammals, so other animal vectors could have been chosen for this role but birds are of particular interest to catfish farmers due to their other direct (predation) and indirect (disease transmission) impacts (Jubirt et al. 2015; Rosser et al. 2017; Cunningham et al. 2018). The short duration of shedding by piscivorous birds in previous studies suggests birds may be more likely to translocate the aAh pathogen among and within farm operations in a production season, rather than serving as a long-term reservoir between seasons.

Timing of fish harvest is a complex and important component of pond profitability. Each additional day fish are in a pond, they increase in value as weight increases, yet costs also accumulate in the form of feed, pond maintenance, aeration, and the chance of mortality and disease can further reduce profitability (Kumar and Engle 2017). It is important to find a balance to maximize fish size while minimizing feed costs and losses to mortality. In our model, harvesting fish at day 300 was optimal, followed by harvesting at day 260, and, finally, 450. Day 300 provided 40 additional days of growth over the day 260 harvest, increasing the value of each fish while minimizing the additional costs from feeding. Conversely, by day 450, fish had reached their peak weight (1.81 kg) and began to decline in value with additional weight; this combined with the additional feed costs caused a dramatic decline in potential profitability.

Routine monitoring has the potential to serve as an effective proactive method of managing aAh. Results from the SEIR model presented here showed routine monitoring incurred approximately \$500 in net loss for a farm. Much of this loss was attributable to an assumed \$50

fee accompanying diagnostic submission, though additional losses would also incur from direct loss of harvestable fish. The frequency of routine diagnostic submission (14 vs. 30 days) showed no significant effect on the profit loss, suggesting diagnostic monitoring at shorter or longer intervals may also be viable options; however, longer intervals would likely reduce the effectiveness of detecting the disease early. It is likely the rarity of aAh outbreaks in recent years (Ch. 2) is a major driver of potential losses. Simulations routinely consisted of replicates with no aAh outbreak, though it was relatively common for diagnostic monitoring to detect an infected fish triggering medicated feed use — increasing costs further. The model could benefit from adding a scenario where medicated feed is only triggered once per year via routine monitoring and all other medication usage is determined by overt outbreaks. This would minimize monitoring costs and still provide surveillance to detect the pathogen early without dramatic losses due to an outbreak. Atypical *A. hydrophila* is not commonly a recurring problem within a single pond (Ch. 2), so detection and treatment of a pond via routine monitoring once per year may be all that is required to minimize the risk of an outbreak. Columnaris and enteric septicemia of catfish (ESC) are notably more common in catfish aquaculture (Wagner et al. 2002) than aAh and would likely show more benefit from some type of routine monitoring program.

The robust nature of the model to disease dynamics variables raises interesting questions about disease management and future routes of research. One would expect the two hypotheses suggesting a fish-centric portal of introduction (H1 and H2) to show similar patterns of model sensitivity. However, the model was most sensitive to different variables for each hypothesis. The latent infection hypothesis (H3) was most sensitive to the transmission rate of the disease, suggesting the flow of individuals from the susceptible to latent states was the most important

driver whereas the infected fingerlings hypothesis (H1) was most sensitive to the rate of individuals moving from the latent state to the infectious state. The ecological mechanism causing this difference is unknown but warrants further study. It is also important to note that while differences in sensitivity between hypotheses were relatively small, approximately \$1000, this is only for a single pond. From the viewpoint of a farm with a large number of ponds, an aAh outbreak could show profit swings of \$20,000 to \$30,000 depending on which vector hypothesis is responsible for disease introduction and the true nature of the disease dynamics.

Catfish aquaculture is a for-profit industry, so practical and economical solutions are crucial to the decision-making and profitability of individual operations. The model constructed here contains a small aspect of economics directly affected by aAh epizootics. Using medicated feed is common practice for this and many other bacterial diseases; however, feed prices are more than doubled during the treatment period, which is 10 days for florfenicol (FWS.gov). So, understanding the costs and benefits of this treatment method are important to economic decisions. Using antibiotic feed resulted in nearly \$6,000 of additional profit for a single pond suggesting the additional cost associated with medicated feed is offset by the increased survival and subsequent harvest of fish. One important caveat to this is the timing of antibiotic use. In this model, medicated feed usage was triggered the day following a positive result from the diagnostic submissions and the submission may occur during routine monitoring or via increased single-day mortality above a given threshold. A longer lag time between positive diagnostics and treatment, or a larger mortality threshold would likely reduce the beneficial effects of the antibiotics and may result in a less economical outcome for the farmer.

The model presented here seeks to provide information on the disease dynamics of aAh in catfish aquaculture ponds. Unfortunately, much of this model has yet to be validated due to

difficulty in acquiring the relevant data. Lab studies have been relatively ineffective at producing consistent epizootic events mirroring those in the commercial industry. Using a compartmental model allows for monitoring states over time in a pond over time. This iterative process can be used to construct a time series of data and then the system dynamics model is fit to observed data to estimate rates and provide information on the epidemiology of the disease and estimate rates.

In addition, since approximately 2015 when the second aAh haplotype (S14-452) began to increase in prevalence across the Mississippi Delta where this work was performed, the number of epizootic cases has sharply declined (Ch. 2). These epizootics were important opportunities for field data collection through working relationships with local catfish operations. Certain regions of the industry have also shown a significant shift toward raising hybrid catfish (*I. punctatus* (f) x *I. furcatus* (m)) which show decreased susceptibility to aAh but are susceptible to diseases like *Edwardsiella piscicida* (Abayneh et al. 2013; Griffin et al. 2014; 2019). This model provides the foundation for future efforts to model the aAh disease and could be adapted to other emerging or otherwise data-lacking diseases within the industry and identify potential mechanisms for minimizing losses to individual operations. As empirical data is collected, the model allows for continual updating and a graphical interface to aid in communicating different aspects disease mechanisms to farmers and the general public.

Table 4.1 Median profits with 95% and 80% confidence intervals for each scenario evaluated. For binary variables, 0 is “no”, 1 is “yes”. All profit values are in USD (\$).

Medication	Hypothesis †	Monitor Frequency	Fish Submitted	Harvest Day	Lower 95% CI (\$)	Upper 95% CI (\$)	Lower 80% CI (\$)	Upper 80% CI (\$)	Median Profit (\$)
0	0	0	0	260	39,212	39,212	39,212	39,212	39,212
0	0	0	0	300	40,310	40,310	40,310	40,310	40,310
0	0	0	0	450	33,765	33,765	33,765	33,765	33,765
0	1	0	0	260	17,252	32,375	18,771	28,139	22,875
0	1	0	0	300	17,890	32,657	19,113	28,640	23,207
0	1	0	0	450	13,641	25,836	14,707	22,784	18,020
0	2	0	0	260	18,333	34,803	19,819	30,798	24,307
0	2	0	0	300	18,890	35,307	20,300	31,011	25,099
0	2	0	0	450	14,998	29,444	16,074	25,853	20,267

Table 4.1 (continued)

Medication	Hypothesis †	Monitor Frequency	Fish Submitted	Harvest Day	Lower 95% CI (\$)	Upper 95% CI (\$)	Lower 80% CI (\$)	Upper 80% CI (\$)	Median Profit (\$)
0	3	0	0	260	17,668	33,929	19,367	29,927	23,432
0	3	0	0	300	18,530	34,367	20,086	30,476	24,095
0	3	0	0	450	14,082	29,309	15,417	25,669	19,228
0	4	0	0	260	18,463	33,687	20,089	30,208	24,366
0	4	0	0	300	19,520	35,629	21,129	32,199	25,776
0	4	0	0	450	15,457	29,715	16,894	25,936	20,766
1	1	0	0	260	19,178	33,869	21,833	32,126	27,927
1	1	0	0	300	19,777	33,941	22,509	32,590	28,239
1	1	0	0	450	15,355	26,739	16,894	25,119	21,645
1	1	14	10	260	24,750	30,565	25,951	29,695	27,931

Table 4.1 (continued)

Medication	Hypothesis †	Monitor Frequency	Fish Submitted	Harvest Day	Lower 95% CI (\$)	Upper 95% CI (\$)	Lower 80% CI (\$)	Upper 80% CI (\$)	Median Profit (\$)
1	1	14	10	300	25,561	31,254	26,622	30,262	28,644
1	1	14	10	450	-	23,693	-	22,961	21,181
1	1	30	10	260	23,367	31,039	24,664	29,760	27,040
1	1	30	10	300	24,041	32,166	25,310	30,996	27,927
1	1	30	10	450	18,162	24,591	19,116	23,588	21,378
1	2	0	0	260	20,436	34,749	23,069	33,583	29,003
1	2	0	0	300	21,240	36,179	23,865	34,144	29,837
1	2	0	0	450	16,562	29,732	18,937	28,470	24,361
1	2	14	10	260	25,581	31,555	26,594	30,784	28,779
1	2	14	10	300	26,100	32,337	27,336	31,409	29,642

Table 4.1 (continued)

Medication	Hypothesis †	Monitor Frequency	Fish Submitted	Harvest Day	Lower 95% CI (\$)	Upper 95% CI (\$)	Lower 80% CI (\$)	Upper 80% CI (\$)	Median Profit (\$)
1	2	14	10	450	-	25,102	-	24,277	22,446
1	2	30	10	260	24,605	32,277	25,701	30,995	28,121
1	2	30	10	300	25,069	33,387	26,402	32,099	29,135
1	2	30	10	450	19,342	26,936	20,590	25,754	22,771
1	3	0	0	260	19,852	34,753	23,275	33,573	28,536
1	3	0	0	300	20,467	35,996	23,556	34,546	29,957
1	3	0	0	450	15,830	30,024	18,688	28,619	24,103
1	3	14	10	260	25,087	30,775	26,365	29,959	28,294
1	3	14	10	300	26,130	31,653	27,117	30,833	29,259
1	3	14	10	450	-	24,782	-	24,084	22,077

Table 4.1 (continued)

Medication	Hypothesis †	Monitor Frequency	Fish Submitted	Harvest Day	Lower 95% CI (\$)	Upper 95% CI (\$)	Lower 80% CI (\$)	Upper 80% CI (\$)	Median Profit (\$)
1	3	30	10	260	23,719	31,765	24,901	30,493	27,390
1	3	30	10	300	24,491	32,784	25,810	31,673	28,508
1	3	30	10	450	18,867	26,089	20,000	25,136	22,465
1	4	0	0	260	21,067	34,846	23,981	33,191	29,253
1	4	0	0	300	20,966	36,390	24,793	34,765	29,906
1	4	0	0	450	16,803	30,545	19,427	29,117	24,328
1	4	14	10	260	25,297	31,371	26,440	30,693	28,879
1	4	14	10	300	25,880	32,211	27,128	31,420	29,600
1	4	14	10	450	-	25,254	-	24,438	22,574
1	4	30	10	260	25,273	32,729	26,334	31,502	28,613

Table 4.1 (continued)

Medication	Hypothesis †	Monitor Frequency	Fish Submitted	Harvest Day	Lower 95% CI (\$)	Upper 95% CI (\$)	Lower 80% CI (\$)	Upper 80% CI (\$)	Median Profit (\$)
1	4	30	10	300	26,037	34,234	26,955	32,529	29,528
1	4	30	10	450	20,610	27,294	21,521	25,957	23,721
1	1	14	25	260	16,797	30,898	18,171	27,450	22,039
1	1	14	25	300	17,059	31,753	18,650	28,398	22,222
1	1	14	25	450	12,200	23,817	13,322	20,782	16,705
1	1	30	25	260	16,729	31,852	18,356	28,206	21,949
1	1	30	25	300	17,630	32,237	18,921	28,768	22,646
1	1	30	25	450	12,698	24,826	13,730	22,007	17,257
1	2	14	25	260	17,782	33,634	19,413	29,682	23,952
1	2	14	25	300	18,204	34,419	19,563	30,815	24,066

Table 4.1 (continued)

Medication	Hypothesis †	Monitor Frequency	Fish Submitted	Harvest Day	Lower 95% CI (\$)	Upper 95% CI (\$)	Lower 80% CI (\$)	Upper 80% CI (\$)	Median Profit (\$)
1	2	14	25	450	13,386	28,137	14,894	24,407	18,782
1	2	30	25	260	17,869	34,166	19,433	30,017	24,068
1	2	30	25	300	18,846	35,090	20,295	31,469	25,157
1	2	30	25	450	14,217	28,958	15,628	26,260	19,662
1	3	14	25	260	16,600	33,114	18,203	29,144	22,502
1	3	14	25	300	17,238	34,112	18,832	29,580	23,146
1	3	14	25	450	12,784	27,393	14,083	23,295	17,667
1	3	30	25	260	17,507	32,918	18,913	28,790	22,939
1	3	30	25	300	18,229	34,828	19,745	29,985	23,826
1	3	30	25	450	13,677	28,071	15,023	24,655	18,879

Table 4.1 (continued)

Medication	Hypothesis †	Monitor Frequency	Fish Submitted	Harvest Day	Lower 95% CI (\$)	Upper 95% CI (\$)	Lower 80% CI (\$)	Upper 80% CI (\$)	Median Profit (\$)
1	4	14	25	260	18,461	33,181	19,809	29,386	23,809
1	4	14	25	300	18,462	35,564	20,229	31,571	24,568
1	4	14	25	450	13,476	27,536	14,956	24,607	19,142
1	4	30	25	260	17,968	33,349	19,589	30,142	24,247
1	4	30	25	300	18,797	35,241	20,389	31,579	25,128
1	4	30	25	450	14,117	31,101	15,373	25,774	19,688

Note: † Hypothesis = 0 represents scenarios with aAh was not present and served as the baseline for pond profit.

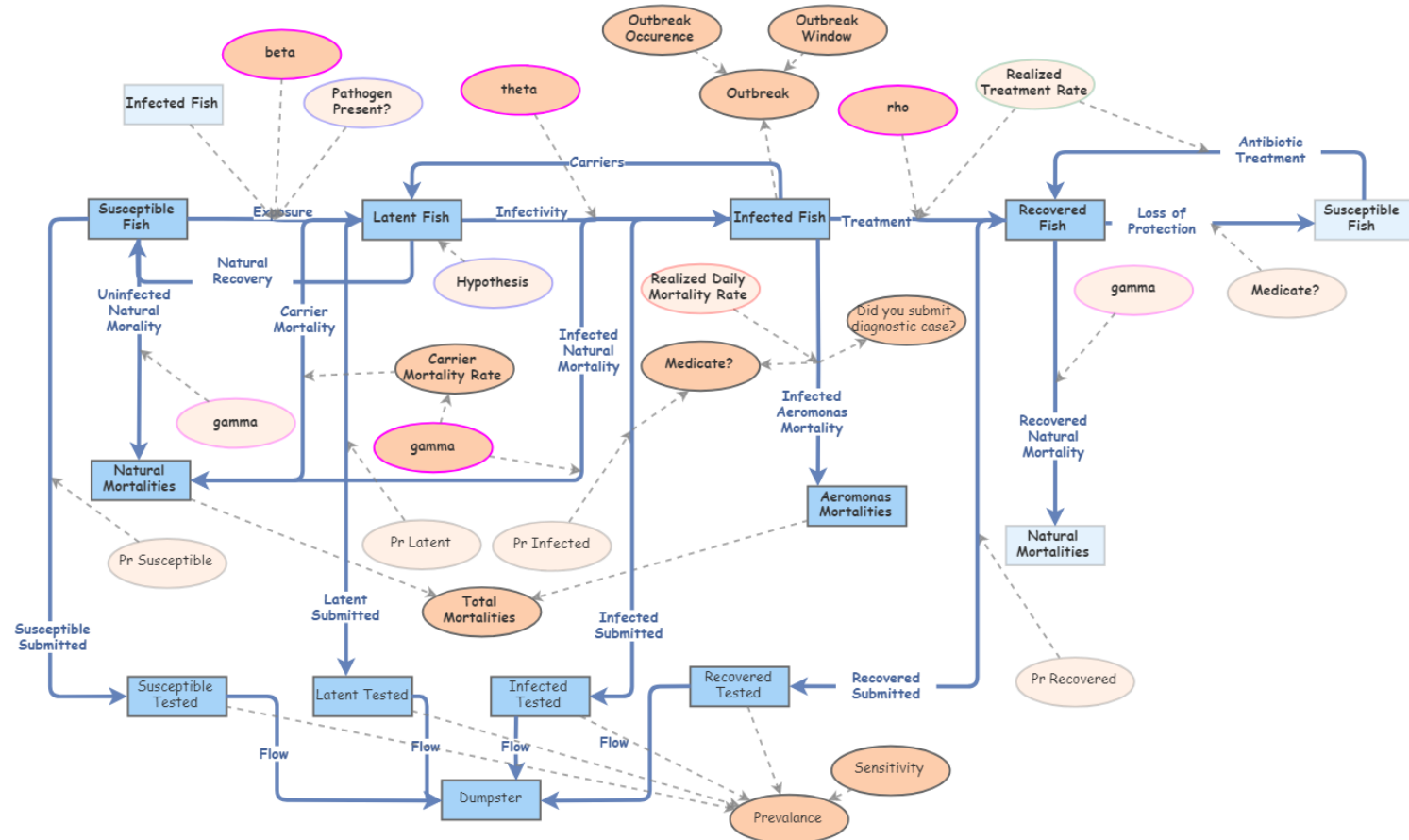


Figure 4.1 Epidemiological (SEIR) model constructed for atypical *Aeromonas hydrophila* (aAh) disease dynamics.

Variables outlined in pink are disease transmission variables and represent the transmission rate (β), progression rate (θ), recovery rate (ρ), natural mortality rate (γ), and disease-specific mortality rate (α ; not shown).

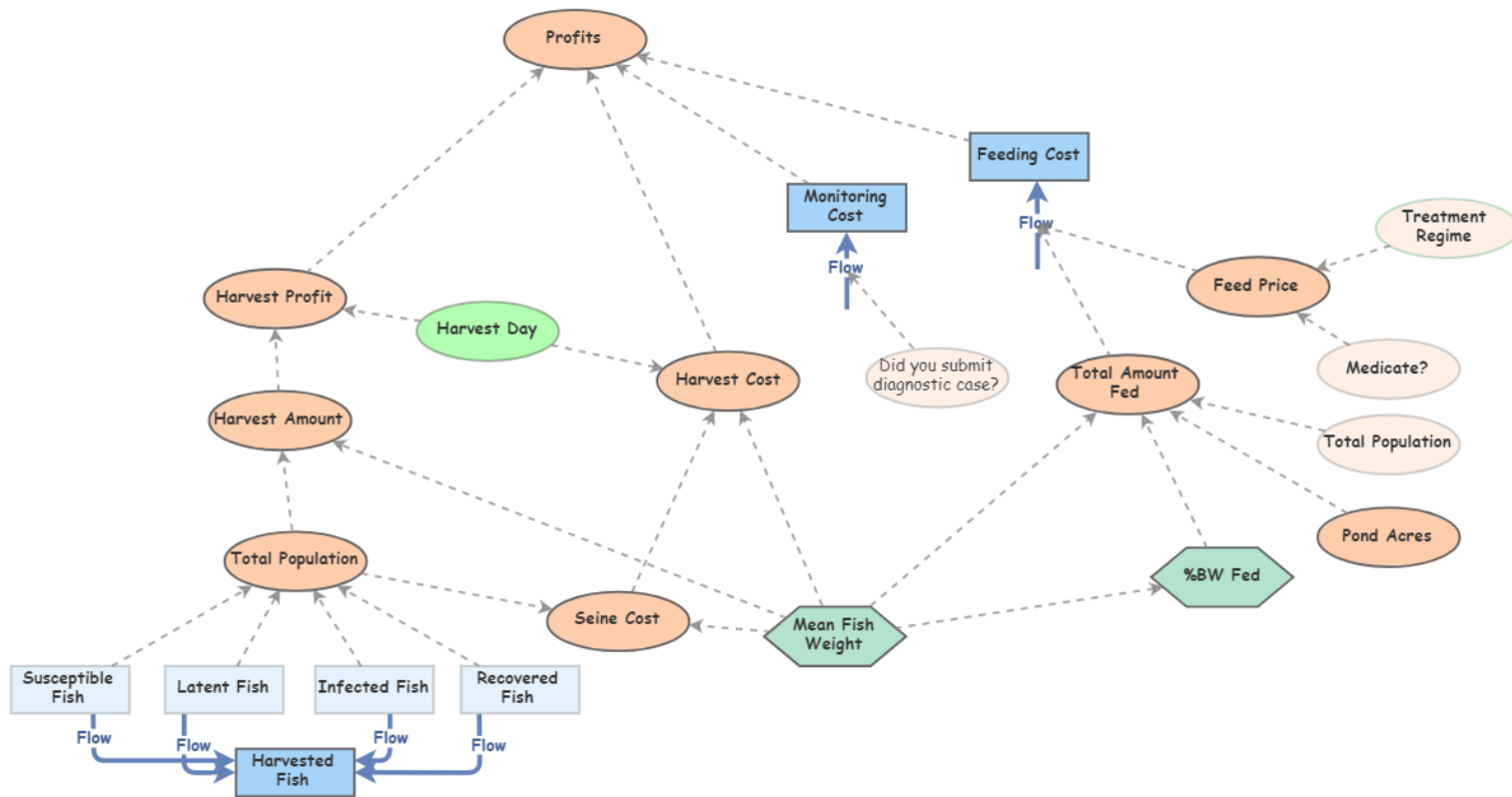


Figure 4.2 Economics portion of the epidemiological model constructed.

Harvest cost and profit were pulsed into the overall *Profits* on the harvest day selected. Feeding costs were the cumulative costs of feeding fish up to the day of harvest and accounts for the difference in feed price if medication is triggered or not.

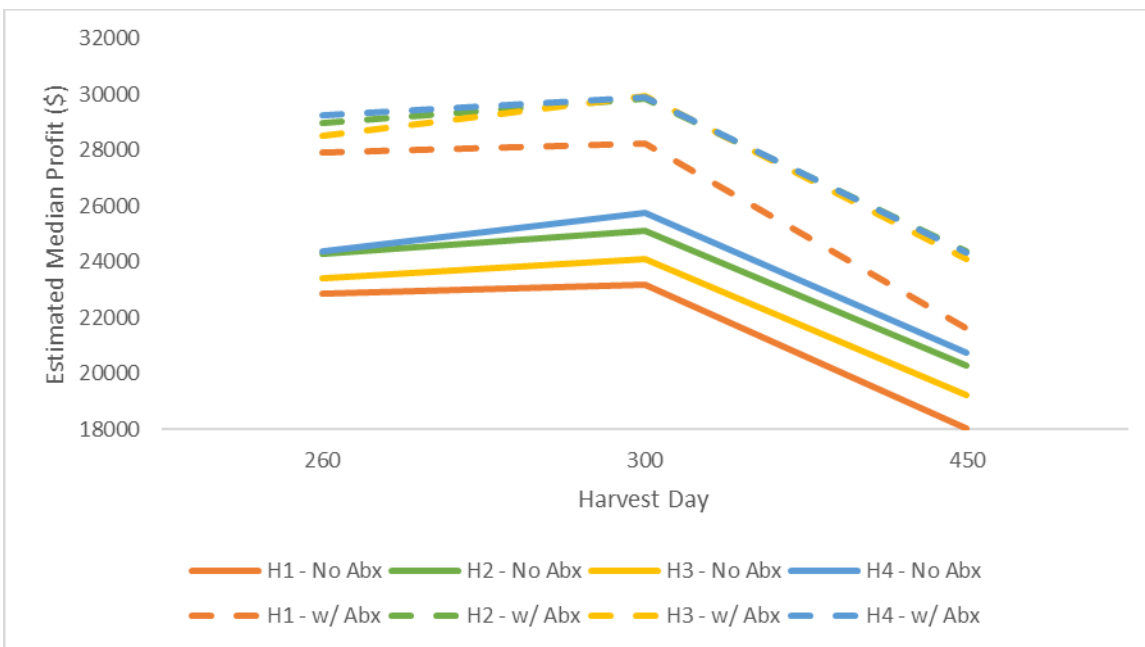


Figure 4.3 Plot of median profit with and without antibiotic usage by harvest day. Solid lines represent no antibiotic usage; dashed lines indicate antibiotic use. Results based on 500 simulations for each scenario. “Abx” = antibiotics.

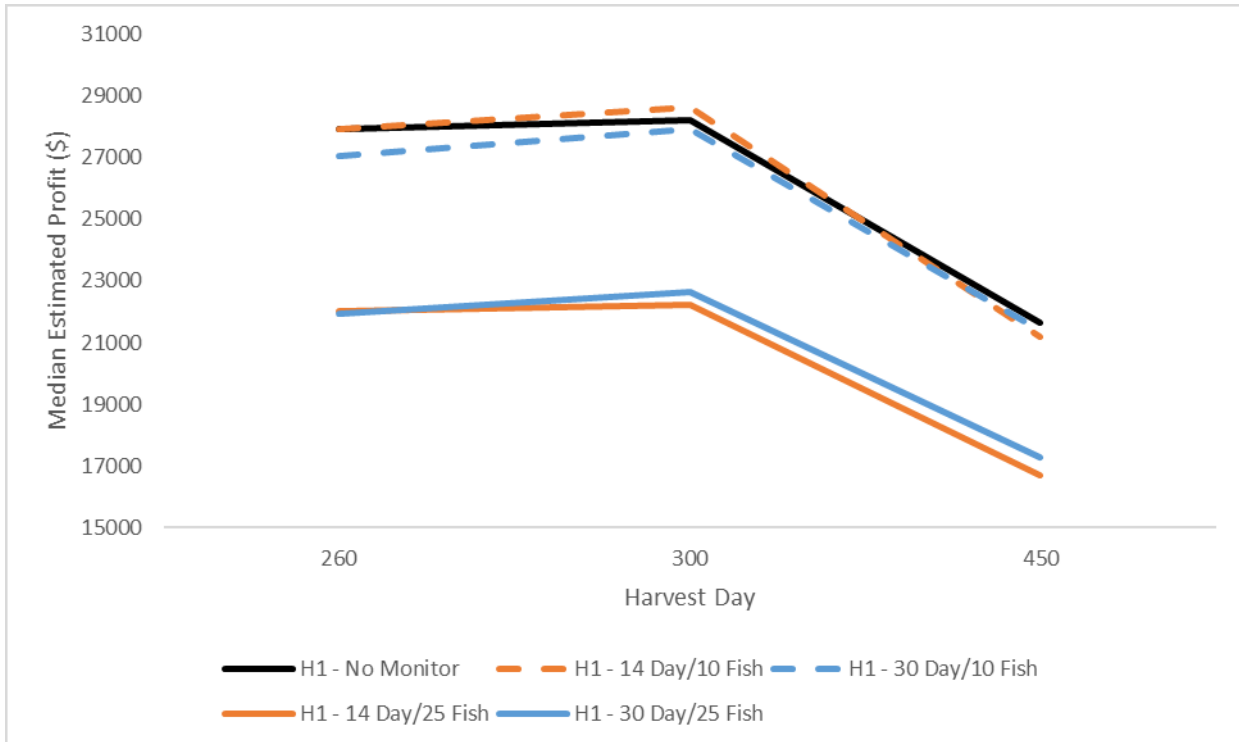


Figure 4.4 Simulated median profit by harvest day given the hypothesis of infected fingerlings. The black, solid line shows the median profit with no diagnostic monitoring. Orange and blue lines represent 14- and 30-day intervals in diagnostic monitoring submissions, respectively. Dashed lines represent scenarios with 10 fish submitted per monitoring, solid lines represent cases with 25 fish submitted.

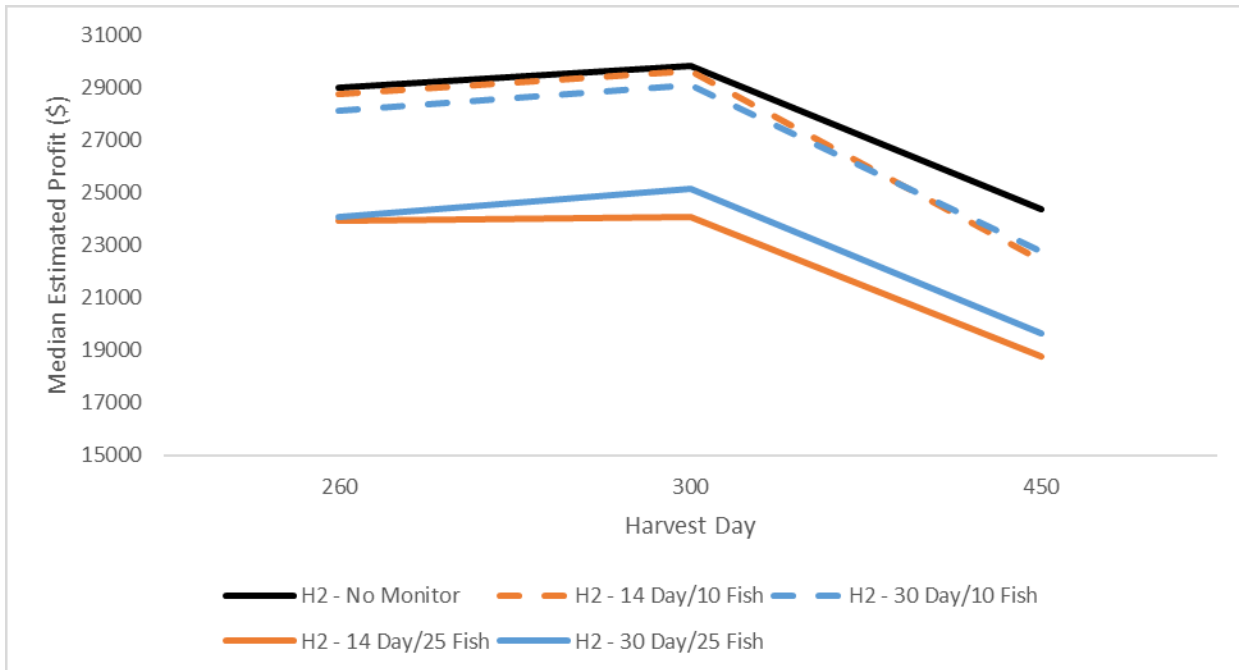


Figure 4.5 Simulated median profit by harvest day given the hypothesis of aAh introduction via birds. The black, solid line shows the median profit with no diagnostic monitoring. Orange and blue lines represent 14- and 30-day intervals in diagnostic monitoring submissions, respectively. Dashed lines represent scenarios with 10 fish submitted per monitoring, solid lines represent cases with 25 fish submitted.

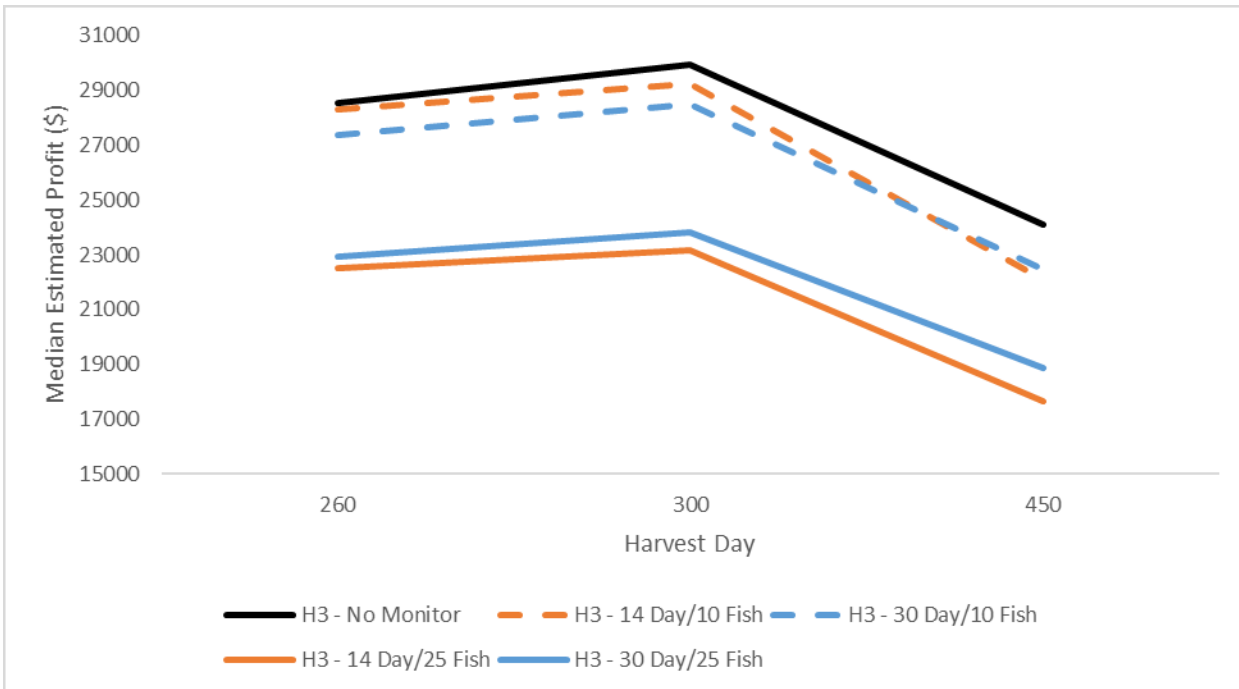


Figure 4.6 Simulated median profit by harvest day given the hypothesis of latent aAh carrier fish. The black, solid line shows the median profit with no diagnostic monitoring. Orange and blue lines represent 14- and 30-day intervals in diagnostic monitoring submissions, respectively. Dashed lines represent scenarios with 10 fish submitted per monitoring, solid lines represent cases with 25 fish submitted.

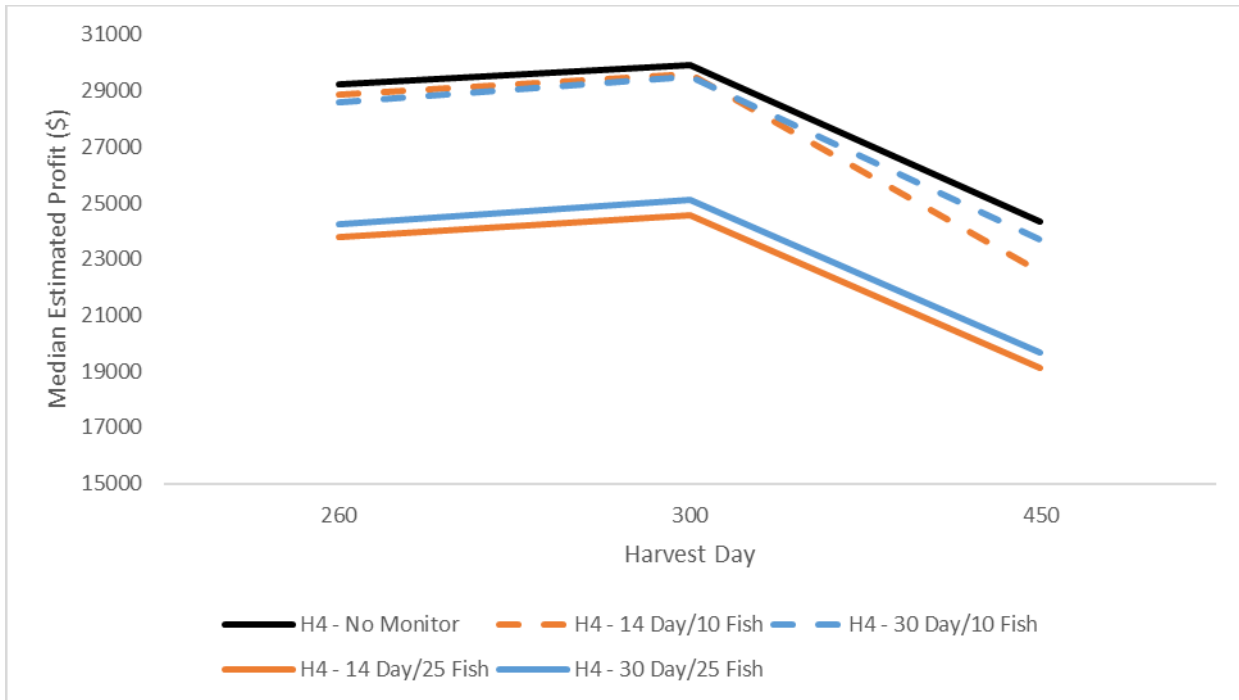


Figure 4.7 Simulated median profit by harvest day given the hypothesis of aAh as a pond resident. The black, solid line shows the median profit with no diagnostic monitoring. Orange and blue lines represent 14- and 30-day intervals in diagnostic monitoring submissions, respectively. Dashed lines represent scenarios with 10 fish submitted per monitoring, solid lines represent cases with 25 fish submitted.

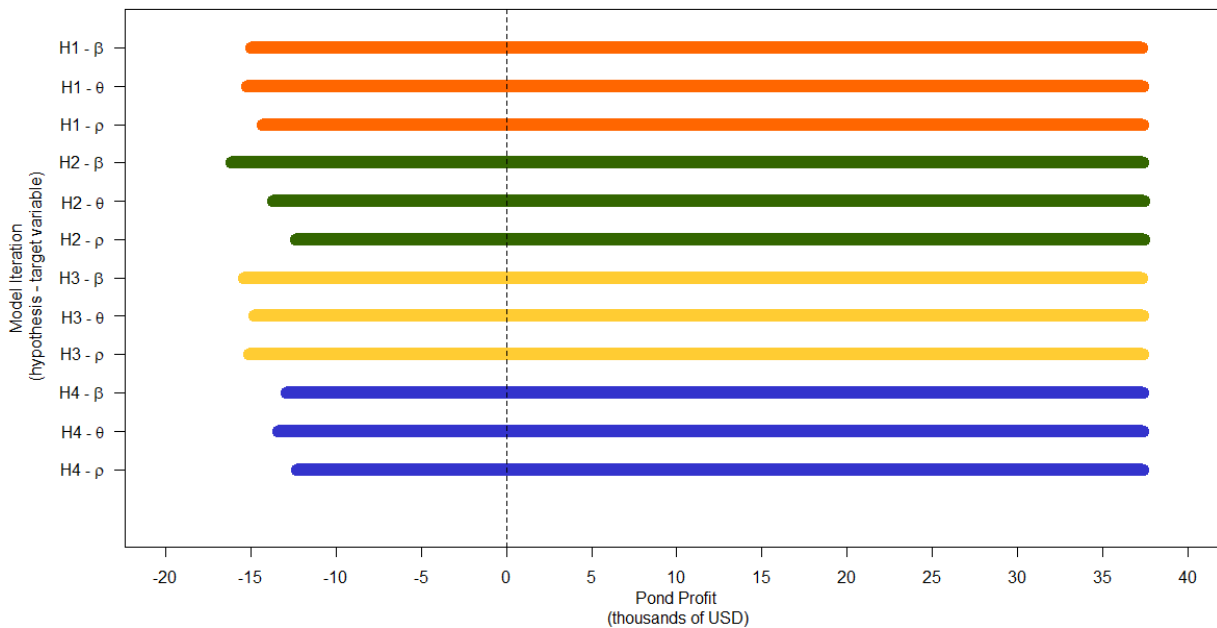


Figure 4.8 Tornado plot of pond profit sensitivity grouped by hypothesis and disease variable. Plot is color-coded by hypothesis for readability. Hypothesis numbers correspond to modes of pathogen introduction via *infected fingerlings*, *bird vector*, *latent infections*, and *pond resident*, respectively. Disease variables are transmission rate (β ; beta), progression rate (θ ; theta), and recovery rate (ρ ; rho). Breakeven point is denoted by the hashed vertical line. Sensitivity based on 1000 iterations and each variable was allowed to vary by 20% of the initial values reported by previous studies. All profit values are in thousands of USD and represent the range of values recorded for each analysis.

REFERENCES

- Abayneh, T., Colquhoun, D. J., and Sørum, H. 2013. *Edwardsiella piscicida* sp. nov., a novel species pathogenic to fish. *Journal of applied microbiology*, 114(3), 644-654.
- Abdelhamed, H., Ibrahim, I., Baumgartner, W., Lawrence, M. L., and Karsi, A. 2017. Characterization of histopathological and ultrastructural changes in channel catfish experimentally infected with virulent *Aeromonas hydrophila*. *Frontiers in microbiology*, 8, 1519.
- Abu-Elala, N. M., Abd-Elsalam, R. M., Marouf, S., Abdelaziz, M., and Moustafa, M. 2016. Eutrophication, Ammonia Intoxication, and Infectious Diseases: Interdisciplinary Factors of Mass Mortalities in Cultured Nile Tilapia. *Journal of Aquatic Animal Health*, 28(3), 187-198.
- Albarral, V., Sanglas, A., Palau, M., Miñana-Galbis, D., and Fusté, M. C. 2016. Potential pathogenicity of *Aeromonas hydrophila* complex strains isolated from clinical, food, and environmental sources. *Canadian journal of microbiology*, 62(4), 296-306.
- Allen, J. L. 1988. Residues of benzocaine in rainbow trout, largemouth bass, and fish meal. *The Progressive Fish-Culturist*, 50(1), 59-60.
- Ansary, A., Haneef, R. M., Torres, J. L., and Yadav, M. 1992. Plasmids and antibiotic resistance in *Aeromonas hydrophila* isolated in Malaysia from healthy and diseased fish. *Journal of Fish Diseases*, 15(2), 191-196.
- Araoju, R. M., Arribas, R. M., and Pares, R. 1991. Distribution of *Aeromonas* species in waters with different level of pollution. *Journal of Applied Bacteriology*, 71, 182-186.
- Austin, B., and Austin, D. A. 2012. Aeromonadaceae representative (*Aeromonas salmonicida*). In *Bacterial fish pathogens* (pp. 147-228). Springer: Netherlands.
- Awan, F., Dong, Y., Liu, J., Wang, N., Mushtaq, M. H., Lu, C., and Liu, Y. 2018. Comparative genome analysis provides deep insights into *Aeromonas hydrophila* taxonomy and virulence-related factors. *BMC Genomics*, 19(1), 712. doi: 10.1186/s12864-018-5100-4
- Baumgartner, W. A., Ford, L. and Hanson, L., 2017. Lesions caused by virulent *Aeromonas hydrophila* in farmed catfish (*Ictalurus punctatus* and *I. punctatus* × *I. furcatus*) in Mississippi. *Journal of Veterinary Diagnostic Investigation*, 29(5), 747-751.

- Bebak, J., Wagner, B., Burnes, B., and Hanson, T. 2015. Farm size, seining practices, and salt use: risk factors for *Aeromonas hydrophila* outbreaks in farm-raised catfish, Alabama, USA. *Preventive veterinary medicine*, 118(1), 161-168.
- Benskin, C. M. H., Wilson, K., Jones, K., and Hartley, I. R. 2009. Bacterial pathogens in wild birds: a review of the frequency and effects of infection. *Biological Reviews*, 84(3), 349-373.
- Bosworth, B. G., Wise, D. J., Terhune, J. S., and Wolters, W. R. 2003. Family and genetic group effects for resistance to proliferative gill disease in channel catfish, blue catfish and channel catfish × blue catfish backcross hybrids. *Aquaculture Research*, 34(7), 569-573.
- Bosworth, B. G., Wolters, W. R., Silva, J. L., Chamul, R. S., and Park, S. 2004. Comparison of production, meat yield, and meat quality traits of NWAC103 line channel catfish, Norris line channel catfish, and female channel catfish× male blue catfish F1 hybrids. *North American Journal of Aquaculture*, 66(3), 177-183.
- Bowser, P. R., and Conroy, J. D. 1985. Histopathology of gill lesions in channel catfish associated with *Henneguya*. *Journal of Wildlife Diseases*, 21(2), 177-179.
- Bowser, P. R., Falls, W. W., VanZandt, J., Collier, N., and Phillips, J. D. (1983). Methemoglobinemia in channel catfish: methods of prevention. *The Progressive Fish-Culturist*, 45(3), 154-158.
- Bowser, P. R., Munson, A. D., Jarboe, H. H., Francis-Floyd, R. and Waterstrat, P. R. 1985. Isolation of channel catfish virus from channel catfish, *Ictalurus punctatus* (Rafinesque), brood-stock. *Journal of Fish Diseases* 8, 557-561.
- Boyd, C. E., Torrans, E. L., and Tucker, C. S. 2018. Dissolved oxygen and aeration in ictalurid catfish aquaculture. *Journal of the World Aquaculture Society*, 49(1), 7-70.
- Brauer, F. 2008. Compartmental models in epidemiology. In *Mathematical epidemiology* (pp. 19-79). Springer, Berlin, Heidelberg.
- Brinkman, N. E., Haugland, R. A., Wymer, L. J., Byappanahalli, M., Whitman, R. L., and Vesper, S. J. 2003. Evaluation of a rapid, quantitative real-time PCR method for enumeration of pathogenic *Candida* cells in water. *Applied and Environmental Microbiology*, 69(3), 1775-1782.
- Bromley, J., Jackson, N. A., Clymer, O. J., Giacomello, A. M., and Jensen, F. V. 2005. The use of Hugin® to develop Bayesian networks as an aid to integrated water resource planning. *Environmental Modelling and Software*, 20(2), 231-242.
- Bustin, S. A., Benes, V., Garson, J. A., Hellemans, J., Huggett, J., Kubista, M., Mueller, R., Nolan, T., Pfaffl, M. W., Shipley, G. L., and Vandesompele, J. 2009. The MIQE guidelines: Minimum Information for publication of Quantitative real-time PCR Experiments. *Clinical Chemistry*, 55, 611-622.

- Cai, W., and Arias, C. R. 2017. Biofilm formation on aquaculture substrates by selected bacterial fish pathogens. *Journal of aquatic animal health*, 29(2), 95-104.
- Cai, W., Willmon, E., Burgos, F. A., Ray, C. L., Hanson, T., and Arias, C. R. 2019. Biofilm and sediment are major reservoirs of virulent *Aeromonas hydrophila* (vah) in catfish production ponds. *Journal of aquatic animal health*, 31(1), 112-120.
- Camus, A. C., Durborow, R. M., Hemstreet, W. G., Thune, R. L., and Hawke, J. P. 1998. Aeromonas Bacterial Infections – Motile Aeromonad Septicemia. *Southern Regional Aquaculture Center (SRAC) Publication 478*.
- Camus, A. C., P. Gaunt, and M. Mauel. 2006. 2006 Annual Case Summary Report. Mississippi State College of Veterinary Medicine, Aquatic Diagnostic Laboratory, National Warmwater Aquaculture Center, Stoneville.
- Chang, M. C., and Huang, T. C. 1981. Effects of the predation of *Tetrahymena pyriformis* on the population of *Aeromonas hydrophila*. *National Science Council Mon.*, 9(7), 552-556.
- Chaudhury, A., Nath, G., Shukla, B.N., and Sanyal, S.C. 1996. Biochemical characterization, enteropathogenicity, and antimicrobial resistance plasmids of clinical and environmental *Aeromonas* isolates. *Journal of Medical Microbiology*, 44, 434-437.
- Chen, H. Q., and C. P. Lu, 1991: Study on the pathogen of epidemic septicaemia occurred in cultured cyprinoid fishes in southeastern China. *J. Nanjing Agric. Univ.* 14, 87–91.
- Cipriano, R. C., Bullock, G. L., and Pyle, S. W. 1984. *Aeromonas hydrophila* and motile aeromonad septicemias of fish. *US Fish and Wildlife Service*, 68, 0-23.
- Colvin, M. E., Peterson, J. T., Kent, M. L., and Schreck, C. B. 2015. Occupancy modeling for improved accuracy and understanding of pathogen prevalence and dynamics. *PLoS one*, 10(3), e0116605. doi:10.1371/journal.pone.0116605.
- Costanza, R., and Ruth, M. 1998. Using dynamic modeling to scope environmental problems and build consensus. *Environmental management*, 22(2), 183-195.
- Cunningham, F. L., Jubirt, M. M., Hanson-Dorr, K. C., Ford, L., Fioranelli, P., and Hanson, L. A. 2018. Potential of double-crested cormorants (*Phalacrocorax auritus*), american white pelicans (*Pelecanus erythrorhynchos*), and wood storks (*Mycteria americana*) to transmit a hypervirulent strain of *Aeromonas hydrophila* between channel catfish culture ponds. *Journal of Wildlife Diseases*, 54(3), 548-552.
- Davis, W. A., J. G. Kane, and V. G. Garagusi. 1978. Human *Aeromonas* infections: a review of the literature and a case report of endocarditis. *Medicine*, 57, 267-277.
- De Figueiredo, J., and Plumb, J. A. 1977. Virulence of different isolates of *Aeromonas hydrophila* in channel catfish. *Aquaculture*, 11(4), 349-354.

- de Jong, M. C. M., Diekmann, O., and Heesterbeek, H. 1995. How does transmission of infection depend on population size. D. Mollison (Ed.), *Epidemic Models: Their Structure and Relation to Data*, Newton Institution Publications, London, pp. 84-94
- Deng, G. C., Jiang, X. Y., Ye, X., Liu, M. Z., Xu, S. Y., Liu, L. H., Bai, Y. Q. and Luo, X. 2009. Isolation, identification and characterization of *Aeromonas hydrophila* from hemorrhagic grass carp. *Microbiol. China*, 36, 1170-1177.
- Dlamini, W. M. (2010). A Bayesian belief network analysis of factors influencing wildfire occurrence in Swaziland. *Environmental Modelling and Software*, 25(2), 199-208.
- Doffitt, C. M., Pote, L. M., and King, D. T. 2009. Experimental *Bolbophorus damnificus* (Digenea: Bolbophoridae) infections in piscivorous birds. *Journal of Wildlife Diseases*, 45(3), 684-691.
- Dorr, B. S., Burger, L. W., Barras, S. C., and Godwin, K. C. 2012. Economic impact of double-crested cormorant, *Phalacrocorax auritus*, depredation on channel catfish, *Ictalurus punctatus*, aquaculture in Mississippi, USA. *Journal of the World Aquaculture Society*, 43(4), 502-513.
- Dunham, R. A., Lambert, D. M., Argue, B. J., Ligeon, C., Yant, D. R., and Liu, Z. 2000. Comparison of manual stripping and pen spawning for production of channel catfish×blue catfish hybrids and aquarium spawning of channel catfish. *North American Journal of Aquaculture*, 62(4), 260-265.
- Dunham, R. A., Smitherman, R. O., and Webber, C. 1983. Relative tolerance of channel x blue hybrid and channel catfish to low oxygen concentrations. *The Progressive Fish-Culturist*, 45(1), 55-57.
- Earn, D. J., Rohani, P., Bolker, B. M., and Grenfell, B. T. 2000. A simple model for complex dynamical transitions in epidemics. *Science*, 287(5453), 667-670.
- Eisen, R. J., and Eisen, L. 2014. Spatial modeling of human risk of exposure to vector-borne pathogens based on epidemiological versus arthropod vector data. *Journal of medical entomology*, 45(2), 181-192.
- Engle, C. R. 2010. *Aquaculture economics and financing: management and analysis*. John Wiley & Sons. 272 pp.
- Engle, C. R. and Pounds, G. L. 1994. Trade-offs between single-and multiple-batch production of channel catfish, *Ictalurus punctatus*: an economics perspective. *Journal of Applied Aquaculture*, 3(3-4), 311-332.
- FAO, 2010. The state of the world fisheries and aquaculture 2010. Food and Agriculture Organization of the United Nations, Rome, Italy, 218 pages.

- Farmani, R., Henriksen, H. J., and Savic, D. 2009. An evolutionary Bayesian belief network methodology for optimum management of groundwater contamination. *Environmental Modelling and Software*, 24(3), 303-310.
- Forsberg, J. A., Eberhardt, J., Boland, P. J., Wedin, R., and Healey, J. H. 2011. Estimating survival in patients with operable skeletal metastases: an application of a bayesian belief network. *PloS one*, 6(5).
- Fry, F. E. 1969. Some possible physiological stresses induced by eutrophication. In *Eutrophication: Causes, Consequences, Correctives*, pp. 531-536. Washington: National Academy of Science.
- Garrett, T. R., Bhakoo, M., and Zhang, Z. 2008. Bacterial adhesion and biofilms on surfaces. *Progress in Natural Science*, 18(9), 1049-1056.
- Gelman, A., and Rubin, D. B. 1992. Inference from iterative simulation using multiple sequences. *Statistical Science*, 7: 457–511.
- Glahn, J. F. and King, D. T. 2004. Bird depredation. In *Developments in Aquaculture and Fisheries Science* (Vol. 34, pp. 503-529). Elsevier.
- Glahn, J. F., and Dorr, B. S. 2002. Captive double-crested cormorant *Phalacrocorax auritus* predation on channel catfish *Ictalurus punctatus* fingerlings and its influence on single-batch cropping production. *Journal of the World Aquaculture Society*, 33(1), 85-93.
- Glahn, J. F., Tomsa, T., and Preusser, K. J. 1999. Impact of great blue heron predation at trout-rearing facilities in the northeastern United States. *North American Journal of Aquaculture*, 61(4), 349-354.
- Green, B. W., and Rawles, S. D. 2010. Comparative growth and yield of channel catfish and channel× blue hybrid catfish fed a full or restricted ration. *Aquaculture Research*, 41(9), e109-e119.
- Griffin, M. J., Camus, A. C., Wise, D. J., Greenway, T. E., Mauel, M. J., and Pote, L. M. 2010. Variation in susceptibility to *Henneguya ictaluri* infection by two species of catfish and their hybrid cross. *Journal of Aquatic Animal Health*, 22(1), 21-35.
- Griffin, M. J., Goodwin, A. E., Merry, G. E., Liles, M. R., Williams, M. A., Ware, C., and Waldbieser, G. C. 2013. Rapid quantitative detection of *Aeromonas hydrophila* strains associated with disease outbreaks in catfish aquaculture. *Journal of Veterinary Diagnostic Investigations*, 25(4), 473-481.
- Griffin, M. J., Greenway, T. E., and Wise, D. J. 2017. *Edwardsiella* spp. Fish viruses and bacteria: Pathobiology and protection, 190-210.

- Griffin, M. J., Pote, L.M., Camus, A.C., Mauel, M.J., Greenway, T.E. and Wise, D.J. 2009. Application of a real-time PCR assay for the detection of *Henneguya ictaluri* in commercial channel catfish ponds. *Diseases of aquatic organisms*, 86(3), 223-233.
- Griffin, M. J., Reichley, S. R., Baumgartner, W. A., Aarattuthodiyil, S., Ware, C., Steadman, J. M., Lewis, M., Gaunt, P.S., Khoo, L.H. and Wise, D. J. 2019. Emergence of *Edwardsiella piscicida* in farmed channel♀, *Ictalurus punctatus* × blue♂, *Ictalurus furcatus*, hybrid catfish cultured in Mississippi. *Journal of the World Aquaculture Society*, 50(2), 420-432.
- Griffin, M. J., Ware, C., Quiniou, S. M., Steadman, J. M., Gaunt, P. S., Khoo, L. H., and Soto, E. 2014. *Edwardsiella piscicida* identified in the southeastern USA by *gyrB* sequence, species-specific and repetitive sequence-mediated PCR. *Diseases of aquatic organisms*, 108(1), 23-35.
- Griffin, M. J., Wise, D. J., Camus, A. C., Mauel, M. J., Greenway, T. E., and Pote, L. M. 2008. A real-time polymerase chain reaction assay for the detection of the myxozoan parasite *Henneguya ictaluri* in channel catfish. *Journal of Veterinary Diagnostic Investigation*, 20(5), 559-566.
- Griffin, M.J., Wise, D.J., Yost, M.C., Doffitt, C.M., Pote, L.M., Greenway, T.E. and Khoo, L.H., 2010. A duplex real-time polymerase chain reaction assay for differentiation between *Bolbophorus damnificus* and *Bolbophorus* type II species cercariae. *Journal of Veterinary Diagnostic Investigation*, 22(4), 615-622.
- Gupta, A., Gupta, P., and Dhawan, A. 2016. *Paenibacillus polymyxa* as a water additive improved immune response of *Cyprinus carpio* and disease resistance against *Aeromonas hydrophila*. *Aquaculture Reports*, 4, 86-92.
- Hallett, S. L., and Bartholomew, J. L. 2006. Application of a real-time PCR assay to detect and quantify the myxozoan parasite *Ceratomyxa shasta* in river water samples. *Diseases of Aquatic Organisms*, 71(2), 109-118.
- Hänninen, M., and Kujala, P. 2012. Influences of variables on ship collision probability in a Bayesian belief network model. *Reliability Engineering and System Safety*, 102, 27-40.
- Hanson, L., Liles, M. R., Hossain, M. J., Griffin, M. J., Hemstreet, W. 2014. Motile Aeromonas Septicemia. In: Fish Health Section Blue Book Edition 2014, Section 1.2.9. American Fisheries Society-Fish Health Section, Bethesda, Maryland
- Harikrishnan, R., Rani, M. N., and Balasundaram, C. 2003. Hematological and biochemical parameters in common carp, *Cyprinus carpio*, following herbal treatment for *Aeromonas hydrophila* infection. *Aquaculture*, 221(1), 41-50.
- Hazen, T. C., Esch, G. W., Dimock Jr, R. V., and Mansfield, A. 1982. Chemotaxis of *Aeromonas hydrophila* to the surface mucus of fish. *Current Microbiology*, 7(6), 371-375.

- Hazen, T. C., Fliermans, C. B., Hirsch, R. P., and Esch, G. W. 1978. Prevalence and distribution of *Aeromonas hydrophila* in the United States. *Applied and Environmental Microbiology*, 36(5), 731-738.
- Hemstreet, B. 2010. An update on *Aeromonas hydrophila* from a fish health specialist for summer 2010. *Catfish Journal*, 24(4).
- Hethcote, H. W. 1989. Three basic epidemiological models. In *Applied mathematical ecology* (pp. 119-144). Springer, Berlin, Heidelberg.
- Ho, B. T., Fu, Y., Dong, T. G., and Mekalanos, J. J. 2017. *Vibrio cholerae* type 6 secretion system effector trafficking in target bacterial cells. *Proceedings of the National Academy of Sciences*, 114(35), 9427-9432.
- Hogarth, R. 1987. Judgment and choice. John Wiley and Sons: Chichester, England.
- Hossain, M. J., Sun, D., McGarey, D. J., Wrenn, S., Alexander, L. M., Martino, M. E., Xing, Y., Terhune, J. S., and Liles, M. R. 2014. An Asian origin of virulent *Aeromonas hydrophila* responsible for disease epidemics in United States-farmed catfish. *Molecular Bio*, 5(3), e00848-14. doi: 10.1128/mbio.00848-14
- Hossain, M. J., Waldbieser, G. C., Sun, D., Capps, N. K., Hemstreet, W. B., Carlisle, K., Griffin, M. J., Khoo, L., Goodwin, A. E., Sonstegard, T. S., Schroeder, S., Hayden, K., Newton, J. C., Terhune, J. S., and Liles, M. R. 2013. Implication of lateral genetic transfer in the emergence of *Aeromonas hydrophila* isolates of epidemic outbreaks in channel catfish. *PLoS One*, 8(11), e80943. doi: 10.1371/journal.pone.0080943
- Hossain, S., De Silva, B. C. J., Wimalasena, S. H. M. P., Pathirana, H. N. K. S., Dahanayake, P. S., and Heo, G. J. 2018. Distribution of antimicrobial resistance genes and class 1 integron gene cassette arrays in motile *Aeromonas* spp. isolated from goldfish (*Carassius auratus*). *Microbial Drug Resistance*, 24(8), 1217-1225.
- Huey, D. W., Simco, B. A., and Criswell, D. W. 1980. Nitrite-induced methemoglobin formation in channel catfish. *Transactions of the American Fisheries Society*, 109(5), 558-562.
- Hurst, T.P. 2007. Causes and consequences of winter mortality in fishes. *Journal of Fish Biology*, 71: 315-345. doi:10.1111/j.1095-8649.2007.01596.x
- Janda, J. M., Abbott, S. L. 2010. The genus *Aeromonas*: taxonomy, pathogenicity, and infection. *Clinical Microbiology Reviews*, 23(1), 35-73.
- Johnson, K., Engle, C., and Wagner, B. 2014. Comparative economics of US catfish production strategies: evidence from a cross-sectional survey. *Journal of the World Aquaculture Society*, 45(3), 279-289.

- Jubirt, M. M., Hanson, L. A., Hanson-Dorr, K. C., Ford, L., Lemmons, S., Fioranelli, P., and Cunningham, F. L. 2015. Potential for great egrets (*Ardea alba*) to transmit a virulent strain of *Aeromonas hydrophila* among channel catfish (*Ictalurus punctatus*) culture ponds. *Journal of Wildlife Diseases*, 51(3), 634-639.
- Kahnemann, D., P. Slovic, and A. Tversky. 1982. Judgment under uncertainty: heuristics and bias. Cambridge University Press: Cambridge.
- Kalácska, M., Sánchez-Azofeifa, G. A., Caelli, T., Rivard, B., and Boerlage, B. 2005. Estimating leaf area index from satellite imagery using Bayesian networks. *IEEE Transactions on Geoscience and Remote Sensing*, 43(8), 1866-1873.
- Kawakani, H., and Hoshimoto, H. 1978. Occurrence and distribution of *Aeromonas* in surface water and algae in river water. *Journal of Faculty of Fisheries and Animal Husbandry, Hiroshima University*, 17(2), 155-164.
- Kelly, A. M. 2004. Broodfish management. In *Developments in Aquaculture and Fisheries Science* (Vol. 34, pp. 129-144). Elsevier.
- Kermack, W. O. and McKendrick, A. G. 1927. A contribution to the mathematical theory of epidemics. *Proceedings of the Royal Society of London. Series A, Containing Papers of a Mathematical and Physical Character*, 115(772), 700-721.
- Khoo, L. 2013. 2012 Annual Case Summary Report. Stoneville, Mississippi, Aquatic Research and Diagnostic Laboratory, Mississippi State University, College of Veterinary Medicine, Thad Cochran National Warmwater Aquaculture Center.
- Kneitel, J. M. 2019. Gause' s Competitive Exclusion Principle. In *Encyclopedia of Ecology* (2nd ed.). pp. 2780. Elsevier.
- Kumar, G., Engle, C., and Tucker, C. 2016. Costs and risk of catfish split-pond systems. *Journal of the World Aquaculture Society*, 47(3), 327-340.
- Kumar, G., Li, M.H., Wise, D.J., Mischke, C.C., Rutland, B., Tiwari, A., Aarattuthodiyil, S., Griffin, M.J., Khoo, L.H., Ott, B., Torrans, L. and Tucker, C.S. 2019. Performance of channel catfish and hybrid catfish in single-batch, intensively aerated ponds. *North American Journal of Aquaculture*, 81: 406-416. doi:10.1002/naaq.10109
- Lallier, R., Leblanc, D., Mittal, K. R., and Olivier, G. 1981. Sero-grouping of motile *Aeromonas* species isolated from healthy and moribund fish. *Journal of Applied Environmental Microbiology*, 42(1), 56-60.
- Leung, T., Campbell, P. T., Hughes, B. D., Frascoli, F., and McCaw, J. M. 2018. Infection-acquired versus vaccine-acquired immunity in an SIRWS model. *Infectious Disease Modelling*, 3, 118-135.

- Levins, R. 1966. The strategy of model building in population biology. *American scientist*, 54(4), 421-431.
- Levy, M. G., Flowers, J. R., Poore, M. F., Mullen, J. E., Khoo, L. H., Pote, L. M., Paperna, I., Dzikowski, R., and Litaker, R. W. 2002. Morphologic, pathologic, and genetic investigations of *Bolbophorus* species affecting cultured channel catfish in the Mississippi Delta. *Journal of Aquatic Animal Health*, 14(4), 235-246.
- Li, M. H., Robinson, E. H., Bosworth, B. G., Oberle, D. F., and Lucas, P. M. 2014. Optimizing soybean meal levels in alternative diets for pond-raised hybrid catfish. *North American Journal of Aquaculture*, 76(1), 61-66.
- Li, M. H., Robinson, E. H., Manning, B. B., Yant, D. R., Chatakondi, N. G., Bosworth, B. G., and Wolters, W. R. 2004. Comparison of the channel catfish, *Ictalurus punctatus* (NWAC103 strain) and the channel× blue catfish, *I. punctatus*×*I. furcatus*, F1 hybrid for growth, feed efficiency, processing yield, and body composition. *Journal of Applied Aquaculture*, 15(3-4), 63-71.
- Liles, M., Hemstreet, W., Waldbieser, G., Griffin, M., Khoo, L., Bebak, J.A., Garcia, J.C., Goodwin, A., Capps, N., Hayden, K., Terhune, J. 2011. Comparative genomics of *Aeromonas hydrophila* isolates from an epidemic in channel catfish [abstract]. *American Society for Microbiology*. Poster No. 1489.
- Lunn, D. J., Thomas, A., Best, N., and Spiegelhalter, D. 2000. WinBUGS – a Bayesian modelling framework: concepts, structure, and extensibility. *Statistics and Computing*, 10, 325-337.
- Manning, B. B., Terhune, J. S., Li, M. H., Robinson, E. H., Wise, D. J., and Rottinghaus, G. E. 2005. Exposure to feed-borne mycotoxins t-2 toxin or ochratoxin-a causes increased mortality of channel catfish challenged with *Edwardsiella ictaluri*. *Journal of Aquatic Animal Health*, 17:2, 147-152.
- Marcot, B. G., Steventon, J. D., Sutherland, G. D., and McCann, R. K. 2006. Guidelines for developing and updating Bayesian belief networks applied to ecological modeling and conservation. *Canadian Journal of Forest Research*, 36(12), 3063-3074.
- Merkhofer, M. W. 1977. The value of information given decision flexibility. *Management Science*, 23(7), 716-727.
- Meyer, F. P. 1970. Seasonal fluctuations in the incidence of disease on fish farms. *American Fisheries Society Symposium Special Publication* 5, 21-29.
- Meyer, F. P., and Bullock, G. L. 1973. *Edwardsiella tarda*, a new pathogen of channel catfish (*Ictalurus punctatus*). *Applied microbiology*, 25(1), 155.

- Mischke, C. C., Griffin, M. J., Wise, D. J., and Greenway, T. E. 2016. Effects of co-stocking smallmouth buffalo, *Ictiobus bubalus*, with channel catfish, *Ictalurus punctatus*. *Journal of the World Aquaculture Society*, 47(2), 212-219.
- Mitchell, A. J., and Plumb, J. A. 1980. Toxicity and efficacy of Furanace on channel catfish *Ictalurus punctatus* (Rafinesque) infected experimentally with *Aeromonas hydrophila*. *Journal of Fish Diseases*, 3(2), 93-99.
- Mott, D. F., and Brunson, M. W. 1995. A historical perspective of catfish production in the southeast in relation to avian predation. *7th Eastern Wildlife Damage Management Conference*, 23-30.
- NOAA. 2015. Fisheries of the United States, 2014. U.S. Department of Commerce, National Marine Fisheries Service, NOAA Current Fishery Statistics No. 2014. Available at: <https://www.st.nmfs.noaa.gov/commercial-fisheries/fus/fus14/index>.
- Nolan, T., Hands, R. E., Ogunkolade, W. and Bustin, S. A., 2006. SPUD: a quantitative PCR assay for the detection of inhibitors in nucleic acid preparations. *Analytical biochemistry*, 351(2), 308-310.
- Ogut, H. 2001. Modeling of fish disease dynamics: a new approach to an old problem. *Turkish Journal of Fisheries and Aquatic Sciences*, 1(1), 67-74.
- Ogut, H. and Bishop, S. C. 2007. A stochastic modelling approach to describing the dynamics of an experimental furunculosis epidemic in Chinook salmon, *Oncorhynchus tshawytscha* (Walbaum). *Journal of fish diseases*, 30(2), 93-100.
- Ogut, H., LaPatra, S. E., and Reno, P. W. 2005. Effects of host density on furunculosis epidemics determined by the simple SIR model. *Preventive Veterinary Medicine*, 71, 83-90.
- Ogut, H., Reno, P. W., and Sampson, D. 2004. A deterministic model for the dynamics of furunculosis in chinook salmon *Oncorhynchus tshawytscha*. *Diseases of Aquatic Organisms*, 62(1-2), 57-63.
- Overstreet, R. M., Curran, S. S., Pote, L. M., King, D. T., Blend, C. K., and Grater, W. D. 2002. *Bolbophorus damnificus n. sp.* (Digenea: Bolbophoridae) from the channel catfish *Ictalurus punctatus* and American white pelican *Pelecanus erythrorhynchos* in the USA based on life-cycle and molecular data. *Systematic Parasitology*, 52(2), 81-96.
- O'Neill, R. V., DeAngelis, D. L., Pastor, J. J., Jackson, B. J., and Post, W. M. 1989. Multiple nutrient limitations in ecological models. *Ecological Modeling*, 46(3-4), 147-163.
- Palumbo, S. A., Morgan, D. R., and Buchanan, R. L. 1985. Influence of temperature, NaCl, and pH on the growth of *Aeromonas hydrophila*. *Journal of Food Science*, 50(5), 1417-1421.

- Pang, M. D., Lin, X. Q., Hu, M., Li, J., Lu, C. P., and Liu, Y. J. 2012. Tetrahymena: an alternative model host for evaluating virulence of *Aeromonas* strains. *PLoS One*, 7(11).
- Pang, M., Jiang, J., Xie, X., Wu, Y., Dong, Y., Kwok, A. H., Zhang, W., Yao, H., Lu, C., Leung, F. C., and Liu, Y. 2015. Novel insights into the pathogenicity of epidemic *Aeromonas hydrophila* ST251 clones from comparative genomics. *Scientific Reports*, 5, 9833. doi: 10.1038/srepo9833
- Pasquale V., Baloda S. B., Dumontet S., and Krovacek K. 1994. An outbreak of *Aeromonas hydrophila* infection in turtles (*Pseudemis scripta*). *Applied Environmental Microbiology*, 60, 1678-1680.
- Pearl, J. 1986. Fusion, propagation, and structuring in belief networks. *Artificial intelligence*, 29(3), 241-288.
- Peatman, E., Mohammed, H., Kirby, A., Shoemaker, C. A., Yildirim-Aksoy, M., and Beck, B. H. 2018. Mechanisms of pathogen virulence and host susceptibility in virulent *Aeromonas hydrophila* infections of channel catfish (*Ictalurus punctatus*). *Aquaculture*, 482, 1-8.
- Plumb, J. A., and Hanson, L. A. 2010. Catfish bacterial diseases. In *Health Maintenance and Principal Microbial Diseases of Cultured Fishes*, pp. 275-313. Wiley-Blackwell, Hoboken, US.
- Plummer, M. 2003. JAGS: A program for analysis of Bayesian graphical models using Gibbs sampling. *Proceedings of the 3rd International Workshop on Distributed Statistical Computing*: 1–10.
- Pollino, C. A., Woodberry, O., Nicholson, A., Korb, K., and Hart, B. T. 2007. Parameterisation and evaluation of a Bayesian network for use in an ecological risk assessment. *Environmental Modelling and Software*, 22(8), 1140-1152.
- Pote, L. M., Hanson, L. A., and Shivaji, R. 2000. Small subunit ribosomal RNA sequences link the cause of proliferative gill disease in channel catfish to *Henneguya* n. sp.(Myxozoa: Myxosporea). *Journal of Aquatic Animal Health*, 12(3), 230-240.
- Pratt, J. W. 1978. Risk aversion in the small and in the large. In *Uncertainty in Economics* (pp. 59-79). Academic Press.
- Pridgeon, J. W., and Klesius, P. H. 2011. Molecular identification and virulence of three *Aeromonas hydrophila* isolates cultured from infected channel catfish during a disease outbreak in west Alabama (USA) in 2009. *Diseases of Aquatic Organisms*, 94(3), 249-253.
- R Core Team 2017. R: A language and environment for statistical computing. R Foundation for Statistical Computing, Vienna, Austria. URL <https://www.R-project.org/>.

- Radu, S., Ahmad, N., Ling, F. H., and Reezal, A. 2003. Prevalence and resistance to antibiotics for *Aeromonas* species from retail fish in Malaysia. *International Journal of Food Microbiology*, 81(3), 261-266.
- Rahman, M. H., Suzuki, S., and Kawai, K. 2001. The effect of temperature on *Aeromonas hydrophila* infection in goldfish, *Carassius auratus*. *Journal of Applied Ichthyology*, 17(6), 282-285.
- Rasmussen-Ivey, C. R., Hossain, M. J., Odom, S. E., Terhune, J. S., Hemstreet, W. G., Shoemaker, C. A., Zhang, D., Xu, D. H., Griffin, M. J., Liu, Y. J., Figueras, M. J., Santos, S. R., Newton, J. C., and Liles, M. R. 2016. Classification of a hypervirulent *Aeromonas hydrophila* haplotype responsible for epidemic outbreaks in warm-water fishes. *Frontiers in Microbiology*, 7, 1615. doi: 10.3389/fmicb.2016.01615
- Reichley, S. R., Ware, C., Greenway, T. E., Wise, D. J., and Griffin, M. J. 2015. Real-time polymerase chain reaction assays for the detection and quantification of *Edwardsiella tarda*, *Edwardsiella piscicida*, and *Edwardsiella piscicida*-like species in catfish tissues and pond water. *Journal of Veterinary Diagnostic Investigation*, 27(2), 130-139.
- Robinson, E. H., and Li, M. H. 2015. *Feed conversion ratio for pond-raised catfish*. Mississippi Agricultural and Forestry Experiment Station.
- Rosser, T. G., Baumgartner, W. A., Alberson, N. R., Noto, T. W., Woodyard, E. T., King, D. T., Wise, D. J., and Griffin, M. J. 2018. *Clinostomum poteae n. sp.* (Digenea: Clinostomidae), in the trachea of a double-crested cormorant *Phalacrocorax auritus* Lesson, 1831 and molecular data linking the life-cycle stages of *Clinostomum album* Rosser, Alberson, Woodyard, Cunningham, Pote & Griffin, 2017 in Mississippi, USA. *Systematic parasitology*, 95(6), 543-566.
- Rosser, T. G., Khoo, L. H., Wise, D. J., Mischke, C. C., Greenway, T. E., Alberson, N. R., Reichley, S.R., Woodyard, E.T., Steadman, J., Ware, C. and Pote, L. M. 2019. Arrested Development of *Henneguya ictaluri* (Cnidaria: Myxobolidae) in ♀ Channel Catfish×♂ Blue Catfish Hybrids. *Journal of aquatic animal health*, 31(2), 201-213.
- Ruth, M., and Cleveland, C. J. 1996. Modeling the dynamics of resource depletion, substitution, recycling and technical change in extractive industries. pp. 301–324 in R. Costanza, O. Segura, and J. Martinez-Alier (eds.), Getting down to earth: Practical applications of ecological economics. Island Press: Washington, DC.
- Schwarz, S., Hood, R. D., and Mougous, J. D. 2010. What is type VI secretion doing in all those bugs?. *Trends in microbiology*, 18(12), 531-537.
- Shafer, G. 1992. Dempster-shafer theory. *Encyclopedia of artificial intelligence*, 1, 330-331.
- Snieszko, S. F. 1974. The effects of environmental stress on outbreaks of infectious diseases of fishes. *Journal of Fish Biology*, 6(2), 197-208.

- Snieszko, S. F. 1978. Control of fish disease. *Marine Fisheries Review*, 40(3), 65-68.
- Snieszko, S.F. 1974. The effect of environmental stress on outbreak of infectious diseases of fishes. *J. Fish Biol.* 6: 197–208.
- Steeby, J. A. and Lovshin, L. L. 1993. Comparison of seines equipped with rubber roller or gathered-netting mud lines for harvesting channel catfish in earthen ponds. *The Progressive Fish-Culturist*, 55(2), 133-136.
- Stone, N. M., Shelton, J. L., Haggard, B. E., and Thomforde, H. K. (2013). *Interpretation of water analysis reports for fish culture*. Stoneville, Mississippi: Southern Regional Aquaculture Center.
- Stults, J. R., Snoeyenbos-West, O., Methé, B., Lovley, D. R., and Chandler, D. P. 2001. Application of the 5' fluorogenic exonuclease assay (TaqMan) for quantitative ribosomal DNA and rRNA analysis in sediments. *Applied and environmental microbiology*, 67(6), 2781-2789.
- Sturtz, S., Ligges, U., and Gelman, A. 2005. R2WinBUGS: a package for funning WinBUGS from R. *Journal of Statistical Software*, 12, 1-16.
- Styer, E. L., Harrison, L. R., and Burtle, G. J. 1991. Communications: Experimental production of proliferative gill disease in channel catfish exposed to a myxozoan-infected oligochaete, *Dero digitata*. *Journal of Aquatic Animal Health*, 3(4), 288-291.
- Sunder, J., Jeyakumar, S., Ahlawat, S. P. S., Rai, R. B., Kundu, A., Senani, S., Chatterjee, R. N., Saha, S. K., and Yadav, S. 2006. Antibiotic resistance pattern of bacterial isolates from fishes of Andaman and Nicobar Islands. *Indian Journal of Fisheries*, 53(2), 231-235.
- Taylor, P. W. 1992. Fish-eating birds as potential vectors of *Edwardsiella ictaluri*. *Journal of Aquatic Animal Health*, 4(4), 240-243.
- Taylor, S., Wakem, M., Dijkman, G., Alsarraj, M., Nguyen, M. 2010. A practical approach to RT-qPCR—publishing data that conform to the MIQE guidelines. *Methods*, 50: S1–S5. doi:10.1016/j.ymeth.2010.01.005.
- Tekedar, H. C., Abdelhamed, H. A., Kumru, S., Blom, J., Karsi, A., and Lawrence, M. L. 2019. Comparative genomics of *Aeromonas hydrophila* secretion systems and mutational analysis of tssD and tssI Genes from T6SS. *Frontiers in Microbiology*, 9, 3216. doi: 10.3389/fmicb.2018.03216
- Thune, R. L., Stanley, L. A., and Cooper, R. K. 1993. Pathogenesis of Gram negative bacterial infections in warm water fish. *Ann. Rev. Fish Dis.*, 3, 17-68.
- Tomás, J. M. 2012. The main *Aeromonas* pathogenic factors. *ISRN microbiology*, 2012.

- Torrans, E. L. 2005. Effect of oxygen management on culture performance of channel catfish in earthen ponds. *North American Journal of Aquaculture*, 67(4), 275-288.
- Torrans, L., Ott, B., and Bosworth, B. 2015. Impact of minimum daily dissolved oxygen concentration on production performance of hybrid female Channel Catfish× male Blue Catfish. *North American journal of aquaculture*, 77(4), 485-490.
- Trust, T. J., and Sparrow, R. A. H. 1974. The bacterial flora in the alimentary tract of freshwater salmonid fishes. *Canadian Journal of Microbiology*, 20(9), 1219-1228.
- Tucker, C.C. and Robinson, E.H., 1990. *Channel catfish farming handbook*. Springer Science and Business Media.
- USDA. 2013a. 2012 Census of Aquaculture, Part II. US Department of Agriculture, the Census of Agriculture (AC-12-A-51), 57 pages.
- USDA. 2013b. Catfish production. National Agricultural Statistics Service (NASS), Agricultural Statistics Board. United States Department of Agriculture, Washington, DC, 10 pages.
- USDA. 2016. Catfish production. National Agricultural Statistics Service (NASS), Agricultural Statistics Board. United States Department of Agriculture, Washington, DC, 6 pages.
- Varis, O. 1997. Bayesian decision analysis for environmental and resource management. *Environmental Modelling and Software*, 12(2-3), 177-185.
- Wagner, B. A., Wise, D. J., Khoo, L. H., and Terhune, J. S. 2002. The epidemiology of bacterial diseases in food-size channel catfish. *Journal of Aquatic Animal Health*, 14(4), 263-272,
- Walsh, S., Copeland, C., and Westlake, M. 2004. Major fish kills in the northern rivers of NSW in 2001: causes, impacts and responses. New South Wales Department of Primary Industries, Fisheries Final Report Series 68, Ballina: New South Wales, Australia.
- Walters, G. R., and Plumb, J. A. 1980. Environmental stress and bacterial infection in channel catfish, *Ictalurus punctatus* Rafinesque. *Journal of Fish Biology*, 17(2), 177-185.
- Wedemeyer, G. 1970. The role of stress in the disease resistance of fishes. In *A Symposium on Diseases of Fishes and Shellfishes* (Vol. 5, pp. 30-35). American Fisheries Society, Bethesda, Maryland.
- Wellborn, T. L. 1988. Channel catfish: life history and biology. *Southern Regional Aquaculture Center Publication No. 180*, Texas Agricultural Extension Service, College Station, Texas, USA: Southern Regional Aquaculture Center.
- Wellborn, T. L. 1990. Channel Catfish Life History and Biology. *Leaflet/Texas Agricultural Extension Service; no. 2402*.

- Wilcox, B. A., and Colwell, R. R. 2005. Emerging and reemerging infectious diseases: biocomplexity as an interdisciplinary paradigm. *EcoHealth*, 2(4), 244-257.
- Wilcox, B. A., and Gubler, D. J. 2005. Disease ecology and the global emergence of zoonotic pathogens. *Environmental Health and Preventive Medicine*, 10(5), 263-272.
- Wise, D. J., Camus, A. C., Schwedler, T. E., and Terhune, J. S. 2004. 15 Health management. In *Developments in Aquaculture and Fisheries Science* (Vol. 34, pp. 444-503). Elsevier.
- Wise, D. J., Greenway, T. E., Byars, T. S., Griffin, M. J., and Khoo, L. H. 2015. Oral vaccination of channel catfish against enteric septicemia of catfish using a live attenuated *Edwardsiella ictaluri* isolate. *Journal of Aquatic Animal Health*, 27:2, 135-143.
- Wise, D. J., Hanson, T. R., and Tucker, C. S. 2008. Farm-level economic impacts of *Bolbophorus* infections of Channel Catfish. *North American Journal of Aquaculture*, 70(4), 382-387.
- Wurts, W. A. 2015. Using Equations to Improve Feeding and Growth of Channel Catfish. *World Aquaculture*, 59.
- Xu, D. H., Pridgeon, J. W., Klesius, P. H., and Shoemaker, C. A. 2012. Parasitism by protozoan *Ichthyophthirius multifiliis* enhanced invasion of *Aeromonas hydrophila* in tissues of channel catfish. *Veterinary Parasitology*, 184(2-4), 101-107.
- Yost, M. C. 2008. The study of the life cycle of *Bolbophorus damnificus* and its pathology in the channel catfish (*Ictalurus punctatus*) (Doctoral dissertation, Mississippi State University).
- Zhang, D., Pridgeon, J. W., and Klesius, P. H. 2014. Vaccination of channel catfish with extracellular products of *Aeromonas hydrophila* provides protection against infection by the pathogen. *Fish and Shellfish Immunology*, 36(1), 270-275.
- Zhang, D., Xu, D. H., and Shoemaker, C. 2016. Experimental induction of motile *Aeromonas* septicemia in channel catfish (*Ictalurus punctatus*) by waterborne challenge with virulent *Aeromonas hydrophila*. *Aquaculture Reports*, 3, 18-23.
- Zhang, D., Xu, D., Shoemaker, C., and Hemstreet, W. 2016. Virulent *Aeromonas hydrophila* in Channel Catfish. <https://www.aquaculturealliance.org/advocate/virulent-aeromonas-hydrophila-in-channel-catfish/>. Accessed on September 30, 2016.
- Zhang, X., Yang, W., Wu, H., Gong, X., and Li, A. 2014. Multilocus sequence typing revealed a clonal lineage of *Aeromonas hydrophila* caused motile *Aeromonas* septicemia outbreaks in pond-cultured cyprinid fish in an epidemic area in central China. *Aquaculture*, 432, 1-6.

APPENDIX A

METADATA FOR ALL ISOLATES COLLECTED AND USED IN THE TEMPORAL
AND SPATIAL ANALYSIS OF THIS STUDY

Table A.1 All isolates used for spatial and temporal analysis of atypical *Aeromonas hydrophila* in the southeastern U.S.

Isolate	[†] Lab	Year	Strain
*ML09-119	Alabama	2009	ML09-119
*S14-452	Delta	2014	S14-452
ALG10-167	Alabama	2010	ML09-119
ALG10-197	Alabama	2010	A. veronii
ML10-115 F2	Alabama	2010	ML09-119
ALG10-160 F1	Alabama	2010	ML09-119
ML10-113	Alabama	2010	ML09-119
ML10-115 F3	Alabama	2010	ML09-119
ML10-052	Alabama	2010	ML09-119
ALG10-064-2	Alabama	2010	ML09-119
ALG10-064	Alabama	2010	ML09-119
ML10-191 F1	Alabama	2010	ML09-119
ALG10-123	Alabama	2010	ML09-119
ALG10-196	Alabama	2010	A. veronii

Table A.1 (continued)

Isolate	[†] Lab	Year	Strain
ALG10-144	Alabama	2010	ML09-119
ALG10-161 F1	Alabama	2010	ML09-119
ALG10-161 F2	Alabama	2010	ML09-119
ALG10-194 F2	Alabama	2010	tAh
ALG10-126 Tilapia	Alabama	2010	tAh
ALG10-140	Alabama	2010	ML09-119
ALG10-163 F2	Alabama	2010	ML09-119
ALG10-064 Fe+	Alabama	2010	ML09-119
ALG10-064-1	Alabama	2010	ML09-119
ML12-061	Alabama	2012	ML09-119
ML12-069	Alabama	2012	ML09-119
ML12-063	Alabama	2012	ML09-119
ML12-062	Alabama	2012	ML09-119
ML12-076	Alabama	2012	ML09-119

Table A.1 (continued)

Isolate	[†] Lab	Year	Strain
IRPS15-28	Alabama	2015	ML09-119
IPRS15-009A	Alabama	2015	ML09-119
ML15-159 B1	Alabama	2015	ML09-119
IPRS15-30	Alabama	2015	ML09-119
IPRS15-034	Alabama	2015	ML09-119
IPRS15-031	Alabama	2015	ML09-119
AL15-079	Alabama	2015	ML09-119
ML15-022-1630	Alabama	2015	ML09-119
C16-00231	Starkville	2016	S14-452
C16-12824-1	Starkville	2016	S14-452
C16-12825	Starkville	2016	S14-452
C16-12827	Starkville	2016	S14-452
C16-13322	Starkville	2016	S14-452
C16-13421-1	Starkville	2016	S14-452

Table A.1 (continued)

Isolate	[†] Lab	Year	Strain
C16-13422-1	Starkville	2016	ML09-119
C16-13424-1	Starkville	2016	ML09-119
C16-13426-1	Starkville	2016	tAh
C16-13569	Starkville	2016	S14-452
C16-13688	Starkville	2016	ML09-119
C16-13689	Starkville	2016	S14-452
C16-13690	Starkville	2016	S14-452
C16-13760	Starkville	2016	S14-452
C16-13763	Starkville	2016	S14-452
C16-14080A	Starkville	2016	S14-452
C16-14080B	Starkville	2016	S14-452
C16-14082	Starkville	2016	S14-452
C16-14202	Starkville	2016	S14-452
C16-14204	Starkville	2016	S14-452

Table A.1

Isolate	[†] Lab	Year	Strain
C16-14297	Starkville	2016	S14-452
C16-14375	Starkville	2016	S14-452
C16-14530	Starkville	2016	ML09-119
C16-14930A	Starkville	2016	S14-452
C16-14930B	Starkville	2016	ML09-119
C16-14959	Starkville	2016	S14-452
C16-14961	Starkville	2016	S14-452
C16-15077	Starkville	2016	ML09-119
C16-15148	Starkville	2016	S14-452
C16-15175A	Starkville	2016	S14-452
C16-15175B	Starkville	2016	ML09-119
C16-15207	Starkville	2016	tAh
C16-15245	Starkville	2016	S14-452
C16-16046	Starkville	2016	ML09-119

Table A.1 (continued)

Isolate	[†] Lab	Year	Strain
C16-16047-1	Starkville	2016	ML09-119
C16-16153-1	Starkville	2016	S14-452
C16-16154	Starkville	2016	S14-452
C16-16432B	Starkville	2016	S14-452
C16-16434A	Starkville	2016	S14-452
C16-16581	Starkville	2016	S14-452
C16-16582	Starkville	2016	S14-452
C16-16748	Starkville	2016	S14-452
C16-16952	Starkville	2016	S14-452
C16-17033	Starkville	2016	S14-452
C16-17034	Starkville	2016	S14-452
C16-17064	Starkville	2016	S14-452
C16-17538	Starkville	2016	ML09-119
C16-17585	Starkville	2016	S14-452

Table A.1 (continued)

Isolate	[†] Lab	Year	Strain
C16-17588	Starkville	2016	S14-452
C16-17589	Starkville	2016	tAh
C16-17637A	Starkville	2016	ML09-119
C16-17637B	Starkville	2016	S14-452
C16-17638	Starkville	2016	S14-452
C16-17734	Starkville	2016	S14-452
C16-17830	Starkville	2016	S14-452
C16-18206-1	Starkville	2016	S14-452
C16-18254	Starkville	2016	S14-452
C16-18256	Starkville	2016	S14-452
C16-18316	Starkville	2016	S14-452
C16-18317	Starkville	2016	S14-452
C16-18324	Starkville	2016	S14-452
C16-19094	Starkville	2016	S14-452

Table A.1 (continued)

Isolate	[†] Lab	Year	Strain
C16-19100	Starkville	2016	S14-452
C16-19102	Starkville	2016	S14-452
C16-19147	Starkville	2016	S14-452
C16-19712	Starkville	2016	S14-452
C16-19713	Starkville	2016	S14-452
C16-19755	Starkville	2016	S14-452
C16-20267	Starkville	2016	S14-452
C16-20657	Starkville	2016	S14-452
A18-190	Starkville	2018	S14-452
A18-092	Starkville	2018	S14-452
A18-139	Starkville	2018	S14-452
A18-126-2	Starkville	2018	S14-452
A18-201	Starkville	2018	tAh
A18-136	Starkville	2018	S14-452

Table A.1 (continued)

Isolate	[†] Lab	Year	Strain
A18-189	Starkville	2018	S14-452
A18-166	Starkville	2018	S14-452
A18-179-1	Starkville	2018	S14-452
A18-126	Starkville	2018	S14-452
A18-128	Starkville	2018	S14-452
A18-206	Starkville	2018	S14-452
A18-088-2	Starkville	2018	tAh
A18-096	Starkville	2018	ML09-119
A18-157	Starkville	2018	S14-452
A18-197	Starkville	2018	S14-452
A18-163	Starkville	2018	S14-452
A18-135	Starkville	2018	S14-452
A18-186	Starkville	2018	S14-452
A18-140	Starkville	2018	S14-452

Table A.1 (continued)

Isolate	[†] Lab	Year	Strain
A18-035	Starkville	2018	tAh
A18-160	Starkville	2018	S14-452
A18-117	Starkville	2018	S14-452
A18-071	Starkville	2018	tAh
A18-198	Starkville	2018	S14-452
A18-115	Starkville	2018	S14-452
A18-180-1	Starkville	2018	S14-452
A18-165	Starkville	2018	S14-452
A18-189 Lesion	Starkville	2018	S14-452
A18-118	Starkville	2018	S14-452
A18-116	Starkville	2018	S14-452
A18-126-Brain1	Starkville	2018	S14-452
A18-213	Starkville	2018	S14-452
A18-014	Starkville	2018	S14-452

Table A.1 (continued)

Isolate	[†] Lab	Year	Strain
A18-170-1	Starkville	2018	S14-452
A18-093	Starkville	2018	S14-452
A18-162	Starkville	2018	S14-452
A18-181	Starkville	2018	S14-452
A18-141	Starkville	2018	S14-452
A18-142	Starkville	2018	S14-452
S13-597	Delta	2013	ML09-119
S13-612A	Delta	2013	ML09-119
S13-612B	Delta	2013	ML09-119
S13-613A	Delta	2013	ML09-119
S13-613B	Delta	2013	ML09-119
S13-614A	Delta	2013	ML09-119
S13-614B	Delta	2013	ML09-119
S13-615A	Delta	2013	ML09-119

Table A.1 (continued)

Isolate	[†] Lab	Year	Strain
S13-615B	Delta	2013	ML09-119
S13-615C	Delta	2013	ML09-119
S13-633	Delta	2013	ML09-119
S13-634	Delta	2013	ML09-119
S13-656	Delta	2013	ML09-119
S13-657	Delta	2013	ML09-119
S13-658	Delta	2013	ML09-119
S13-660	Delta	2013	ML09-119
S13-700	Delta	2013	ML09-119
S14-230	Delta	2014	tAh
S14-296	Delta	2014	ML09-119
S14-448A	Delta	2014	ML09-119
S14-448B	Delta	2014	ML09-119
S14-451	Delta	2014	S14-452

Table A.1 (continued)

Isolate	[†] Lab	Year	Strain
S14-455	Delta	2014	S14-452
S14-458	Delta	2014	S14-452
S14-533	Delta	2014	ML09-119
S14-603	Delta	2014	ML09-119
S14-604	Delta	2014	ML09-119
S14-605	Delta	2014	ML09-119
S14-606	Delta	2014	ML09-119
S14-699	Delta	2014	ML09-119
PB15-921-1	Delta	2015	ML09-119
PB15-921-2	Delta	2015	ML09-119
S15-016	Delta	2015	S14-452
S15-130	Delta	2015	S14-452
S15-246	Delta	2015	S14-452
S15-247	Delta	2015	S14-452

Table A.1 (continued)

Isolate	[†] Lab	Year	Strain
S15-265	Delta	2015	S14-452
S15-266A	Delta	2015	S14-452
S15-266B	Delta	2015	S14-452
S15-267	Delta	2015	S14-452
S15-268	Delta	2015	S14-452
S15-269	Delta	2015	ML09-119
S15-272	Delta	2015	S14-452
S15-295	Delta	2015	ML09-119
S15-308	Delta	2015	S14-452
S15-309	Delta	2015	S14-452
S15-400	Delta	2015	S14-452
S15-401	Delta	2015	S14-452
S15-451	Delta	2015	S14-452
S15-452	Delta	2015	S14-452

Table A.1 (continued)

Isolate	[†] Lab	Year	Strain
S15-591A	Delta	2015	S14-452
S15-591B	Delta	2015	S14-452
S16-004	Delta	2016	S14-452
S16-070	Delta	2016	S14-452
S16-219A	Delta	2016	S14-452
S16-219B	Delta	2016	S14-452
S16-220A	Delta	2016	S14-452
S16-220B	Delta	2016	S14-452
S16-229	Delta	2016	S14-452
S16-232	Delta	2016	S14-452
S16-345	Delta	2016	tAh
S16-346	Delta	2016	tAh
S16-349	Delta	2016	S14-452
S16-367	Delta	2016	S14-452

Table A.1 (continued)

Isolate	[†] Lab	Year	Strain
S16-415	Delta	2016	S14-452
S16-456	Delta	2016	S14-452
S16-535	Delta	2016	S14-452
S16-539A	Delta	2016	S14-452
S16-539B	Delta	2016	S14-452
S16-546	Delta	2016	ML09-119
S16-547	Delta	2016	ML09-119
S16-548	Delta	2016	tAh
S16-549	Delta	2016	tAh
S16-704	Delta	2016	S14-452
S17-131	Delta	2017	S14-452
S17-151	Delta	2017	S14-452
S17-177	Delta	2017	S14-452
S17-196	Delta	2017	S14-452

Table A.1 (continued)

Isolate	[†] Lab	Year	Strain
S17-221	Delta	2017	S14-452
S17-278	Delta	2017	S14-452
S17-286	Delta	2017	S14-452
S17-293	Delta	2017	S14-452
S17-299	Delta	2017	S14-452
S17-343	Delta	2017	S14-452
S17-344	Delta	2017	S14-452
S17-380	Delta	2017	S14-452
S17-401	Delta	2017	S14-452
S17-406	Delta	2017	S14-452
S17-494	Delta	2017	S14-452
S17-859	Delta	2017	S14-452
S17-886	Delta	2017	S14-452
S17-888	Delta	2017	S14-452

Table A.1 (continued)

Isolate	†Lab	Year	Strain
S18-167	Delta	2018	A. sobria
S18-316	Delta	2018	A. sobria
S18-331	Delta	2018	S14-452
S18-400	Delta	2018	S14-452
S18-404	Delta	2018	S14-452
S18-567	Delta	2018	S14-452
S18-568	Delta	2018	S14-452
S18-569	Delta	2018	S14-452
S18-570	Delta	2018	S14-452
S18-571	Delta	2018	S14-452
S18-607	Delta	2018	S14-452
S18-641	Delta	2018	S14-452

* Indicate type strains of the two recognized haplotypes.

†Lab indicates which of the three diagnostic labs each isolate was originally submitted to and cultured from.